Project Number: CM-TAC-0021

Utilizing the Quartz Crystal Microbalance with Dissipation to Bind Cecropin P1 to *Escherichia coli*

A Major Qualifying Project Report:
submitted to the Faculty
of the
WORCESTER POLYTECHNIC INSTITUTE
In partial fulfillment of the requirements for the
Degree of Bachelor of Science
by

_____

Christine Cronin

and

_____

Andrea L. Kadilak

Date: March 28, 2008

Approved:

_____

Professor Terri A. Camesano, Advisor

Abstract

The main goal of this project was to study the binding and deactivation potential of the antimicrobial peptide (AMP) cecropin P1 with eleven strains of *E. coli* with varying lipopolysaccharide (LPS) membrane structure, using the quartz crystal microblance with dissipation (QCM-D). A decrease in frequency and an increase in dissipation from the QCM-D indicated an increase in the mass deposited on the gold crystals. A live/dead kit was used to determine the amount of bacteria bound to the gold crystal surface and the percentage dead with and without cecropin P1. The QCM-D showed four of the eleven strains preferentially bound to cecropin P1, while the live/dead kit showed six strains preferentially bound to cecropin P1. Three strains of *E. coli* (O157:H7, O113:H4, and O35:K-:H10) showed preferential binding with cecropin P1 and resulted in a higher percentage of the bacteria dead when in the presence of the AMP.

Acknowledgements

We would like to begin by thanking our advisor, Professor Terri A. Camesano, Department of Chemical Engineering at Worcester Polytechnic Institute for giving us the opportunity to work on this interesting project and conduct our research in the new state of the art laboratories at Gateway Park.

Also, we are very appreciative of all of the help given to us by Professor Camesano's graduate students Joshua Strauss, Paola Pinzon-Arango, and Yatao Liu. In particular, we would like to especially thank Joshua Strauss for all of his guidance and teaching throughout this project.

Finally, we would like to thank Dr. Howard Ochman of the University of Arizona and Kim Ziebel of Health Canada for kindly donating several strains of *E. coli* necessary for this research.

Table of Contents

ABSTRACT ..... **I**

ACKNOWLEDGEMENTS ..... **II**

TABLE OF CONTENTS ..... **III**

LIST OF FIGURES ..... **V**

LIST OF TABLES ..... **VI**

1 INTRODUCTION **1**

2 LITERATURE REVIEW **6**

2.1 E. COLI OVERVIEW 6
2.1.1 Recent E. coli Outbreaks in the United States *6*
2.1.2 Causes of E. coli Outbreaks *7*
2.1.3 Disease-causing E. coli Strains *9*
2.1.4 Cellular Structure *12*
2.2 ANTIMICROBIAL PEPTIDES 16
2.2.1 Derivations *16*
2.2.2 Structure and Characteristics of AMPs *19*
2.2.3 Cecropin P1 ..... *22*
2.3 AMP AND BACTERIAL INTERACTIONS 24
2.3.1 How and Why AMPs Attack Bacterial Membranes *24*
2.3.2 Models for Attack *26*
2.4 QUARTZ CRYSTAL MICROBALANCE WITH DISSIPATION (QCM-D) 29
2.4.1 How the QCM-D Works *29*
2.4.2 Theory of the QCM-D *30*
2.4.3 Relevant Research Using the QCM and QCM-D *32*

3 METHODOLOGY **39**

3.1 MAKING AGAR PLATES 39
3.2 PLATING BACTERIA 39
3.3 PRE-CULTURING BACTERIA 40
3.4 GROWTH CURVES 40
3.5 COUNTING BACTERIA 42
3.6 CONTACT ANGLES 43
3.7 QCM-D 43
3.7.1 Cleaning procedure for QCM-D and crystals *44*
3.7.2 QCM-D Experimental Procedure *44*
3.8 LIVE/DEAD KIT ON GOLD CRYSTALS TO CHARACTERIZE CELL VIABILITY 46

4 RESULTS **48**

4.1 GROWTH CURVES 48
4.2 COUNTING CHAMBER 50
4.3 CONTACT ANGLE 52
4.4 QCM-D 52
4.5 LIVE/DEAD KIT 59

5 CONCLUSIONS AND RECOMMENDATIONS **67**

5.1 NUMBER OF E. COLI CELLS PRESENT ON GOLD CRYSTALS 67
5.2 PERCENTAGE OF E. COLI DEAD 71

6 REFERENCES **72**

APPENDIX A: QCM-D FREQUENCY AND DISSIPATION PLOTS **75**

APPENDIX B: QCM-D FREQUENCY AND DISSIPATION SHIFTS 86
APPENDIX C: LIVE/DEAD CELL COUNT RAW DATA 88
APPENDIX D: LIVE/DEAD TABLES 94
APPENDIX E: GROWTH CURVES 95
APPENDIX F: FREQUENCY AND DISSIPATION RESULTS TABLE 101

List of Figures

Figure 1: A simplified version of the difference between Gram-positive bacteria (left) and Gram-negative bacteria (right) (http://filebox.vt.edu/users/chagedor/biol_4684/Methods/bacterial.gif). 13
Figure 2: Representation of the three different regions of the LPS structure. R, SR and S refer to the LPS structure as being Rough-type, Semi-rough type and Smooth-type (Epand et al., 1999). 14
Figure 3: Organizational chart explaining the classification of *E. coli* bacteria using the O-antigen unit of the LPS. 15
Figure 4: Alpha helix structure as seen in the AMP cecropin P1 (http://www.csusm.edu/jayasinghe/MoviesAminations/files/page34-1000-thumb.jpg). 22
Figure 5: Carpet Model of AMP activity against bacteria (Reddy et al., 2004). 27
Figure 6: "Barrel-Stave" Model for AMP activity against bacteria (Reddy et al., 2004). 28
Figure 7: Growth curve for *E. coli* O113:H21. 48
Figure 8: Semi-log plot of *E. coli* O113:H21. 49
Figure 9: Example of counting chamber image for *E. coli* O113:H21 at 0.495A. 50
Figure 10: *E. coli* O113:H21 Bacteria Population Averages. 51
Figure 11: QCM-D frequency and dissipation shifts for *E. coli* O157:H12 with cecropin P1 cys on a gold crystal surface. 53
Figure 12: QCM-D frequency and dissipation shifts for *E. coli* O55:H7 without cecropin P1cys on a gold crystal surface. 55
Figure 13: Bar graph of measured frequency shift measured in QCM-D plots when *E.coli* was added, with and without cecropin P1 bound to the gold crystal surface. Note that the error bars represent the standard deviation. 56
Figure 14: Bar graph of measured dissipation shift measured in QCM-D plots when *E.coli* was added, with and without cecropin P1 bound to the gold crystal surface. Note that the error bars represent the standard deviation. 57
Figure 15: Live/Dead picture of *E. coli* O117:K98:H4 with (top) and without (bottom) cecropin P1 cys on a gold QCM-D crystal. 61
Figure 16: Graph of the number of *E. coli* cells present per live/dead picture with cecropin P1 and without cecropin P1. 62
Figure 17: Graph of percentage of *E. coli* cells dead per live/dead picture with cecropin P1 and without cecropin P1. 63
Figure 18: Amount of bacteria present per picture in live/dead kit versus frequency change measured by QCM-D. 68

List of Tables

Table 1: Antimicrobial peptides found in animals (Brogden et al., 2003). 18
Table 2: Source information for *E. coli* strains used, where EPEC stands for enteropathogenic *E. coli*, EHEC stands for enterohemorrhagic *E.coli*, VTEC stands for vero-toxin producing *E. coli*, and the sugar backbone type refers to the number of sugars in the lipopolysaccharide backbone 41
Table 3: Water contact angle on gold crystals with varying concentrations of cecropin P1 cys. 52
Table 4: Statistical significance for results of average frequency shift in QCM-D plots when *E. coli* was added, comparing crystals with and without bound cecropin P1. 58
Table 5: Statistical significance for results of average dissipation shift in QCM-D plots when *E. coli* was added, comparing between crystals with and without bound cecropin P1..... 59
Table 6: Statistic significance for results of average number of *E. coli* cells present per live/dead picture. 64
Table 7: Number of *E. coli* present on crystal per picture with cecropin P1 and without cecropin P1..... 94
Table 8: Percentage of *E. coli* dead per picture with cecropin P1 and without cecropin P1. 94

1 Introduction

Escherichia coli, commonly referred to as *E. coli*, is a pathogenic species of bacteria known to many people worldwide. *E. coli* has been most widely recognized as a food contaminant that can cause intestinal lesions, hemorrhaging in the digestive tract, kidney failure, and in extreme cases death. One of the most dangerous strains identified as of yet is *E. coli* O157:H7, which has caused three major outbreaks in the United States in the past two years. In the first of these three outbreaks, nearly 200 people throughout the United States were affected by consuming contaminated fresh spinach in September and October of 2006 (CDC, Oct 6, 2006). Only a few months later in November and December, over 70 Americans became ill because of shredded lettuce contaminated by *E. coli* O157:H7 distributed by chains of Taco Bell (CDC, Dec 14, 2006). The most recent outbreak was triggered by contaminated Topps Ground Beef Patties, which left 40 people affected across eight states, 21 of whom were hospitalized, and two of whom developed kidney failure (CDC, Oct 26, 2007).

Clearly, contamination by *E. coli* is a major issue that must be addressed by the American agriculture, food, and health industries. However, despite technological advances in agriculture, increased disease awareness in the food industry, and major medical advancements, *E. coli* contamination is not easy to combat or prevent. In fact, there are many problems in each of these sectors that may complicate or even worsen current issues concerning *E. coli* outbreaks.

In recent years, agriculture, particularly the cattle and beef industries, has witnessed a large increase in demand, and has expanded in order to meet this demand. However, this expansion has caused larger, more crowded farms and slaughterhouses. These conditions contribute a great deal of stress to the cattle, which may cause them to shed parasites and bacteria such as *E. coli* in their feces (Miller et al., 1998). If *E. coli* are excreted during transport or at the slaughterhouse facilities, the meat may become contaminated. This meat is then shipped from the slaughterhouse to various locations throughout the United States, and may possibly cause a widespread outbreak.

The food industry has also played a major role in the increasing occurrence of *E. coli* outbreaks. According to recent studies, Americans are constantly consuming more of their meals outside of their homes, most often in restaurants (Miller et al., 1998). In these situations, consumers have even less control over how well their food is cooked, how fresh their food is, or where the food is obtained. These factors also make outbreaks more difficult to trace back to a single location, since consumers are not always certain of the source of their food.

Finally, the medical industry may have also contributed to the increasing danger of *E. coli* outbreaks through overuse of antibiotics. Because antibiotics are often prescribed when it may not be a bacterial infection and many patients do not finish their antibiotics after the full length of time, certain strains of bacteria have become resistant to these particular treatments. Since bacteria can multiply in only 20 minutes, they undergo mutations much more frequently and can quickly adapt to antibiotics used to kill them. In

fact, some strains are resistant to multiple forms of common drug treatment. Thus, sometimes patients can become infected with a normally treatable disease, but if they possess a resistant strain, antibiotics may be completely ineffective (Brogden et al., 2003).

Antimicrobial peptides (AMPs) have been shown to be an effective new method to combat certain strains of bacteria and other microbes. AMPs are naturally produced by certain insects, amphibians, and mammals to act as a defensive agent against pathogens (Brogden et al., 2003). An AMP that has been found to be particularly effective against *E. coli* is cecropin P1, which was first derived from porcine small intestine, and therefore this was the AMP chosen for experiments in this project (Bomen et al., 1993). It is believed that the generally positively-charged AMPs interact with the negatively charged bacterial membranes. Specifically, AMPs have been shown to penetrate bacterial membranes and disrupt the ion and molecular balances of the cell, which causes the cell to lyse and immediately die (Shai, 1999). Since AMPs fully lyse the cells, there is no way for the bacteria to survive their attack. Furthermore, because it is the inherent structure of the membrane which the AMPs attack, the bacteria cannot become resistant to AMP therapy. Therefore, AMPs show much promise in the medical field to combat bacteria that may be resistant to any antibiotics used as previous treatment.

However, not much is known about the mechanism of AMP attack, the conditions necessary for effectiveness, and where exactly the AMPs adhere to the bacterial membrane. Although research has been conducted concerning the effectiveness of AMPs

in solution against certain strains of bacteria, this may not be a feasible for applications to the food industry. Instead, AMPs could be bound to the certain surfaces, such as stainless steel cutting boards, and used as a preventative method against outbreaks of bacteria such as *E. coli*.

This project has employed a novel technique using a quartz crystal microbalance with dissipation (QCM-D) to study the interactions between bound AMPs and bacteria. The QCM-D works by oscillating a quartz crystal with a gold electrode and measuring the frequency and dissipation changes as a solution is run over the surface. Decreases in frequency indicate an increase in mass deposited on the crystal surface, while an increase in dissipation indicates more energy lost by the film deposited on the crystal (Q-Sense, 2007). These measurements can be used to characterize the layer adsorbed to the surface of the crystal. Prior studies have used the QCM-D to characterize the adsorption of cells (Fredriksson et al., 1998; Otto et al., 1999; Schofield et al., 2007), proteins (Höök et al., 1998), and other biomolecules (Jenkins et al., 2004; Kwon et al., 2006; Carter et al., 1995), but no previously published research has utilized the QCM-D to study AMP-bacterial interactions.

The aim of this project was to better understand the interactions between the AMP cecropin P1 and ten different pathogenic strains of *E. coli* along with one non-pathogenic laboratory strain. This was done by binding cecropin P1 with an added cysteine group to the surface of the gold electrode of a QCM-D crystal and then passing an *E. coli* culture through the flow chamber. Change in contact angle was used to confirm that cecropin P1

was deposited on the crystal. For the duration of the experiment, the frequency and dissipation changes were monitored and used to better understand the adsorption and binding processes. Additionally, *E. coli* adherence to crystals with cecropin P1 was compared to crystals without the AMP. Finally, a protocol involving a live/dead kit was used to determine the effectiveness of bound AMPs in killing *E. coli* and compare its effectiveness between all eleven strains.

This is the first study to apply the QCM-D to directly measure binding between *E. coli* and AMPs, which will lead to better methods for applying AMP technology to bacterial detection. Finally, this project may open doors for new food industry applications of AMPs to help combat *E. coli* outbreaks.

2 Literature Review

2.1 E. coli Overview

2.1.1 Recent *E. coli* Outbreaks in the United States

E. coli outbreaks have become a hot topic in the media in the past few years. This has affected many parts of the United States and several industries, including fast food and agriculture. In October of 2007, 21.7 million pounds of frozen Topp's ground beef patties contaminated with *E. coli* O157:H7 were recalled (CDC, Oct 26, 2007). *E. coli* outbreaks have the potential to affect a large area since products are routinely shipped from state to state. This Topp's outbreak infected 40 people in eight states (Connecticut, Florida, Indiana, Maine, New Jersey, New York, Ohio and Pennsylvania), hospitalized 21 people, and resulted in the kidney failure of two patients (CDC, Oct 26, 2007).

Another *E. coli* O157:H7 outbreak occurred almost a year earlier from November-December of 2006 at Taco Bell Restaurants and affected the East coast of the United States. In this case, it was not tainted beef that was the problem, but contaminated lettuce that the restaurant chain used. This outbreak affected 71 people in five states (New Jersey, New York, Pennsylvania, Delaware and South Carolina) leaving fifty-three people hospitalized and eight people who developed kidney failure (CDC, Dec 14, 2006).

The contamination of raw, packaged spinach, which was perhaps one of the most severe cases of *E. coli* contamination, occurred only months before the Taco Bell incident during the months of September and October of 2006. This outbreak of *E. coli* O157:H7 left 199 people ill throughout 26 states, hospitalized 102 of those affected, resulted in

kidney failure for 31 of those ill, and caused the death of three people (CDC, Oct 6, 2006). These are just a few of the many examples that show how *E. coli* contamination poses a serious health risk to consumers.

2.1.2 Causes of *E. coli* Outbreaks

Large-scale *E. coli* outbreaks that infect people throughout the United States have become more common in the past 20 years, and because of this, the CDC has declared *E. coli* O157:H7 and other enterohemorrhagic *E. coli* (EHEC) strains to be "emerging pathogens" (CDC, 1994). However, evidence has shown that this emergence is not merely caused by natural evolution of the species, but may have been triggered by human behaviors. Miller et al. (1998) attribute the increasing prevalence of *E. coli* outbreaks to changes in the cattle industry and consumer eating habits in recent decades.

With growing demand for beef products in the United States, the cattle industry has expanded significantly in recent years, and because of this, many practices have changed to account for the increased supply of cattle. Bacterial infection problems might begin with the location and climate of the farm itself. Miller et al. (1998) state that many dairy and other cattle farms are moving from the upper Midwestern states to lower Midwestern or Southwestern states that have a warmer climate which might better support the growth of *E. coli* bacteria. Additionally, on the farms it is theorized that wild birds that come in contact with infected manure and then cattle could cause disease in the live animals (Miller et al., 1998). These issues are often compounded by ill-treatment of the cattle on the farms, where feedlots are considerably more crowded on modern cattle farms than

previously. This crowding on the farms and subsequent crowding in trucks while the cattle are being transported to slaughterhouses can cause a significant amount of stress for the animals, which could in turn "allow cattle to shed *E. coli* in feces" (Miller et al., 1998).

Modern practices in cattle slaughtering, meat processing, and meat distribution may also be contributing to *E. coli* outbreaks occurring in the United States. The actual number of slaughterhouses in the United States has decreased in recent years, and therefore the size of remaining slaughterhouses has increased considerably in order to keep up with the supply of cattle and demand for meat (Miller et al., 1998). Because of this enlargement of sites, slaughterhouses encounter problems similar to cattle farms concerning the stress of animals. Additionally, because there are fewer slaughterhouses, each site receives animals from a larger area (Miller et al., 1998). Thus, the animals often have a much longer trip on over-crowded trucks during which they are deprived of food. This stressful environment could cause the cattle to excrete *E. coli* in their manure, which could contaminate the carcasses before they even reach the facility. Once the cattle reach the slaughterhouse, there are even more vectors of disease transport. For instance, beef grinding facilities often receive beef from multiple suppliers, and often grind unused meat from the previous day with fresh meat, which could mix contaminated meat with uncontaminated meat and make the origin of contamination more difficult to trace (Miller et al., 1998). Finally, once again because there are fewer slaughterhouses in the country, a single site may transport meat to many regions of the country, and thus contamination could affect a larger amount of people than it would have in the past.

Finally, consumer habits have evolved considerably in modern society, which could make many people more vulnerable to infection by *E. coli*. According to Jensen and Unnevehr (1995), half of all meals eaten by Americans are consumed away from home, most of which are eaten at a restaurant. When eating at a restaurant, consumers are not actively involved in the preparation of the food, and don't have as much control over how well their food is cooked. In addition, approximately 25% of American survey participants responded that they prefer hamburgers rare or medium rare (Miller et al., 1998). Although rare or medium rare steaks are safe to eat because cooking the surface kills the microorganisms, eating rare or medium rare hamburgers is dangerous because microorganisms can penetrate the surface of ground beef hamburgers. Since such a small amount of *E. coli* O157:H7 is required to cause an infection, it is even easier for consumers to become ill if they are not diligent about their eating habits.

2.1.3 Disease-causing *E. coli* Strains

While some strains of *Echerichia coli* aid digestion and naturally reside in the intestinal tracts of animals, certain strains are highly pathogenic to humans and have caused several outbreaks in the United States, such as the Topps Ground Beef, Taco Bell and Spinach outbreaks discussed earlier. Strains of *E. coli* that have been found to be particularly harmful to the human digestive system are those categorized as enteropathogenic *E. coli* or EPEC. EPEC strains can cause intestinal lesions in humans and perpetuate infection in the intestinal system by adhering to the membranes of microvilli (Mouenuddin et al., 1989). Several strains or serotypes of *E. coli* used in the experiments detailed in this

paper, specifically *E. coli* O55:H7 and O26:K60:H11, have been characterized as EPEC. According the Mouenuddin et al. (1989), who studied data and analyzed samples submitted to the United States Center for Disease Control (CDC) for 50 outbreaks of diarrheal disease in American infants between the years of 1934 and 1987, EPEC strains accounted for 56% of these disease outbreaks. Additionally, they found that 64% of these EPEC strains were resistant to multiple antibiotics (Mouenuddin et al., 1989). Thus, it is quite clear that EPEC strains of *E. coli* are prevalent amongst cases of outbreak and may be difficult to treat due to resistance to typical drug therapy that might be used on affected patients. Because of this, these strains of *E. coli* are good candidates for our study concerning antimicrobial peptide (AMP) treatment, since AMPs such as cecropin P1 used in our research completely lyse the cells and bacteria can develop no resistance to them.

In addition to EPEC strains, enterohemorrhagic *E. coli* (EHEC) strains can commonly cause disease outbreaks. EHEC strains are often even more dangerous than EPEC because they can cause internal hemorrhaging of the intestinal lining (Miller et al., 1998). Six out of the eleven strains used in our experiments with cecropin P1 are categorized as EHEC, specifically O26:K60:H11, O55:H7, O113:H21, O117:K98:H4, O157:H7, and O172:K-. Since *E. coli* O157:H7 is so widely found in outbreak samples, it is defined by the CDC as an emerging pathogen, or "an infectious agent whose incidence in humans has increased dramatically within the past 20 years or one that has the probability of increasing in the future" (CDC, 1994). *E. coli* O157:H7 is so dangerous because it possesses "hypermutable genetic sequences," so the bacteria can vary and diversify

greatly even within a single population, and possibly become resistant to antibiotics used to treat it (Miller et al., 1998). Furthermore, since O157:H7 is naturally found in the acidic fore-stomachs of cattle where fermentation occurs, it can withstand acidic environments, thrive on acidic foods, and can produce Shiga-like toxin which is extremely dangerous to those infected (Miller et al., 1998). As is quite evident, EHEC strains such as O157:H7 are often the culprits of widespread *E. coli* outbreaks and are capable of antibiotic resistance, and therefore valid candidates for AMP and cecropin P1 treatment.

Strains of *E. coli* can also be classified as verotoxin producing *Escherichia coli* (VTEC). VTEC strains are considered to be major causes of disease, especially in developing countries, as they result in contamination of food and are a food-borne illness (Stephan et al., 2000). Three of the strains used in this project can be classified as VTEC: O113:H4, O113:H21 and O157:H7 (the latter two are also EHEC strains). VTEC strains are very harmful to people and can lead to watery or bloody diarrhea, hemorrhagic colitis, thrombotic-thrombocytopenic purpura (a rare blood clotting disorder) and haemolytic-uraemic syndrome (HUS) (Stephan et al., 2000). In research done on VTEC strains by Stephen et al., the researches found that those exposed to an environment more prone to VTEC strains were more likely to be carriers of the bacteria. The research showed that 6% of a Canadian farming family were VTEC carriers where as 9% of slaughter house workers were carriers of the a VTEC strain (Stephan et al., 2000).

2.1.4 Cellular Structure

In order to better understand the reasons why certain strains of *E. coli* are pathogenic and can cause illness in humans, it is important to understand the cellular structure of *E. coli*. Several molecules of the *E. coli* cell wall are believed to play a role in pathogenic activity of certain strains and also the interactions between these strains and AMPs, specifically the cell wall or membrane, lipopolysaccharide, fimbriae, and pili.

2.1.4.1 Cell Wall and Cell Membrane

Due to their size, *E. coli*, like many prokaryotes, do not have the ability to engulf particulate matter for nourishment. Instead, the bacteria are dependent on the diffusion of solutes across their boundary layer. This is accomplished by ensuring that there is efficient diffusion of nutrients and waste by having a high surface area to volume ratio (Beveridge and Graham, 1991). The boundary layer of the bacterial cell is an important component in the survival of the bacteria and makes up a large portion of the cell's mass.

The cell wall is the prime stress bearing structure that resides above the plasma membrane (Beveridge and Graham, 1991). Gram-positive and Gram-negative are the two different classifications of bacterial cell wall formations. The outer layer of the Gram-negative bacteria cell, known as the outer membrane, surrounds the peptidoglycan layer, which surrounds the periplasm layer. These three layers are called the cell wall. The plasma membrane and the cell wall are what constitute the makeup of Gram-negative bacteria (Beveridge, 1999). In contrast, Gram-positive bacteria contain only one lipid bilayer, the plasma membrane (Beveridge and Graham, 1991). Figure 1 is a simplified

visual explanation of the difference between Gram-positive and Gram-negative bacteria structures.

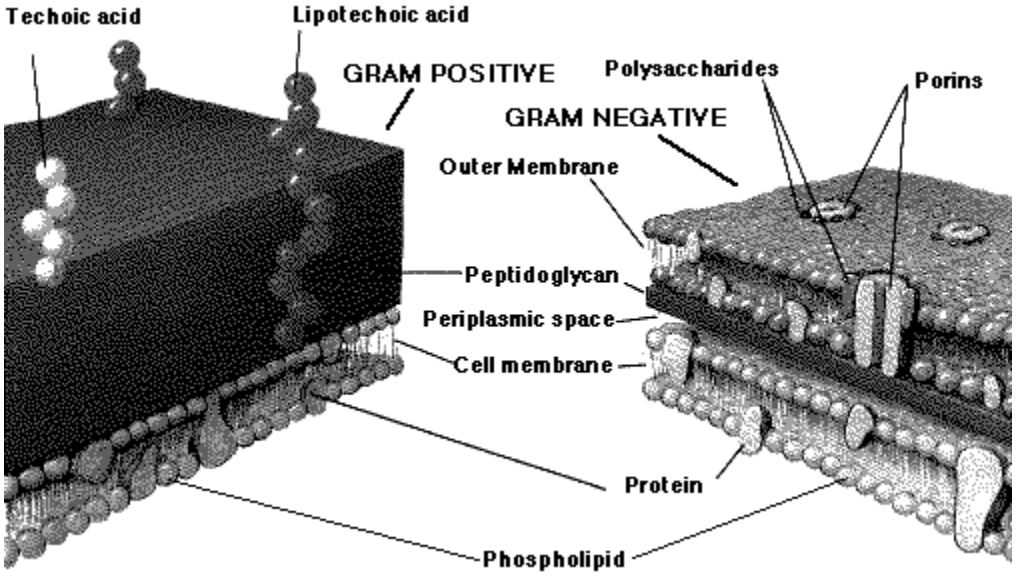

Figure 1: A simplified version of the difference between Gram-positive bacteria (left) and Gram-negative bacteria (right) (http://filebox.vt.edu/users/chagedor/biol_4684/Methods/bacterial.gif).

The cell walls Gram-negative bacteria are more intricate than those of Gram-positive bacteria.

In addition, only Gram-negative bacteria possess outer membrane vesicles, which are extrusions from the surface that entrap part of the periplasm layer, which can be discharged from the surface of the cell during bacterial growth (Beveridge, 1999). Furthermore, the turgor pressure for Gram-negative cells can range from 2 to 5 atm (210 to 252 kPa), but is 5 to 10 times higher for Gram-positive cells (Beveridge and Graham, 1991)

2.1.4.2 Lipopolysaccharide (LPS)

This project will be studying the binding potential of antimicrobial peptides (AMPs) to various strains of *E. coli*. While the possible mechanism of this binding will be discussed later, it is important to understand the role of the lipopolysaccharide (LPS) on bacteria behavior. The LPS is divided into three regions; the O-antigen, the core (outer and inner), and lipid A (Epand et al., 1999), as shown in Figure 2.

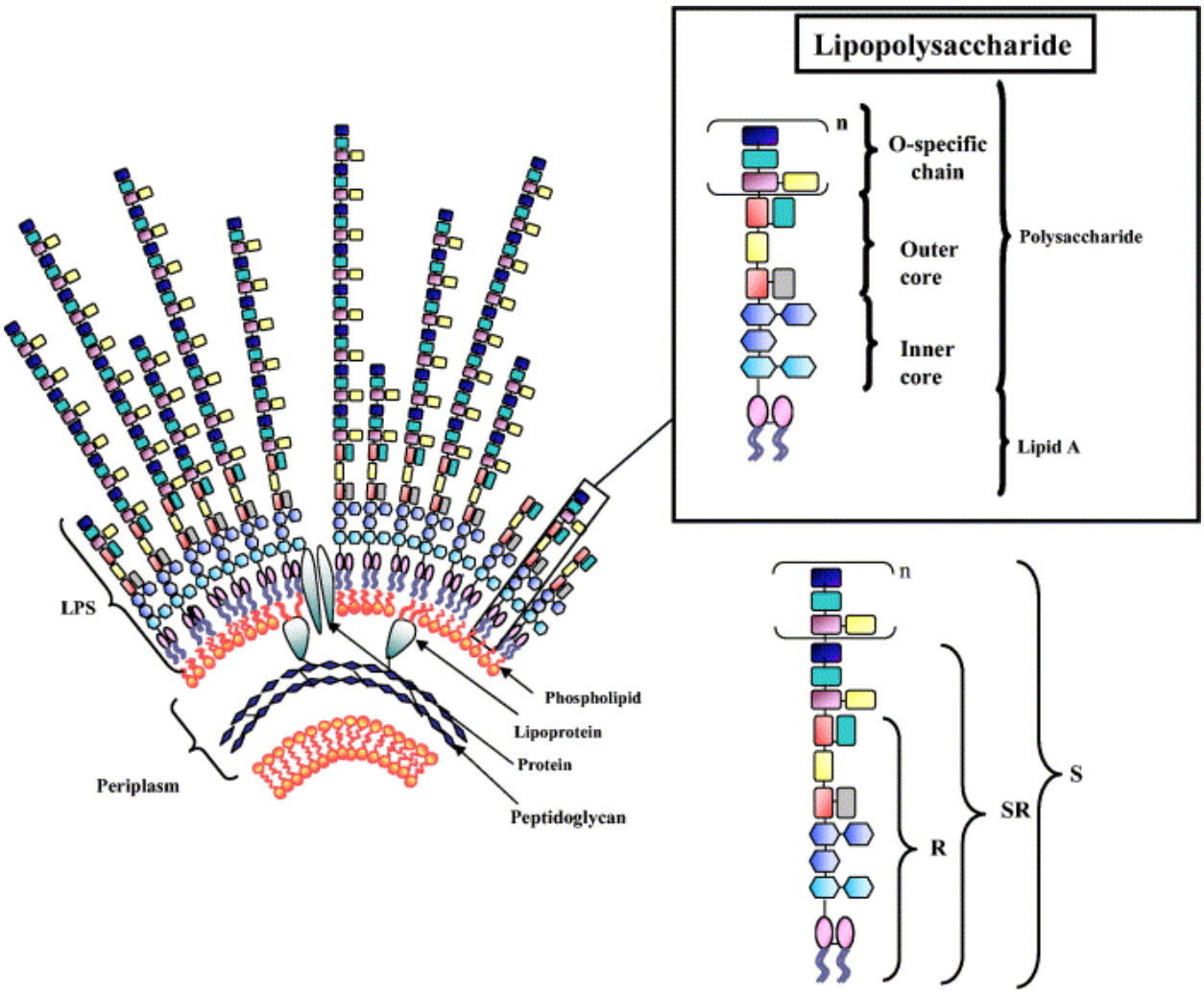

Figure 2: Representation of the three different regions of the LPS structure. R, SR and S refer to the LPS structure as being Rough-type, Semi-rough type and Smooth-type (Epand et al., 1999)**.**

Both the O-antigen and the core regions are made up of polysaccharide chains, whereas lipid A is primarily made up of fatty acids and phosphate groups that are bonded to a carbohydrate backbone. The charge on the lipid A molecules is negative which makes the Gram-negative bacteria likely to bind to cationic peptides (Epand et al., 1999). It would then make sense to hypothesize that the charged interaction at this outer membrane of the bacteria plays a role in the binding and potentially deactivation of the bacteria.

The chart below can be used to explain the difference between the smooth, semi-rough and rough classification of the LPS structure:

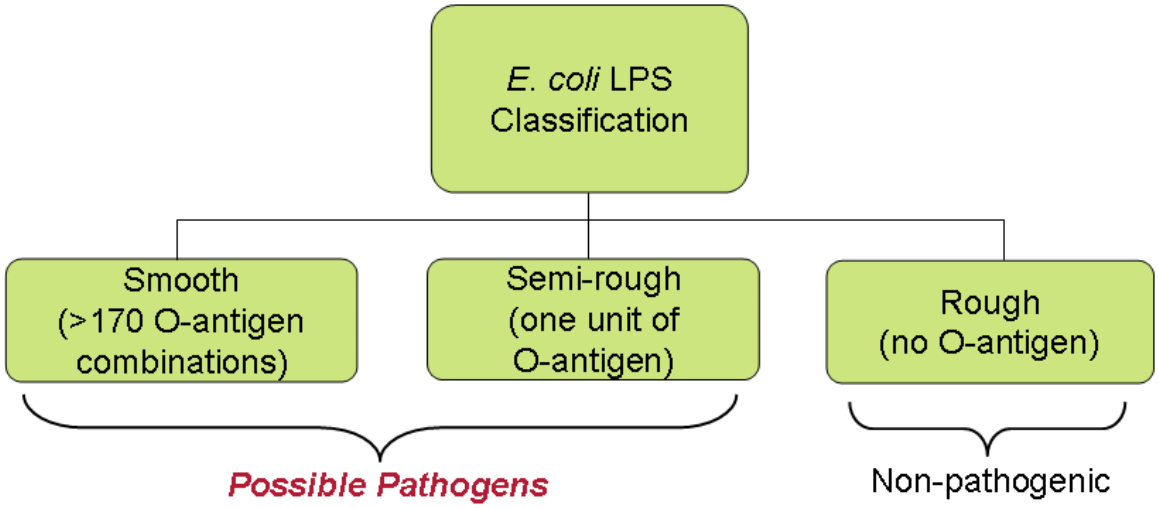

Figure 3: Organizational chart explaining the classification of *E. coli* bacteria using the O-antigen unit of the LPS.

Smooth LPS structures have multiple O-antigen combinations, semi-roughstrains have one unit of O-antigen, and rough strains have no O-antigens. Bacteria with smooth or semi-rough LPS structures can be pathogenic, while rough LPS structures are found in non-pathogenic laboratory strains.

2.1.4.3 Fimbriae and Pili

Since this project is studying the binding potential of various strains of *E. coli* with cecropin P1, it is worth noting the pili (fimbriae) are believed to be the major structure that causes bacterial adhesion. Fimbriae, which are also referred to as pili, are rigid, straight, filamentous motility appendages found on the surface of certain bacteria and are generally between 4 and 7 nm in diameter and between 0.2 and 20 mm in length (An and Friedman, 1998). Therefore, these appendages are much longer than they are wide. It is believed that the fimbriae will be responsible for binding to the cecropin coated gold surface of the crystals.

2.2 Antimicrobial Peptides

Antimicrobial peptides (AMPs) are one method of defense against pathogens (such as *E. coli*) that are found in organisms including humans, other mammals, amphibians, insects, and plants. As Reddy et al. (2004) explain, most AMPs share several common properties such as a net positive charge or net negative charge, hydrophobicity, an active membrane, and are less than 10kDa in size. However, there are also many differences between AMPs that can be used to classify these peptides.

2.2.1 Derivations

Since they were first discovered, AMPs have been isolated from many species of plants and animals, serving as natural defense agents against microorganisms. In 1981, Bozman and his colleagues isolated and characterized the first AMP, known as cecropin, from the pupae of the moth *Hyalophora cecropia* (Bulet et al., 1999). Following this discovery, researchers isolated many of the first AMPs from other insect samples. AMPs from

insects are typically grouped into three categories; peptides with intramolecular disulfide bonds forming hairpin-like β-sheets or α-helical-β-sheet mixed structures, peptides forming amphipathic α-helices and peptides with an overrepresentation in proline and/or glycine residues. Thanatin, which is an antimicrobial peptide derived from the bug *Podisus maculiventris*, is an example of this first category and it contains cysteine residues that a part of the disulfide bridge. The second set of insect AMPS are usually proline rich, like abaecin, which is found in the honeybee *Apis mellifera*. An example of the last category for insect AMPs is diptericin from the black blowfly *P. terranovae*, which is gyceine-rich (Bulet et al., 1999).

Currently, the most promise for AMP use in replacement of traditional drug therapy exists with AMPs derived from domesticated animals. Domesticated animals such as cattle, sheep, goats, pigs, horses, and poultry are the source of nearly 50 AMPs that have been recently isolated, which can be viewed in Table 1 (Brogden et al., 2003). These AMPs serve as a natural defense against microorganisms occurring in the wild, and are often found in bone marrow cells, such as polymorhponuclear leukocytes; white blood cells, specifically macrophages; and in the mucosal epithelial cells of the intestinal tract and respiratory system (Brogden et al., 2003). In bone marrow and white blood cells, AMPs may act in conjunction with antibodies to counteract microorganisms that could infect the animal. In the respiratory system and digestive tract, the AMPs provide a barrier against any microorganisms that might be breathed in or consumed. Cecropin P1 is found naturally in the mucosal epithelial cells of the small intestine of pigs (Brogden et al., 2003).

Table 1: Antimicrobial peptides found in animals (Brogden et al., 2003).

Animal species	Peptide	Tissue/cell type
Cattle	Anionic peptides	
	BNBD-1–3, 6–11, 13	neutrophils
	BNBD-4	bone marrow, distal small intestine, trachea, lung, spleen, colon, bovine alveolar macrophages
	BNBD-5	bovine alveolar macrophages
	BNBD-12	bone marrow, distal small intestine, trachea, colon
	TAP	nasal epithelium, trachea, bronchioles, alveolar macrophages
	LAP	alveolar macrophages, tongue
	EBD	alveolar macrophages, intestine
	BMAP27	bone marrow myeloid cells
	BMAP28	bone marrow myeloid cells
	BMAP34	neutrophils, bone marrow myeloid cells, spleen, testis
	Bac5, Bac7	neutrophils
	Indolicidin	neutrophils
	Dodecapeptide	neutrophils
Sheep	Anionic peptides	turbinates, trachea, pulmonary tissue, liver, small intestine
	Sheep BD-1	tongue, trachea, rumen, reticulum, omasum, colon
	Sheep BD-2	ileum, colon
	SMAP28	neutrophils
	SMAP29	bone marrow myeloid cells
	SMAP34	bone marrow myeloid cells
	OaBac5α, β	neutrophils
	OaBac6	sheep genomic library
	OaBac7.5	bone marrow myeloid cells
	OaBac11	sheep genomic library
	Dodecapeptide	bone marrow myeloid cells
Goats	Goat BD-1	tongue, respiratory tract
	Goat BD-2	intestine
	ChBac5	neutrophils
Pigs	Porcine BD-1	respiratory tract, digestive tract, thymus, spleen, lymph node, brain, liver, kidney, urinary bladder, testis, skin, heart, muscle, bone marrow, neutrophils, alveolar macrophages, umbilical cord
	PMAP23	bone marrow myeloid cells
	PMAP36	bone marrow myeloid cells
	PMAP37	bone marrow myeloid cells
	PR-39	intestinal epithelium, neutrophils
	βPR-39	porcine liver genomic library
	Cecropin P1	small intestine
	Prophenin-1, 2	leukocytes
	Protegrin 1-5	leukocytes
Horses	eNAP-1	neutrophils
	eCATH-1, eCATH-2, eCATH-3	neutrophils
Poultry	Gal 1/CHP1	heterophils
	Gal 1α/CHP2	heterophils
	Gal 2	heterophils
	Gal 3	tongue, bursa of Fabricius trachea, skin, oesophagus, air sacs, large intestine, kidney
	THP 1	heterophils
	THP 2	heterophils
	THP 3	heterophils
	GPV-1	

Many AMPs derived from domestic animal are the basis upon which synthetic AMPs are being manufactured (Brogden et al., 2003). Additionally, research is being conducted concerning methods to trigger production of AMPs within animal subjects, either for humans to consume directly as food products, such as milk or meat, or so the AMPs can be isolated and administered as treatment separately (Brogden et al., 2003). Finally, not only do these domestic animals serve as a source of AMPs, but also act as models concerning how mammalian systems may react to AMP therapy. One study infected lambs with acute pneumonia and treated the lambs in vivo with the AMP SMAP29 derived from sheep bone marrow, which is cationic and has an α-helical shape similar to cecropin-P1. Researchers found that lung tissue of the lambs treated with SMAP29 contained a much lower concentration of bacteria than untreated lambs (Brogden et al., 2003). Thus, AMPs derived from domestic animals are a very practical source of the peptides and also show considerable promise for applications to medical treatment for humans.

2.2.2 Structure and Characteristics of AMPs

Although all AMPs have essentially the same purpose of acting as a defensive agent against micriobial infection, each AMP is unique in its structure and effectiveness. Because of this, and since so many AMPs have been already been isolated while more are constantly discovered, researchers have developed several categories for these specialized peptides.

2.2.2.1 Cationic AMPs

Cationic AMPs, or AMPs with a net positive charge, are much more commonly found than anionic AMPs, particularly in domestic animals. Since so many cationic AMPs have

been isolated, a number of classification systems have been proposed by researchers studying the nuclear magnetic resonance (NMR) structures of the peptides, but most of the systems have similar main groups. For example, Reddy et al. (2004) classify the AMPs into five groups: (1) α-Helical AMPs, (2) cysteine rich AMPs, (3) β-Sheet AMPs, (4) AMPs rich in regular amino acids, and (5) AMPs with rare modified amino acids. Brogden et al. (2003) similarly list linear, amphipathic α-helical peptides as a main group, but group cysteine-rich and β-sheet AMPs together and have a separate group for praline-rich linear peptides. In either case, AMPs are generally categorized by their secondary structure, particularly α-helices or β-sheets, and amino acids common in the AMP's sequence.

An example of an α-helical AMP is cecropin P1, which is the AMP used in the experiments disucssed in this report. The structure and effectiveness of cecropin P1 will be discussed in the following section. Cysteine rich AMPs contain many cysteine residues and can be found in many organisms, including humans. Similarly, praline rich AMPs contain multiple praline residues in the peptide sequence. β-Sheet AMPs form a single β-hairpin structure and usually contain disulfide bonds. Horseshoe crab peptides, tachyplesins and polyphemusin II are examples of β-Sheet AMPs. AMPs that are rich in regular amino acids contain a large number of regular amino acids. Histatin (which is a peptide found in human saliva) is an example of an AMP that is rich in regular amino acids. The last classification of AMPs is those with rare modified amino acids. An example of this would be Nisin, which is a protein produced by the bacteria *Lactococcus lactis* as a defensive agent against other types of bacteria (Reddy et al., 2003).

Additionally, Epand et al. (1999) defined categories for AMPs with thio-ether rings and peptaibols. Peptides with thio-ether rings contain a small ring-like structure that is enclosed by a thio-ether bond, while peptaibols have a high amount of α-amino-isobutyric acid (Aib) residues.

2.2.2.2 Anionic AMPs

Anionic AMPs are defined as AMPs with a net negative charge. Although less common than cationic AMPs, which have a net positive charge, anionic AMPs have also been shown to be effective against various microbes. Specifically, in 1992 researchers found an anionic AMP, ovine pulmonary surfactant, to be effective against the bacteria *Mennheimia haemolytica, Escherichia coli,* and *Klebsiella pneumonaie* (Brogden et al., 2003). Anionic AMPs have also been found in samples of cattle bronchoalveolar lavage fluid in neonatal calves (Brogden et al., 2003). In these animals, it is believed that a number of anionic AMPs have a "regulatory role in pulmonary metabolism… via negative feedback inhibition" (Brogden et al., 2003).

Although the mechanism for anionic AMP activity is not as clear as that for cationic AMPs, it is theorized that the zinc which activates the anionic AMPs forms a cationic salt bridge across the cell membrane (Brogden et al., 2003). This salt bridge allows the AMPs to pass through the membranes of the bacteria and into the cytoplasm, where they interrupt protein formation by possibly attaching to the ribosomes (Brogden et al., 2003).

2.2.2.3 Insect-derived AMPs

There are also many peptides derived from insects. Therfore, AMPs derived from insects are often classified separately. Bulet et al. (1999) divided the peptides from insects into three categories: cysteine-containing peptides (such as insect defensins, drosomycin and thanatin), proline-rich peptides with emphasis on the O-glycosylated antimicrobial peptides (like drosocin, lebocins and formaecins), and glycine-rich molecules (gloverins) (Bulet et al., 1999).

2.2.3 Cecropin P1

As stated previously, cecropin P1 was originally isolated from pig small intestine and is categorized as a linear, amphipathic, α-helical AMP.

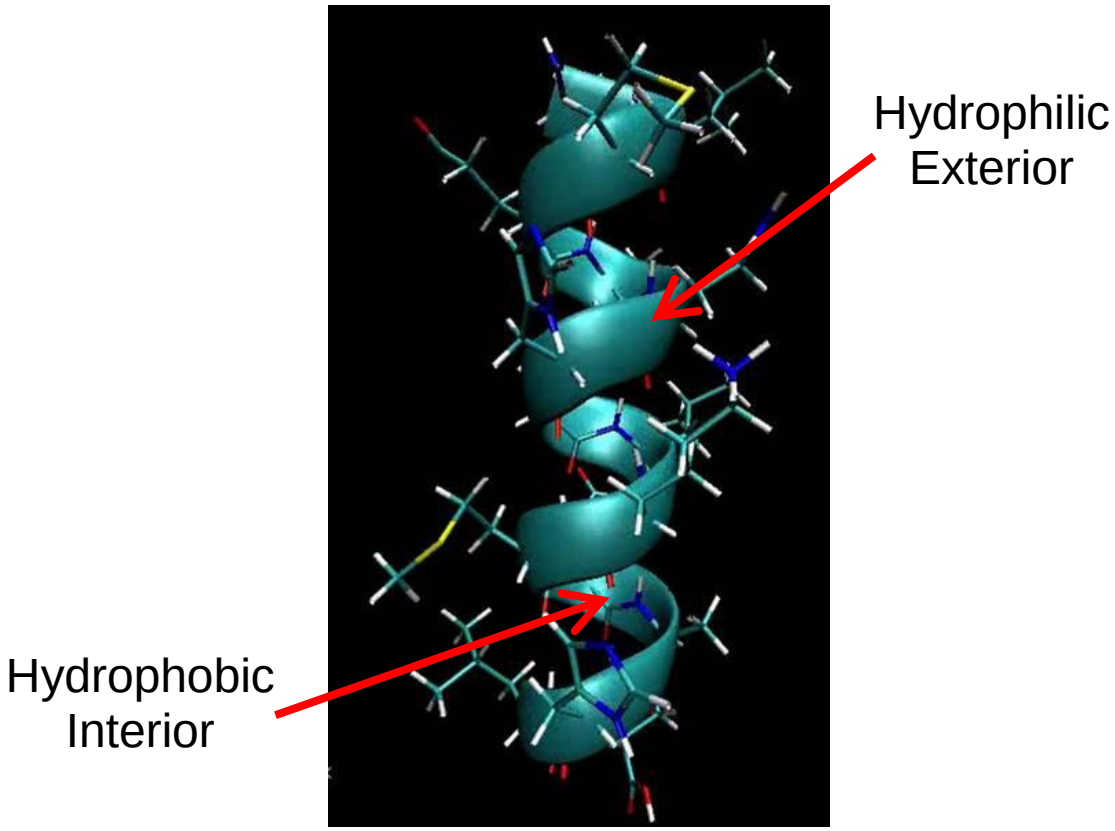

Figure 4: Alpha helix structure as seen in the AMP cecropin P1 (http://www.csusm.edu/jayasinghe/MoviesAminations/files/page34-1000-thumb.jpg).

The α-helix is arranged with hydrophobic amino acids on the inside and hydrophilic amino acids on the outside of the structure, and it is believed that this amphipathic helix is what allows the AMP to pass through the bacterial membranes (Brogden et al., 2003). Cecropin P1 also possesses a Ser-Glu-Gly sequence which is believed to act as a hinge-like mechanism to help the AMP come in contact with microorganisms (Brogden et al., 2003). Furthermore, cecropin P1 has a basic N-terminus and a hydrophobic C-terminus, the carboxyl group of which is believed to be the main cause of its high effectiveness against Gram negative bacteria such as *E. coli* (Brogden et al., 2003). According to Reddy et al. (2004), cecropin P1 is active against many parasites in addition to bacteria.

Additionally,cecropin P1 has potent and rapid antibacterial activity (Brogden et al., 2003). Cecropin P1's swift action against bacteria was shown by Bomen et al. (1993), who compared the activity of cecropin P1 and PR-39 on three different strains of *E.* coli. Both cecropin P1 and PR-39 are AMPs found in the upper small intestine of pigs and both are most effective against Gram negative bacteria, such as *E. coli*, and also effective against some Gram positive bacteria. Bomen et al. (1993) found that cecropin P1 completely lysed the bacteria instantaneously, while PR-39 experienced an eight minute lag time before it affected the bacteria and only caused the cells to swell, not completely lyse. It has been shown that cecropins, including cecropin P1, form channels with their amphipathic α-helices as stated previously, which are believed to be the reason cecropin P1 was found to penetrate both the inner and the outer membranes of the *E. coli* (Bomen et al., 1993). Furthermore, this study found that cecropin P1 was not only more effective than the other AMP tested, PR-39, but was also more effective than treatment using a

traditional antibiotic, tetracycline (Bomen et al., 1993). This study showed that cecropin P1 is a fast-acting AMP and was highly effective against *E. coli*, a major cause of food-related illness in the United States.

Although the preliminary studies on AMP inactivation of *E.* coli were useful, no one has directly proven the binding between *E. coli* and AMPs directly. Bomen et al. (1993) applied the AMP solution to a well in a media plate seeded with *E. coli* so the AMPs could dissolve through the agar. However, in our study we are employing a novel technique of binding cecropin P1 with an added cysteine group to a gold crystal using a quartz crystal microbalance with dissipation (QCM-D). This technique allows us to study how site-bound AMPs interact with bacteria, specifically several strains of *E. coli*, not just how AMPs behave in solution.

2.3 AMP and Bacterial Interactions

Not all strains of bacteria will readily bind to AMPs. One study found that some AMPs are active against one bacterial strain, but not against others (Hancock et al., 2000). As discussed earlier in the *E. coli* overview section, the major component of the outer membrane of Gram-negative bacteria is the LPS. Studies by Rosenfeld et al. (2006) showed that in order to promote bacteria binding and death, the AMPs have to pass through the outer membrane and reach the inner phospholipid layer where the binding and deactivation can occur.

2.3.1 How and Why AMPs Attack Bacterial Membranes

While a substantial amount is known about bacteria and AMPs, there has not been much research into the interactions between the two and therefore the mechanisms of their interaction are not well understood.

Rosenfeld et al. (2006) found no correlation between the AMP's antimicrobial activity and its ability to specifically bind to the LPS of the bacterial membrane. However, a correlation can be made between AMP activity and other bacteria characteristics. For example, research by Epand et al. (1999) concluded that peptides have an affinity for binding to membrane lipids and that, in many cases, the magnitude of this binding is believed to be affected by the positive charge on the peptide interacting with the anionic lipid of the bacteria. In the case of cecropin P1, the net positive charge is caused by basic amino acids along the outer, hydrophilic face of the α-helix (Shai, 1999). Furthermore, Shai (1999) explains that this net positive charge of cationic AMPs not only causes its affinity for binding to negatively-charged bacterial membranes, but also prevents them from attacking normal, zwitterionic mammalian cells, making them ideal for human medical applications.

Since bacteria cannot change the charge on their outer membrane in the same way that they can mutate their DNA, bacteria and other microbes cannot become resistant to the defense provided by AMPs. This is very important when considering medical applications, since many strains of bacteria have become resistant to commonly used drug treatments because of overuse of antibiotic medications. However, since bacteria are completely lysed by AMPs effective against the given strain and even mutations cannot

change their fundamental membrane structure, there is no chance for resistance against AMPs to occur. These characteristics indicate that AMPs could possibly be used as a weapon against dangerous drug-resistant bacteria.

2.3.2 Models for Attack

No single mechanism can explain all AMP and bacterial interactions, and it is possible that there are numerous modes of action for different peptides and bacteria strains. One theory propsed is that the peptide attacks the lipid bilayer of the bacterial membrane. Also, charge may be a contributing factor. For example, most peptides are cationic and in Gram-negative bacteria, such as *E. coli*, the outer membrane contains anionic molecules (Epand et al., 1999). This is one possible explanation as to why some AMPs seem to have an affinity for binding to bacteria. However, a conclusion has been reached regarding how the peptides penetrate the membrane.

In a study by Rosenfeld et al. (2006), the authors refer to two previously suggested mechanisms for the AMP-LPS interaction. The first possible mechanism to explain the AMP attack on bacterial membranes is that the peptides directly bind to the LPS, making the LPS unavailable to the LPS binding protein and therefore the LPS is unable to the transfer to its primary receptor (Scott et al., 2000). The second possible mechanism is that the peptide binds directly to the primary receptor which prevents the LPS from binding to the receptor (Scott et al., 2000).

Research by Vunnam et al. (1997) was conducted on the effect that chirality of the peptide has on its binding activity. However, this research showed no chiral selectivity with *E. coli*.

2.3.2.1 Carpet Model

There are two models used to explain the binding of AMPs: the Carpet Model and the Barrel Stave Model. Below is Figure 4 from Reddy et al. (2004) which illustrates the Carpet Model as a possible mechanism for AMP and bacteria interaction:

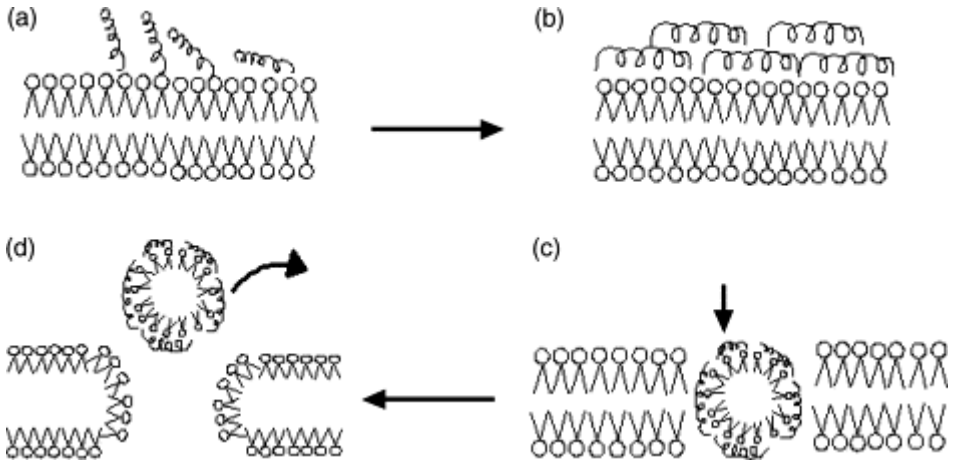

Figure 5: Carpet Model of AMP activity against bacteria (Reddy et al., 2004).

As Reddy et al. (2004) explain, first the peptide monomers bind to the phospholipid head groups (a). Next, the peptide monomers align on the membrane surface so that the hydrophilic residues face the phospholipid head group (b). Then the peptides face the hydrophobic core of the membrane (c) before disintegration of the membrane occurs (d). However, in order for the disruption of the membrane to occur, the peptide must reach relatively high concentrations at certain areas of the membrane to form the micelles (Shai, 1999). If the peptide does not reach the minimum inhibitory concentration (MIC),

then the AMP will only disrupt ion concentrations within the cell, but not directly cause the cell to lyse (Shai, 1999).

2.3.2.2 Barrel Stave Model

The Barrel Stave model is the second model that can be used to explain the binding of AMPs. In the Barrel Stave model, the hydrophobic surfaces of the peptide face each other on the inside of the α-helix,while the hydrophillic surfaces of different AMP molecules interact with one another. Figure 5 from Reddy et al. (2004) which shows the Barrel Stave model:

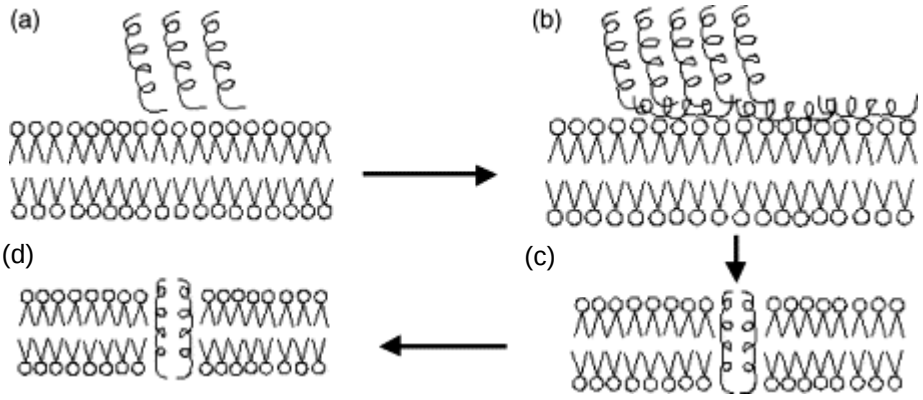

Figure 6: "Barrel-Stave" Model for AMP activity against bacteria (Reddy et al., 2004).

In this model, the peptide monomers first bind to the cell membrane in an α-helical confirmation (a). Then more peptide molecules bind to the cell membrane (b). Next, the peptide helices insert themselves into the hydrophobic core of the membrane (c) which leads to the formation of a pore through the membrane (d) (Reddy et al., 2004). This pore formation increases the membrane's permeability to large molecules, which in turn causes disruption of ion gradients, allows harmful molecules to diffuse into the cell, and

allows important molecules and cellular structures to leave the cell (Shai, 1999). Combined, all of these factors cause the cell to lyse and die.

2.4 Quartz Crystal Microbalance with Dissipation (QCM-D)

The quartz crystal microbalance with dissipation (QCM-D) is a relatively new technology, receiving its patent as recently as 1996. The QCM-D is based on the quartz crystal microbalance (QCM), which was first developed in 1921 and first used with a liquid substrate in 1980 (Rodahl et al., 1997). The QCM has increasingly been used by researchers to monitor the formation of biofilms (Fredriksson et al., 1998; Otto et al., 1999; Schofield et al., 2007) and adsorption of proteins (Höök et al., 1998) and other biomolecules (Jenkins et al., 2004; Kwon et al., 2006; Carter et al., 1995). These researchers needed an instrument that could also measure dissipation so they could more accurately interpret results when the Sauerbrey relation was not valid, and thus the QCM-D was developed. The following section discusses how the QCM-D operates, the theories needed to interpret its data output, and previous research using the QCM and QCM-D.

2.4.1 How the QCM-D Works

The QCM and QCM-D work by using a piezoelectric crystal oscillator which shuts on and off as a liquid solution is running through the chamber containing the crystal. This allows the instrument to determine the decay of the frequency (Δf) of the crystal by measuring the voltage across electrodes on the crystal (Rodahl et al., 1997). The change in frequency the QCM or QCM-D measures is then used to calculate the mass deposited on the surface of the crystal according to the Sauerbrey relation discussed in the following section.

The QCM-D, however, also measures the change in dissipation (ΔD). The dissipation factor (D) is defined as the energy dissipated per oscillation divided by the total energy stored in the system (Q). The dissipation relates to the stiffness or rigidity of the layer deposited on the crystal, where a small ΔD indicates slow energy dissipation and a rigid film, and a large ΔD indicates rapid energy dissipation and a soft film (Q-Sense, Inc., 2007). Dissipation is important to record, particularly for QCM-D experiments using biomolecules, because if ΔD is larger, the layer is less rigid and the Sauerbrey relation is not applicable. Thus, the D factor is relevant for four reasons: to verify the validity of the Sauerbrey relation, monitor swelling/hydration, viscoelastic modeling and for insight into structural changes (Q-Sense, Inc., 2007).

All experiments reported in this paper were conducted using the Q-Sense (Gothenburg, Sweden) Model E-4 QCM-D equipped with gold crystals that measured 14 mm in diameter and had a resonance frequency of 5 MHz.

2.4.2 Theory of the QCM-D

The theory of the QCM-D is described by the Sauerbrey equation (1) shown below,

$$\Delta m = -\frac{C}{n}\Delta f \qquad (1)$$

where Δm is the adsorbed mass on the crystal, C is the mass sensitivity constant, n is the overtone number and Δf is the change in frequency (Sauerbrey, 1959). Essentially, the Sauerbrey equation states that the change in mass on the surface is directly proportional

to the change in frequency of the oscillating crystal multiplied by negative one. Thus, a negative change frequency would indicate an increase in the mass deposited on the crystal surface and vice versa (Kwon et al., 2006).

Additionally, the dissipation factor (D) discussed previously is mathematically expressed as,

$$D = \frac{1}{Q} \tag{2}$$

which is defined as the energy dissipated per oscillation divided by 2π times the total energy stored in the system (Q-Sense, Inc., 2007). This dissipation factor can also be understood as the sum of all energy losses of the system. Therefore, a higher D would indicate more energy lost by the system and a soft film, which a lower D would indicate less energy lost by the system and a relatively rigid film deposited on the crystal surface. It is very important that this dissipation factor is recorded along with the frequency because the Sauerbrey relation is not always valid, particularly for the deposition of cells or other biomolecules. According to Höök et al (1998), the Sauerbrey relation is often not valid for these biological applications because cell or biomolecule layers aren't rigid, may trap liquid between their molecules, and may slip on the electrode surface as it oscillates. All of these conditions may cause a dissipation of energy not taken into account by the Sauerbrey relation.

These two relationships are the basis for interpreting the data obtained from the QCM-D and will be important in understanding the results and discussion portion of this paper.

2.4.3 Relevant Research Using the QCM and QCM-D

Although QCM-D is relatively new, researchers have quickly adopted the technology due to its extreme sensitivity in the range (Jenkins et al, 2004). Thus, the QCM-D is easily applicable as a biosensor, whether this is to detect cells or other biomolecules. Recently, the QCM-D has been used to better understand the stages of cell adhesion to a surface and biofilm formation. QCM-D has also been utilized in research concerning adsorption of biomolecules such as starches, biopolymers, proteins, and antibodies (Jenkins et al, 2004).

2.4.3.1 Cell Adhesion and Biofilm Formation

QCM and QCM-D can be used to study cellular adhesion to surfaces. These techniques are particularly useful for this application because adhesion can be measured without disturbing the cells system (Otto et al., 1999). Fredricksson et al. (1998) studied how effectively the QCM could measure the *E.coli* cellular adhesion to the surface of the gold crystal. At this time, it was known that the QCM could detect the adhesion of 10^5 or 10^6 cells to the crystal surface, but Fredricksson et al. (1998) wanted to determine whether the QCM was sensitive enough to detect adhesion of a very small number of cells. For each experiment, between 70 and 80 monkey kidney eptithelial (MKE) cells or Chinese hamster ovary (CHO) cells were attached to either hydrophilic or hydrophobic surfaces, and both the frequency and dissipation changes were measured. Since the Sauerbrey relation is only valid when the surface is covered by an evenly distributed monolayer, and the small number of cells used in this study did not constitute a monolayer, the researches recognized that it was important to monitor the dissipation of the system. By plotting the change in frequency (Δf) and the change in dissipation (ΔD) in relation to each other, they

were able to determine that the QCM was not only able to detect the cells adhering to the surface, but was also able to detect differences in binding between cell types and surface types.

The QCM-D has also been an integral part of research concerning the phases of cell adhesion at a liquid-solid interface. Otto et al. (1999) researched whether the two main theories used to explain bacterial adhesion, DLVO theory and thermodynamics, were accurate when compared to experimental results. DLVO theory, which stands for the names of its creators Derjaguin, Landau, Verwey and Overbeek, describes intermolecular forces as a function of the separation distance between the cell and the surface, in terms of the balance between van der Waals forces and repulsive electrostatic interactions (Otto et al., 1999). Although DLVO theory is accurate at low ionic strengths, body fluids and environmental systems often exhibit higher ionic strengths, where it is much more difficult to predict cell-surface interactions. Meanwhile, the thermodynamic model considers the balance between the interfacial free energies of the surfaces and media (Otto et al., 1999). To determine whether these theories accurately predicted cell adhesion behavior experimental results, Otto et al. (1999) studied the frequency and dissipation changes observed when fimbriated and non-fimbriated *E. coli* strains were adsorbed to surfaces of varying hydophicities and ionic strengths. The cells bound more favorably with increasing media ionic strength between 0.06M and 0.1225M, but adsorption decreased at higher values of ionic strength (Otto et al., 1999). Further, more cells attached to the hydrophilic portions of the hydrophobicity gradient on the crystal surface and the effect of the hydrophobicity was more pronounced (Otto et al., 1999).

Finally, using D/*f* plots, the researchers were able to propose five phases of cell adhesion detected by the QCM-D: (1) cell binding, or initial cell contact with the surface; (2) secretion of microexudates, proteins that aid adhesion; (3) spreading of the cell surface, causing increased contact area; (4) Modification of adhesion properties, such as strength of adhesion; and (5) changes in the rigidity of the cytoskeleton, which causes change in dissipation (Otto et al., 1999).

The effectiveness of the QCM-D as a means of studying cell adhesion has been well-documented in preliminary studies, but this work is still in the early stages. Few researched to date have used QCM-D to investigate microbial biofilms. Biofilms are attached communities of microbes that form on medical implant devices, in the environment, or even in industrial settings. As stated previously, the QCM-D provides the ability to monitor the formation of these biofilms at a solid-liquid interface without disturbing the system. Schofield et al. (2007) used the QCM-D to monitor the biofilm formation of *Streptococcus mutans*, bacteria often found as a biofilm in dental plaque, on gold crystals under both continuous flow and "attach and flow" conditions. For continuous flow conditions, they passed *S. mutans* cells continuously through the QCM-D chamber for 120 minutes, but for "attach and flow" conditions, they pumped *S. mutans* for 20 minutes and then turned the pump off for 120 minutes to allow cells to attach via passive diffusion (Schofield et al., 2007). Growth media was passed through flow chamber overnight for both flow conditions (Schofield et al., 2007). Biofilms formed under continuous flow systems were more dissipative per unit mass, meaning that they experienced a greater change in dissipation per frequency change, and thus were more

complex than the “attach and flow” biofilms. Also, there was a greater increase in frequency when the “attach and flow” biofilms were rinsed with water, which indicates that more cells washed away, and therefore continuous flow biofilms were more stable (Schofield et al., 2007). As this study demonstrates, the frequency and dissipation measurements taken by the QCM-D can potentially provide useful qualitative data to better understand the process of bacterial biofilm formation.

2.4.3.2 Biomolecule Adsorption

The QCM is useful for detecting biomolecule adsorption and for studying degradation of biomolecules deposited to the crystal surface. Jenkins et al. (2004) used QCM to detect the biodegradation of starch due to *Bacillus subtilis* bacteria. Previously, carbon dioxide meters had been used to measure the biodegradability of biopolymers such as starch, but they were not sensitive enough to pick up very small mass changes in the beginning of the degradation process (Jenkins et al., 2004). Using QCM, Jenkins et al. (2004) could detect very small changes in mass on the crystal surface. They first applied and dried the starch to the crystal surface, and then deposited the bacteria on the crystal by submersing the crystal in a bioreactor. The change in frequency was measured and correlated to the amount of starch remaining, assuming that an increase in frequency meant a decrease in the mass on the crystals, vice versa. The researchers suggested that the QCM might play a role in future experiments geared at investigating how organisms break down different biopolymers, thus extending the utility of this technique.

In another biopolymer study, Kwon et al. (2006) used the QCM-D to monitor the adsorption of dextran to silica and alumina surfaces. The researchers intended to use

these experiments to better understand the interactions between minerals in the environment and extracellular polymeric substances (EPS), which are biopolymers secreted by microbes to aid in adhesion, biofilm formation, and mineral binding (Kwon et al., 2006). EPS play a role in heavy metals mobilization and in the fate of chlorinated hydrocarbons in soils and aquifers. To mimic the surfaces of the minerals found in the environment, they used aluminum oxide (Al_2O_3) and silicon dioxide (SiO_2) crystals instead of the gold crystals generally used in experiments involving the adsorption of biomolecules. Since a QCM-D was used in this experiment, the frequency and the dissipation were measured, while in the previous study by Jenkins et al. (2003) only the frequency was measured by the QCM. The dextran QCM-D experiments showed that as higher concentrations of dextran were applied, there were larger changes in frequency and dissipation, indicating more mass attached to the crystal surfaces (Kwon et al., 2006). Particularly, more dextran was adsorbed to the alumina surface whereas more dextran was washed from the silica surface during rinsing, suggesting the dextran was more strongly attached to the alumina surface. Additionally, they compared the changes in dissipation to the changes in frequency ($\Delta D/\Delta f$) and found this ratio to be considerably different between alumina and silica, suggesting that dextran had altered conformation on the two substrates. Specifically, only one general trend for silica was observed in the $\Delta D/\Delta f$ plot, while there were multiple slopes for the alumina plot, suggesting differences in adsorption mechanisms and the conformation of dextran (Kwon et al., 2006). This was a ground breaking study for each surface since it showed that very subtle changes in biopolymer properties could be accurately detected.

The QCM and QCM-D have also been widely used in experiments concerning protein adsorption at solid-liquid interfaces. Höök et al. (1998) utilized the QCM to measure frequency and dissipation changes during the adsorption of four different proteins: myoglobin, hemoglobin, human serum albumin (HSA), and ferritin. They recognized the limitations of the Sauerbrey relation and the QCM which only measured frequency to biomolecule adsorption applications. In an effort to solve this problem, they researched and developed a mechanism to measure and record instantaneous dissipation much like in the modern QCM-D. Their main finding was that for all proteins deposited and adsorbed on the crystal surface, the QCM recorded a rapid initial frequency decrease, indicating a large bulk deposition, followed by a slower frequency decrease as the surface is saturated with the proteins (Höök et al., 1998). However, when the change in frequency (Δf) and the change in dissipation (ΔD) were plotted in relation to each other, the behavior varied between proteins. The D-*f* plots for hemoglobin were very simple, with one obvious trend while the plots for ferritin and HSA were much more complex. This complexity was attributed to the various stages of protein adsorption that the QCM is able to distinguish. From this study, one can conclude that by measuring both frequency and dissipation, the QCM-D is sensitive enough to differentiate between different stages of protein adsorption and differenced among proteins. Therefore, the QCM-D is an important tool to better understand the mechanisms of protein adsorption at solid-liquid interfaces and is useful for applications including the biocompatibility of implant materials and biofouling (Höök et al., 1998).

Finally, the QCM and QCM-D have been very important in better understanding the interactions between antibodies and antigens. The QCM was particularly important in research concerning the development of a short-term vaccine for *Vibrio cholera* O139. O139 is particularly virulent strain of cholera that recently appeared in India in 1992 (Carter et al., 1995). This strain has a different LPS structure than the O1 serotype commonly associated with the worldwide pandemic and possesses the same cholera toxin as the O1 strain, but much more of it, and the toxin is encoded in different chromosomal locations (Carter et al., 1995). Thus, drugs that work against the O1 serotype are not effective against O139 and those who are immune to O1 through vaccines or previous infection are not immune to O139 (Carter et al., 1995). Through their research, Carter et. al (1995) aimed to create a short-term vaccine for the dangerous O139 cholera serotype by using the QCM to differentiate between strains. They did so by adsorbing the antibody anti-*V. cholerae* O139 derived from rabbit serum, which would only bind to the O139 serotype and not the O1 serotype, to the crystal surface of the QCM and then incubating at 37°C for an hour (Carter et al., 1995). Carter et al. (1995) were able to successfully identify cholera O139, and suggested that crystals be pre-coated with the antibody so they are faster and easier to use in the field. Thus, QCM and QCM-D are not only valuable technology in research labs, but also in the field, since they are portable, easy to operate, and much faster than traditional assay techniques.

3 Methodology

3.1 Making Agar Plates

Agar plates containing the growth media Luria-Bertani (LB) agar (Sigma, St. Louis, MO) were used to culture the bacteria used in this experiment. The same procedure was followed when making plates for all eleven strains of bacteria.

First, the chosen media (for example: LB) was measured out to 35 g/L and the appropriate amount was chosen assuming approximately 20 mL per plate. A flask was filled with a small amount of MilliQ water and media was added. The remainder of the flask was filled with water and mixed on magnetic stirrer on low heat until the media was dissolved. Aluminum foil was taped over the top of the flask and placed in autoclave on setting 1 for 20 minutes. After the cycle was finished, the flask was cooled for approximately 10 minutes in the autoclave. LB media was poured into Petri dishes, ensuring that there were no bubbles, without putting arms or hands over the dish to avoid contamination. Once cooled, the top was placed on the Petri dishes and the plates were placed, inverted, in the hood overnight.

3.2 Plating Bacteria

Bacteria were maintained on agar plates, using the following protocol.

The bacteria were cultured and allowed to grow to an absorbance of 0.3 at a wavelength of 600nm. Under the hood, the plastic inoculation loop was shaken out of container, making sure not reach inside container. Next, the lid from the plate was removed

carefully, making sure not to hold hands or arms over the plate. The inoculation loop was briefly submerged in the culture broth and used to spread the bacteria on the plate. The plates were then covered with Parafilm around the edges and incubated inverted at 37°C for approximately 24 hours.

3.3 Pre-culturing Bacteria

Experiments were run with eleven different strains of bacteria. The night before a growth curve, counting chamber, or QCM-D experiment was to be conducted, the particular strain to be used was pre-cultured using the method outlined below.

First, 10 mL of LB broth was placed in a 250 mL flask and the edge of the flask was flamed both before and after and poured under the hood. Still under the hood, a plastic inoculation loop was shaken out of the container, while making sure not to reach inside container to avoid contamination. Next, the lid of the Petri dish was removed, making sure not to cross arms or hands over the opened Petri dish, to avoid contamination. A single colony was scraped off with the inoculation loop and mixed around inside the flask. The Petri dish was then covered and the pre-culture flask was allowed to incubate overnight at 37^{o}C in an agitator.

3.4 Growth Curves

Eleven different strains of *E. coli* were used in this project (Table 2).

Table 2: Source information for *E. coli* strains used, where EPEC stands for enteropathogenic *E. coli*, EHEC stands for enterohemorrhagic *E.coli*, VTEC stands for vero-toxin producing *E. coli*, and the sugar backbone type refers to the number of sugars in the lipopolysaccharide backbone .

Name of *E. coli* Strain	Sugar Backbone Type	Pathotype/Behavior	Source
HB101	n/a	n/a	American Type Culture Collection (ATCC); #33694
O26:K60:H11	3	EPEC, EHEC	Culture Collection University of Gothenburg (CCUG), Gothenburg, Sweden; 29190
O35:K-:H10	5	not as commonly found	ATCC; #23525
O55:H7	3	EPEC, EHEC	Dr. Howard Ochman, University of Arizona; ECOR #37
O113:H4	n/a	VTEC	Kim Ziebel, Health Canada
O113:H21	4	EHEC	Dr. Howard Ochman, University of Arizona; ECOR #30
O117:K98:H4	5	EHEC	CCUG, Gothenburg, Sweden; 11418
O157:H7	4	EHEC	ATCC; #43895
O157:H12	n/a	non-VTEC	Kim Ziebel, Health Canada
O157:H16	n/a	non-VTEC	Kim Ziebel, Health Canada
O172:K-:H-	5	EHEC	CCUG, Gothenburg, Sweden; 36540

The following procedure was followed to culture each of the eleven strains and to quantify bacterial growth as a function of time.

Approximately 50 mL of LB broth was poured into a 250 mL flask, sterilizing the lip of the flask both before and after pouring. 500µL of bacteria from the overnight pre-culture were then added to the flask. Next, the bacteria in the flask were incubated on setting six and 37^{o}C in the shaker bath. The absorbance was recorded every half hour until it

reached 0.25A. Then the absorbance was recorded every 10 minutes until it reached approximately 0.8A. After this point, the absorbance was recorded every 15-20 minutes until the growth slowed. Finally, the measured absorbance was plotted versus time.

3.5 Counting Bacteria

A counting chamber was used to determine the population of bacteria at various points in time during the exponential stage of growth. Samples of each strain of *E. coli* at 5 different absorbance values (ranging from approximately 0.2 to 0.9) were counted. A PBS (phosphate buffer saline) solution was used to keep cells alive, but prevent further growth. The following procedure was used to conduct counting chamber experiments.

10 mL of bacteria culture was centrifuged at approximately 4000 RPM for 10 minutes. The LB media was then removed and replaced with 10 mL of phosphate buffered saline (PBS) at pH 7.4 (Sigma, St. Louis, MO). The bacteria/PBS solution was then vortexed until the pellet in the bottom of the centrifuge was dissolved. This cleaning process was repeated three times to ensure that all growth media had been removed.

Next, the counting chamber slide was cleaned and assembled with a cover slip fastened on top. Approximately 20 μL of culture was then injected into the well. The counting chamber was placed under a microscope where the bacteria and grid were found. The bacteria were counted in ten random locations on the grid. After this was completed, the counting chamber was cleaned by sonication for 10 minutes in MilliQ water and this was done for each absorbance of each strain of *E. coli*. A spreadsheet program (in this case,

Microsoft Excel) was used to graph the average bacteria population per grid square versus absorbance.

3.6 Contact Angles

Contact angle is a common technique from physical chemistry that can be used to characterize the uniformity and hydrophobicity of a substrate. The contact angle for the gold crystals used in this experiment was determined by the procedure below. For this experiment, a Ramé-Hart model 100-00 (Mountain Lakes, NJ) goniometer was used along with the accompanying DROPimage (Noetcong, NJ) software.

The contact angle was found by placing the gold crystal on the goniometer and filling the device with 40 μL of water. 2 μL of water was dropped on the crystal and the more the drop was spread out, the greater the hydrophilic tendencies of the gold crystal, which means a lower contact angle. This process was repeated with a minimum for 4 drops in 4 different locations on the gold crystals and the results were recorded.

3.7 QCM-D

QCM-D was the major experimental technique used for this project. In order to keep the QCM-D running smoothly, the cleanliness of the gold crystals and the machine were maintained on a daily basis. A Q-Sense, Inc (Gothenburg, Sweden) model E-4 QCM-D was used for all experiments along with a software package including Q-Soft 401 and Q-Tools to record and analyze results. 5 MHz gold crystals that were 14 mm in diameter were used for all QCM-D experiments. Additionally, the cecropin P1 modified with an extra cysteine group that was deposited on certain crystals was obtained from New England Peptide (Gardner, MA).

3.7.1 Cleaning procedure for QCM-D and crystals

The QCM-D and the crystals were cleaned in order to remove any organic and biological before and after each experiment under a chemical fume hood.

3.7.1.1 Cleaning the Gold Crystals (Ammonia Peroxide Mix)

The crystals first underwent UV (which is ultraviolet light at a wavelength of 285 nm) treatment for 5-10 minutes by placing the crystals in the Petri dish, removing the lid, placing under the hood and then turning on the UV light. Next, a 5:1:1 mixture of MilliQ-water, ammonia (25%) (Sigma, St. Lous, MO) and hydrogen peroxide (30%) (Sigma, St. Louis, MO) was heated to 75°C. The crystals were then placed in the heated solution for 5 minutes and then thoroughly rinsed with MilliQ water. The crystals were dried with nitrogen gas and then underwent another 5-10 minutes of UV treatment.

3.7.1.2 Cleaning the QMC-D

When cleaning the QCM-D, specified cleaning crystals were first mounted into the chambers. Approximately 10 mL of 2% Hellmanex (Hellma GmbH and Co., Germany) solution was pumped through at a flow of 300 µL/min followed by approximately 20 mL of MilliQ water. Air was allowed to run through the chambers to rid any excess liquid and then the chambers were emptied and dried completely with nitrogen air.

3.7.2 QCM-D Experimental Procedure

Each of the eleven strains of *E. coli* was tested in the QCM-D using the same protocol. First, the gold crystals were placed in the chambers and all appropriate connections were made. MilliQ water was passed through all four chambers at 100µL/min for

approximately 10 minutes to allow the QCM-D to equilibrate. The computer was then turned on and the program QSoft 401 was opened, and the temperature control was set to 23°C. The frequency and dissipation plots were given time to stabilize and then measurement was stopped and restarted.

MilliQ water was passed through the machine for approximately 5 minutes with stable plots and then the QCM-D pump was stopped and the MilliQ water was replaced with PBS. The flow was reversed for approximately 30 seconds, before being run in the forward direction, in order to prevent air bubbles from disrupting the sensitive measurement devices. PBS was run through all four chambers of the QCM-D at 50µL/min until the frequency and dissipation plots stabilized, which generally took approximately 30 minutes. Once this stabilization occurred, the QMC-D pump was stopped again and the PBS was replaced with 10µM cecropin-P1 cys solution for two out of the four chambers at a flow rate of 50µL/min and run for approximately 120 minutes. The 10µM cecropin-P1 cys solution was made from 1mL of 100µM Cecropin-P1 cys solution diluted in 13mL of PBS. Again, the flow was reversed, before being run in the forward direction, for approximately 30 seconds in order to prevent air bubbles.

Approximately 2 hours after the addition of the cecropin-P1 cys solution and after the plot had stabilized, the QCM-D pump was stopped and PBS was run through all four chambers, again reversing the flow first in order to prevent air bubbles. The PBS was run through the chambers at a flow of 50µL/min to wash off any excess cecropin-P1 cys that did not bind to the gold surface until the frequency and dissipation plots stabilized, or for

approximately 30 minutes. At this point, the QCM-D pump was stopped and the PBS was replaced with $1x10^8$ cells/mL of *E. coli* in PBS, which was passed through all four chambers at 50µL/min for approximately 120 minutes. Again, the flow was reversed first in order to prevent any air bubbles.

After the *E. coli* in PBS solution was passed through the QCM-D and the frequency and dissipation graphs stabilized, PBS was run through all four chambers at 50µL/min for approximately 30 minutes to wash off any excess *E. coli* cells that were not firmly deposited. Next, the measurement was stopped in QSoft, the QCM-D pump was stopped, and the gold crystals were removed from all four chambers in order to use the live/dead kit to evaluate the presence of live/dead bacteria on the crystals. Once the experiments were completed, the crystals and the QCM-D was cleaned and discussed previously.

3.8 Live/Dead Kit on Gold Crystals to Characterize Cell Viability

After the QCM-D experiment was run, a live/dead kit was used to determine the fraction of bacteria alive on all four of the crystals. The dyes used were 20µM propidium iodide and 5µM Syto 9 (Molecular Probes, Eugene, OR) and were diluted using dimethyl sulfoxide (DMSO) (Sigma, St. Louis, MO). The microscope used was a Nikon Eclipse E400, specifically the 60x objective, equipped with FITC and Texas Red filters attached to the Mercury-100W lamp (Chiu, Technical Corp). The Syto 9 dyed all cells, alive and dead, green when viewed under the FITC filter, whereas the propidium iodide dyed all dead cells red when viewed under the Texas Red filter. Additionally, the accompanying software Spot Advanced was used to capture and merge the pictures.

First, each gold crystal was placed in a small Petri dish with approximately 3 mL of PBS, enough to cover the crystal, and the live/dead kit was removed from the freezer and allowed to defrost. Syto 9 (5.01 μL) and propidium iodide (7.5 μL) were added to the crystals in the microscope room, making sure to block as much light as possible because Syto 9 and propidium iodide are light sensitive. The concentrations of Syto 9 and propidium iodide that were added to the Petri dish were determined by the given manufacturer's data. Next, the Mercury Lamp was turned on and the crystals were viewed under both FITC and Texas Red filters. Images were taken at fifteen randomly selected locations, once under each filter. These images were then overlapped and the amounts of live and dead bacteria were counted. When there were multiple crystals with cecropin P1 and multiple crystals without cecropin P1, the average of the live/dead values were calculated.

4 Results

4.1 Growth Curves

Growth curves were determined for each strain of *E. coli* that was used in this project. A representative growth curve for *E. coli* O113:H21 is shown in Figure 7. The growth curves for the remaining 10 strains of bacteria can be found in Appendix E. The growth curve allows us to consistently harvest bacteria at the same phase of growth.

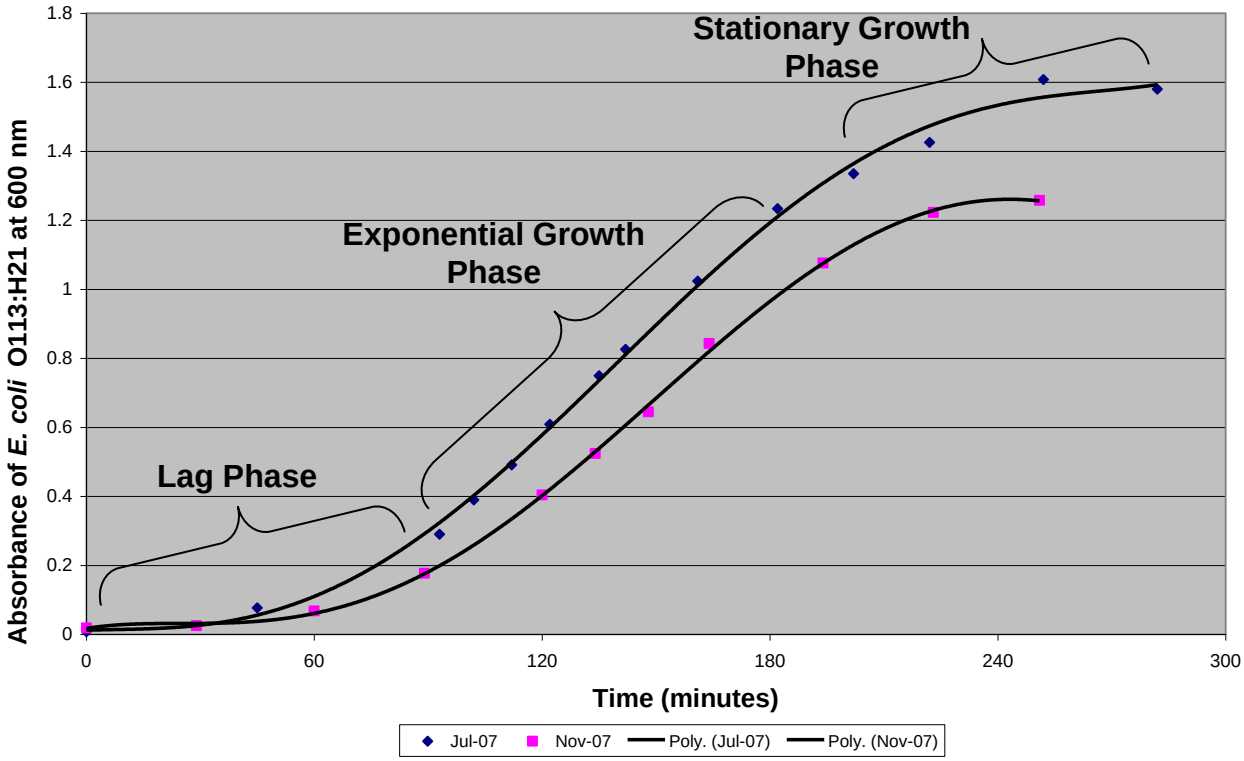

Figure 7: Growth curve for *E. coli* O113:H21.

As Figure 7 illustrates, there are several important stages of bacterial growth that can be observed in growth curves. The first stage is referred to as the lag stage. This phase of bacterial growth is relatively slow and generally lasts between 0.0A and 0.3A. Next is the exponential growth phase, which generally extends between 0.3A and 0.8A. During this

phase, growth is relatively fast and the cells are at their healthiest, and can be used for many applications, including QCM-D experiments. Semi-log plots, such as Figure 8 shown below, can give further insight into growth behaviors during exponential growth.

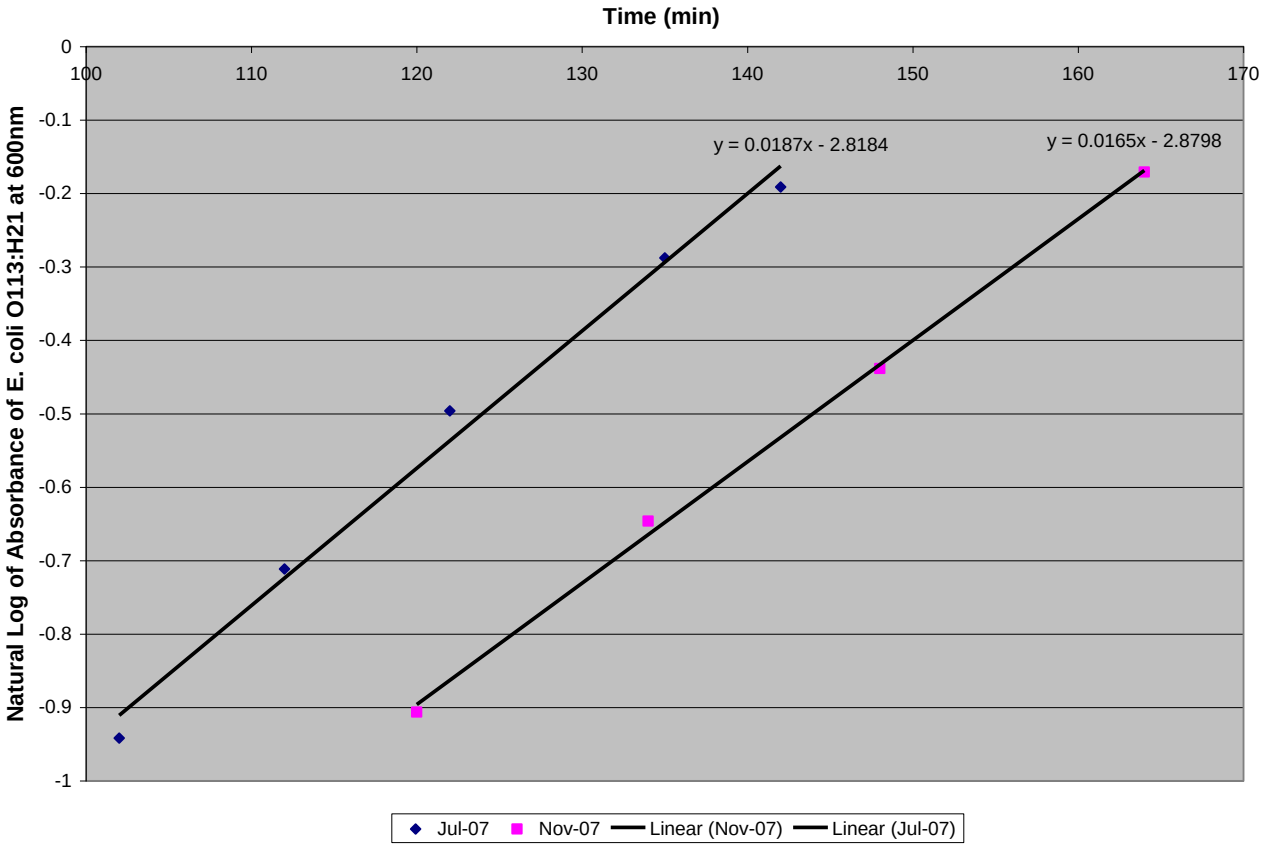

Figure 8: Semi-log plot of *E. coli* O113:H21.

In the semi-log plot, the natural log of the absorbance of the *E. coli* is plotted versus time. The slopes of the lines attaching the data points vary directly with the growth rate during the exponential stage. In Figure 8, the slopes are 0.0187 and 0.0165, indicating there is only a small variation between different trials for a given stage, and that the experiments are reproducible.

The final stage shown on a growth curve is the stationary growth phase, during which the growth of the bacteria slows. After the stationary growth phase, cells undergo the death phase, which cannot be detected by a spectrophotometer because the machine only detects how many cells are present, not whether they are alive or dead.

4.2 Counting Chamber

Counting chamber experiments were conducted for all strains of *E. coli* used in this project. Figure 9 shows an example of one image (out of 10) from a specific absorbance.. This image is of *E. coli* O113:H21 at an absorbance of 0.495.

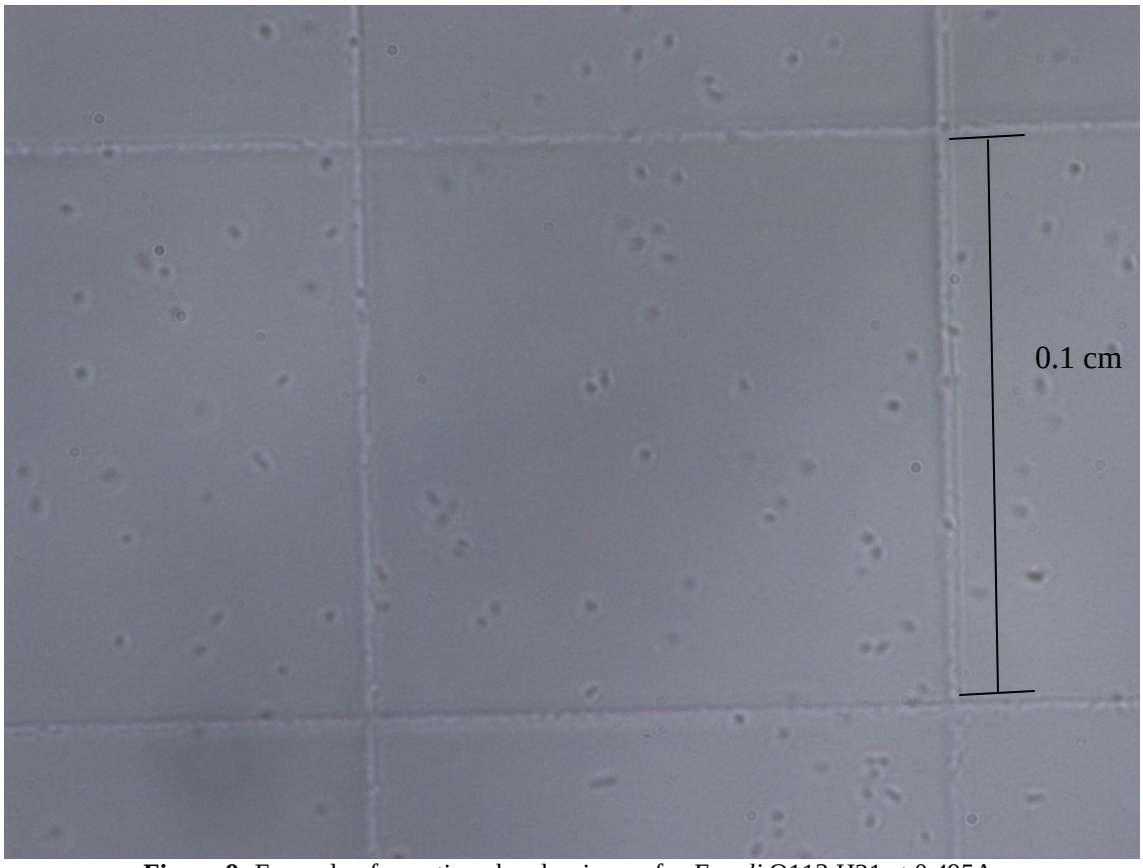

Figure 9: Example of counting chamber image for *E. coli* O113:H21 at 0.495A.

The number of bacteria was counted inside each square (performed for 10 random squares at five different absorbance values for each strain of *E. coli*). This data was then

put into an excel spreadsheet to develop a calibration plot that can be used to determine the population of bacteria at a given absorbance value. The calibration curve for *E. coli* O113:H21 is shown in Figure 10.

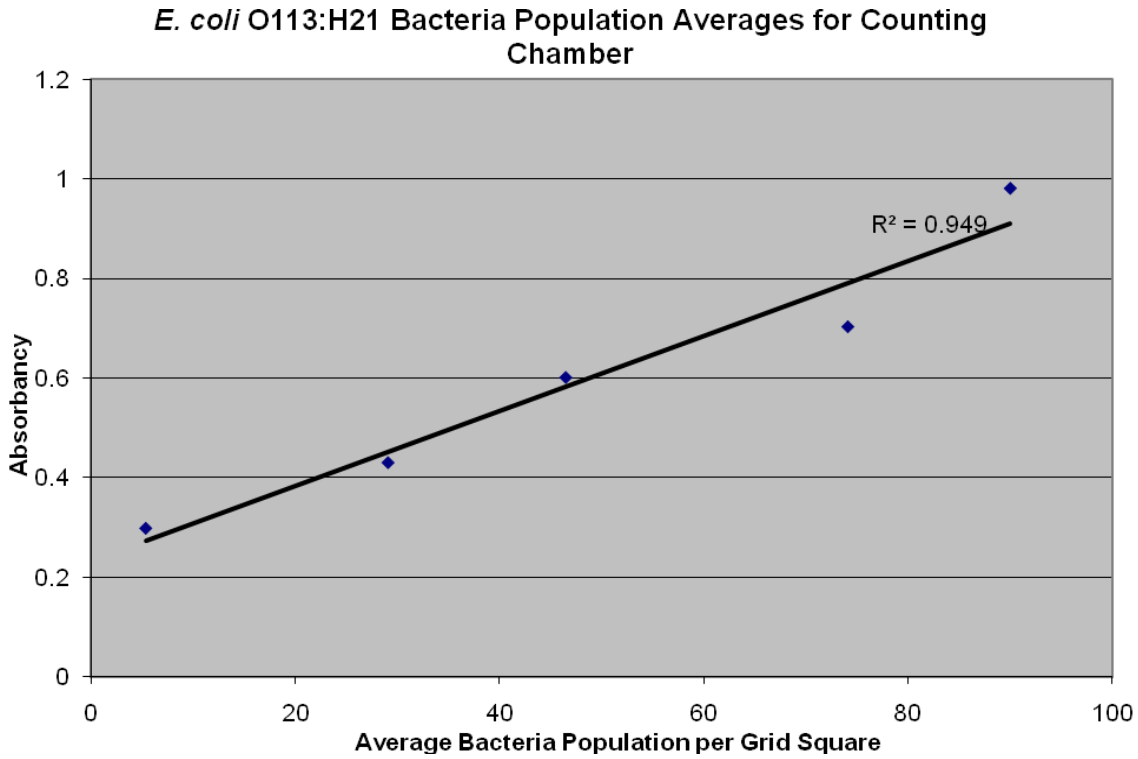

Figure 10: *E. coli* O113:H21 Bacteria Population Averages.

For experiments conducted with the QCM-D, a concentration of $1x10^{8}$ cells/mL was desired. From the calibration curves, like the one above, the average bacteria population per grid square was determined for a given absorbance. The dimensions of one grid square on the counting chamber were given by the manufacturer as 0.01cm x 0.01 cm x 0.001 cm, which is equivalent to $1x10^{-7}$ mL. Calculations, like the one shown below, were conducted to determine how much bacteria rinsed in PBS had to be added to 12 mL of PBS in a centrifuge tube in order to reach the desired $1x10^{8}$ cells/mL concentration.

$$\frac{50 cells}{1x10^{-7} mL} = 5x10^{8} cells/mL$$

$$\frac{5x10^{8} cells/mL}{1x10^{8} cells/mL} = 5$$

$$\frac{12 mL}{x} = \frac{5}{1}$$

$$\frac{12 mL}{5} = 2.4 mL$$

Therefore, in this example, 2.4 mL of *E. coli* O113:H21 rinsed in PBS needed to be added to 12 mL of PBS in order to obtain a concentration of $1x10^{8}$ cells/mL.

4.3 Contact Angle

The contact angle of water droplets was determined for surfaces including clean gold crystal and 1 μm cecropin P1 cys, 2 μm cecropin P1 cys, and 10 μm cecropin P1 cys deposited on the surface of the crystal,after a QCM-D experiment.

Table 3: Water contact angle on gold crystals with varying concentrations of cecropin P1 cys.

	Gold	1 μm CP1-cys	2 μm CP1-cys	10 μm CP1-cys
Water	75 ± 1°	54 ± 3°	48 ± 3°	39 ± 2°

The high contact angle of the water on the clean gold crystal indicated that the surface was hydrophobic, since the water droplet did not spread out when applied to the crystal. However, as cecropin of increasingly higher concentrations was passed through the QCM-D chamber, the contact angle decreased showing a decrease in hydrophobicity of the surface. This change in hydrophobicity, shown by the decreasing contact angle when cecropin P1 was deposited on gold in Table 3, confirms that cecropin P1 did bind to the crystal surfaces.

4.4 QCM-D

The QCM-D was used to monitor the frequency and dissipation changes when cecropin P1 cys was added to the gold crystal surfaces and also Δ*f* and ΔD when each of the *E. coli* strains was added to crystals with and without the antimicrobial peptide. Figure 11 illustrates an example of the frequency and dissipation changes when *E. coli* O157:H12 was added to a gold crystal with cecropin P1.

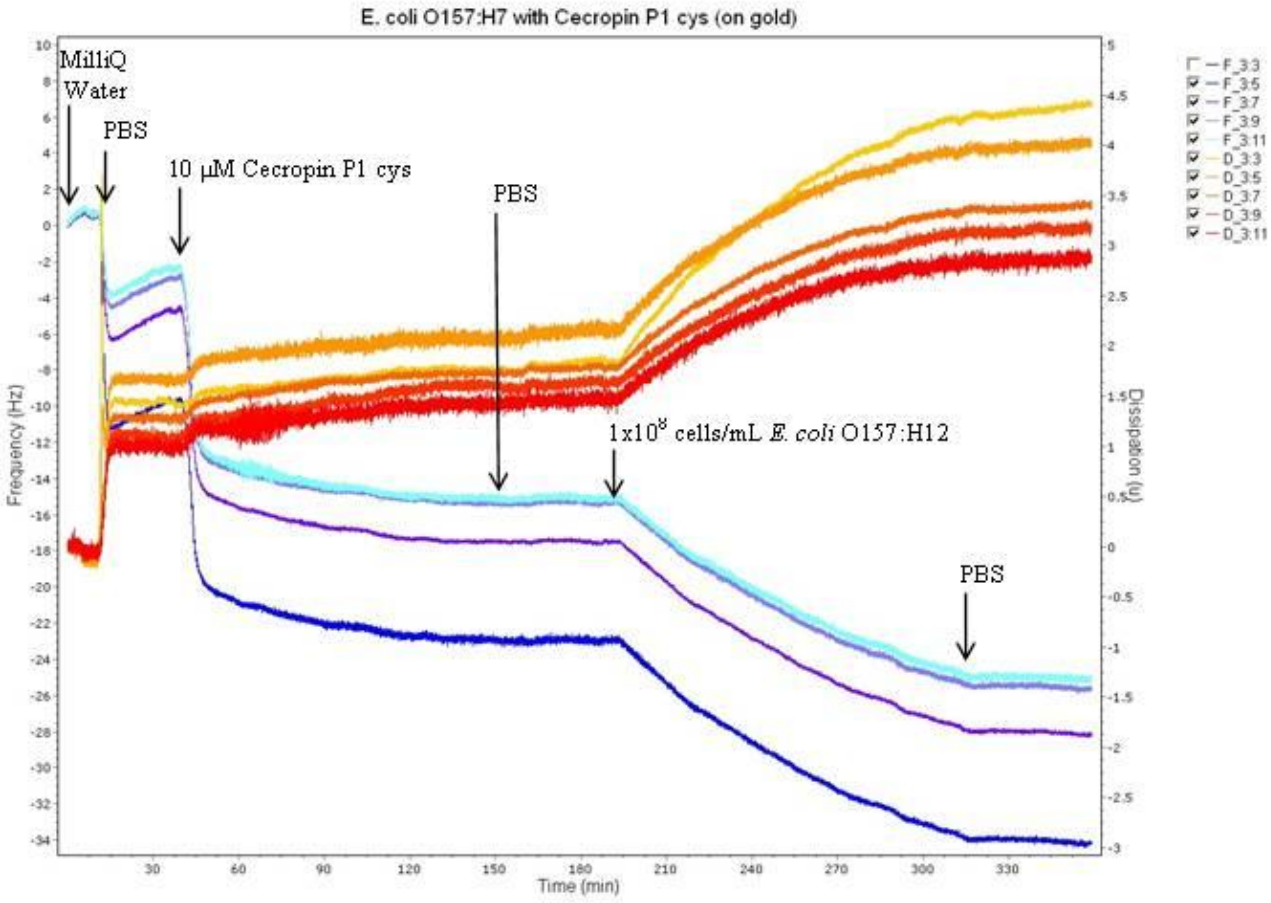

Figure 11: QCM-D frequency and dissipation shifts for *E. coli* O157:H12 with cecropin P1 cys on a gold crystal surface.

The arrows on the graph show when different solutions were passed through the QCM-D flow chamber and the frequency and dissipation changes can be observed. MilliQ water was first used to equilibriate the crystal, and then PBS to accustom the machine to this different bulk liquid, since both the cecropin P1 and *E. coli* were dissolved in PBS. The average frequency shift when PBS was added was -2.8 Hz and the average dissipation shift was 1.305μ. Once the cecropin P1 was added, the frequency underwent a rapid drop and then re-equilibriated as the AMP was bound to the gold surface, which indicates an increase in mass of cecropin P1 deposited on the crystal. The average change in frequency when cecropin P1 was added for all plots and all strains was -12.2 Hz.

Additionally, a small increase in dissipation was observed, which suggests an increase in the "softness" of the deposited film. The average dissipation change when cecropin P1 was added for all plots and strains was 0.168μ. Later, when the *E. coli* was added after a PBS wash to rinse off excess cecropin P1, similar trends of decreasing frequency and increasing dissipation indicate deposition of *E. coli* cells to the surface. Finally, with the last PBS wash, there is little to no change in frequency or dissipation, showing that most of the *E. coli* adhered fairly strongly to the surface with bound cecropin P1 cys. These common trends were observed in all of the QCM-D experiments with cecropin P1, and the graphs can be observed in Appendix A.

However, different trends in the QCM-D frequency and dissipation plots were observed when cecropin P1 was not added to the gold crystal surface before the *E. coli*. The graph below illustrates typical trends for the QCM-D experiments without cecropin P1.

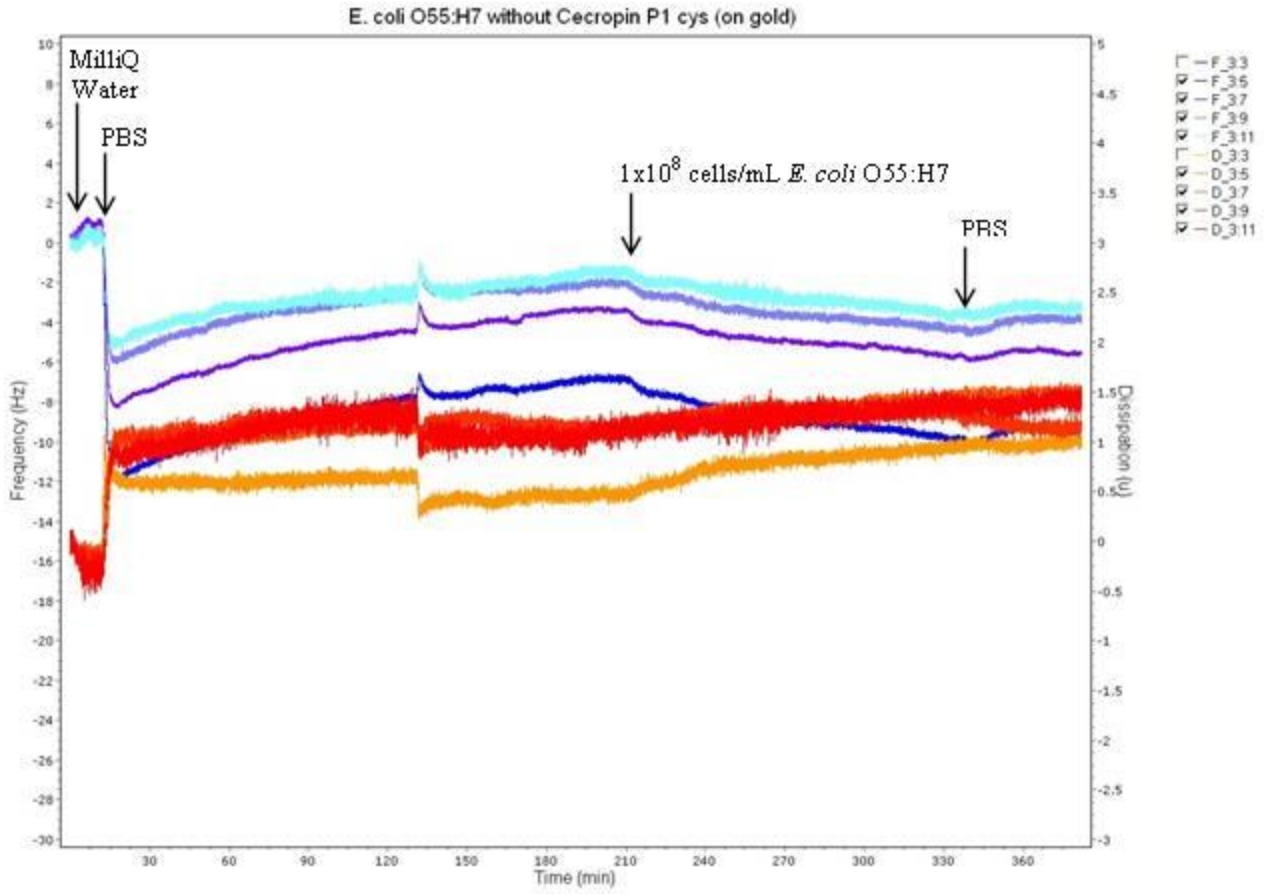

Figure 12: QCM-D frequency and dissipation shifts for *E. coli* O55:H7 without cecropin P1cys on a gold crystal surface.

Once again, the arrows on the graph indicate when different solutions were added to the QCM-D. When PBS was run through the QCM-D instead of cecropin P1, it is clear that the frequency did not decrease as much and the dissipation did not increase as much when the *E. coli* was added, suggesting that the not as much *E. coli* adhered to the crystal surface. Furthermore, when the crystal was rinsed with PBS after the *E. coli*, the frequency increased by a small amount, indicating that some of the cells were washed off. This suggests that the *E. coli* did not attach to the surface as well as when the cecropin P1

was bound to the gold crystal first. These frequency and dissipation changes were similar for all of the other QCM-D experiments conducted without cecropin P1, and these graphs can be observed in Appendix A.

The frequency and dissipation changes observed in the QCM-D plots were measured and recorded for all experiments, and the shifts for every solution change can be seen in Appendix B. The most important frequency and dissipation measurements were the shifts once the *E. coli* was added, because these showed whether more *E. coli* cells adhered to the surfaces with bound cecropin P1 cys than the surfaces without the AMP.

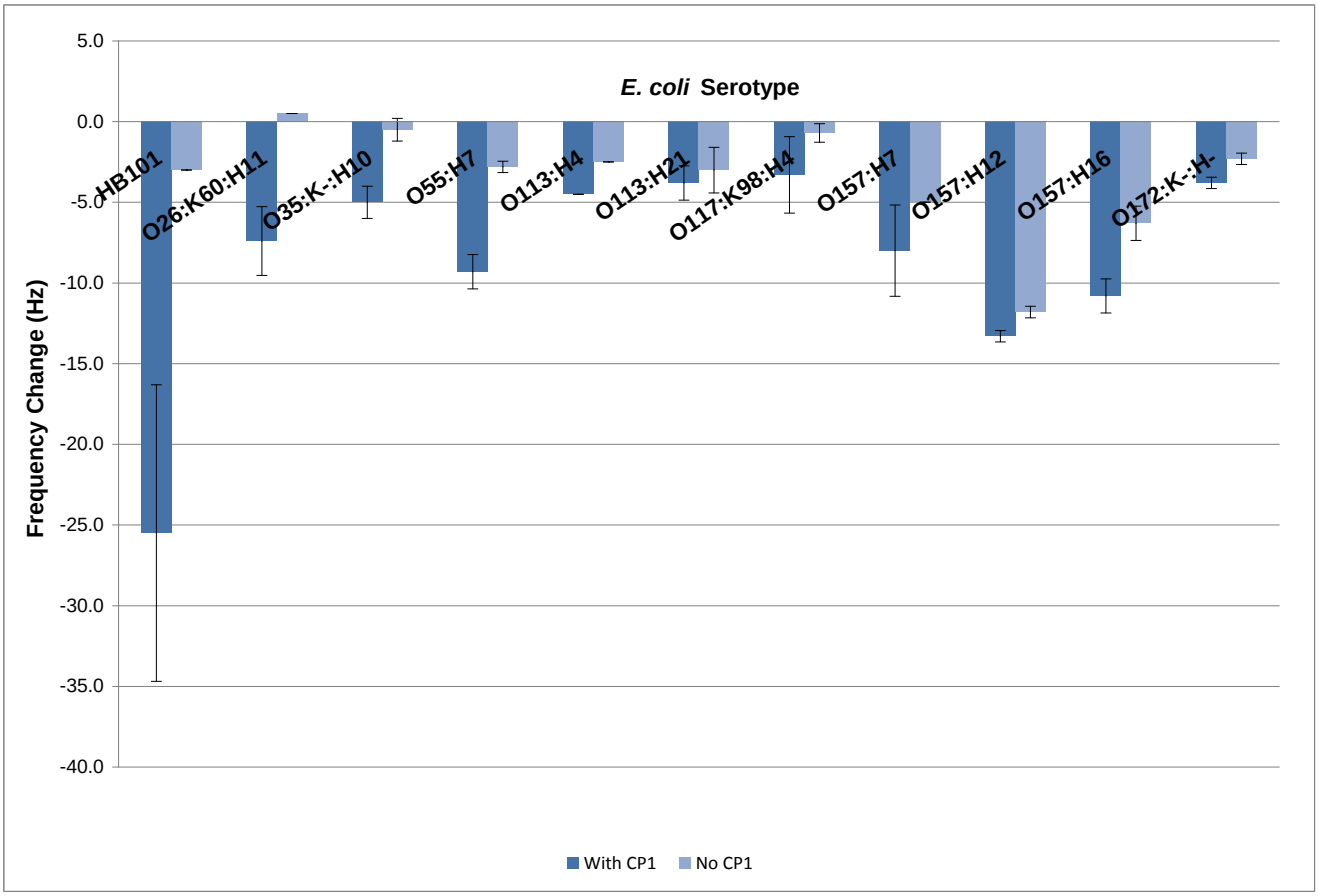

Figure 13: Bar graph of measured frequency shift measured in QCM-D plots when *E.coli* was added, with and without cecropin P1 bound to the gold crystal surface. Note that the error bars represent the standard deviation.

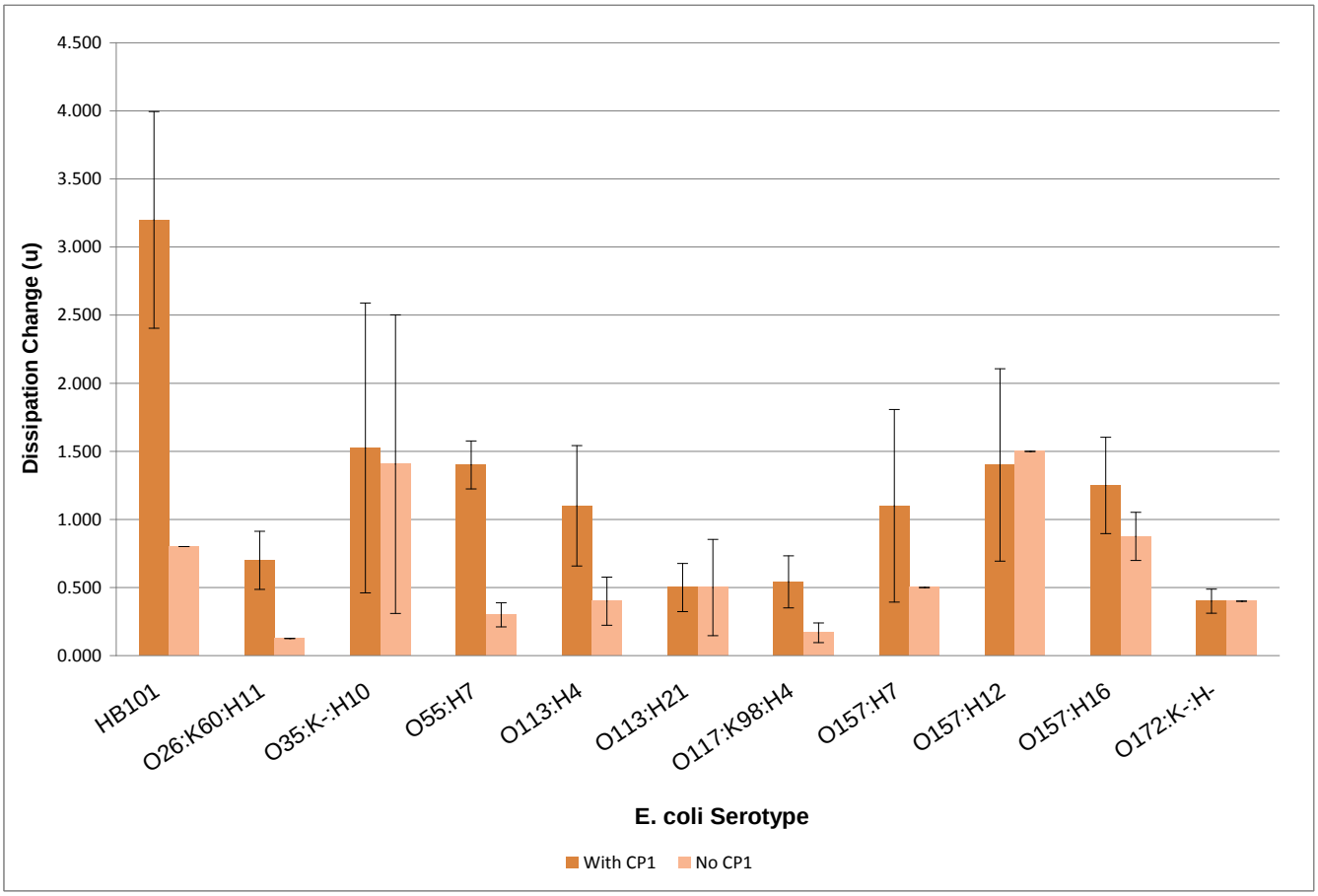

Figure 14: Bar graph of measured dissipation shift measured in QCM-D plots when *E.coli* was added, with and without cecropin P1 bound to the gold crystal surface. Note that the error bars represent the standard deviation.

The frequency decrease was greater when cecropin P1 was bound to the gold crystals for all eleven strains. This indicates that more mass, or more cells, was deposited onto the crystals with bound cecropin P1 cys, which suggests that the *E. coli* were strongly attracted to the AMP.

However, not all of the differences between the crystals with and without cecropin P1 were statistically significant, according to our statistical analysis (Table 5). A one-way ANOVA test was run using SigmaStat 2.03 software.

Table 4: Statistical significance for results of average frequency shift in QCM-D plots when *E. coli* was added, comparing crystals with and without bound cecropin P1.

***E. coli* Strain**	**P-value**	**Statistically Significant**
HB101	0.295	NO
O26:K60:H11	0.045	YES
O35:K-:H10	<0.001	YES
O55:H7	0.014	YES
O113:H4	<0.001	YES
O113:H21	0.588	NO
O117:K98:H4	0.138	NO
O157:H7	0.546	NO
O157:H12	0.051	NO
O157:H16	0.051	NO
O172:K-:H-	0.051	NO

For this test, the p-value had to be ≤ 0.05 for the difference to qualify as statistically significant, meaning that the difference could not be caused by random chance. Only four out of the eleven strains (O26:K60, O35:K-:H11, O55:H7, and O113:H4) showed a statistically significant difference between the *E. coli* frequency shifts for crystals with and without cecropin P1.

As the table and graph of dissipation changes show, the dissipation increased more when cecropin P1 was bound to the gold crystal for seven out of the eleven strains (HB101, O26:K60:H11, O55:H7, O113:H4, O117:K98:H4, O157:H7, and O157:H16). This once again suggests that, for these strains, the *E. coli* adhered better to the surfaces with the cecropin P1. The table below illustrates the statistical significance of the differences

between crystals with and without cecropin P1 for the dissipation change when *E. coli* was sent through the QCM-D.

Table 5: Statistical significance for results of average dissipation shift in QCM-D plots when *E. coli* was added, comparing between crystals with and without bound cecropin P1.

***E. coli* Strain**	**P-value**	**Statistically Significant**
HB101	0.245	NO
O26:K60:H11	0.104	NO
O35:K-:H10	0.891	NO
O55:H7	0.016	YES
O113:H4	0.173	NO
O113:H21	1.000	NO
O117:K98:H4	0.033	YES
O157:H7	0.614	NO
O157:H12	0.860	NO
O157:H16	0.312	NO
O172:K-:H-	1.000	NO

As the table above shows, only one strain of *E. coli* (O55:H7) showed a statistically significant difference between the crystals with and without cecropin P1.

4.5 Live/Dead Kit

It is important to note that no previous research has been conducted on whether the bound AMP inactivated bacteria. The live/dead kit was used to take pictures of the various strains of *E. coli* when deposited on the gold crystals for experiments run with and without cecropin P1. The dye Syto 9 (Molecular Probes, Eugene, OR) dyed all bacteria present on the slide while propidium iodide (Molecular Probes, Eugene, OR) dyed only membrane compromised (dead) bacteria. When these two pictures were merged, an image overlay was created where the live bacteria versus dead bacteria could be counted. Thus, the red cells represent dead bacteria and the green cells indicate live bacteria.

Images, representative ones in Figure 13, which are of *E. coli* O117:K98:H4 with (top) and without (bottom) cecropin P1, were yielded using this method.

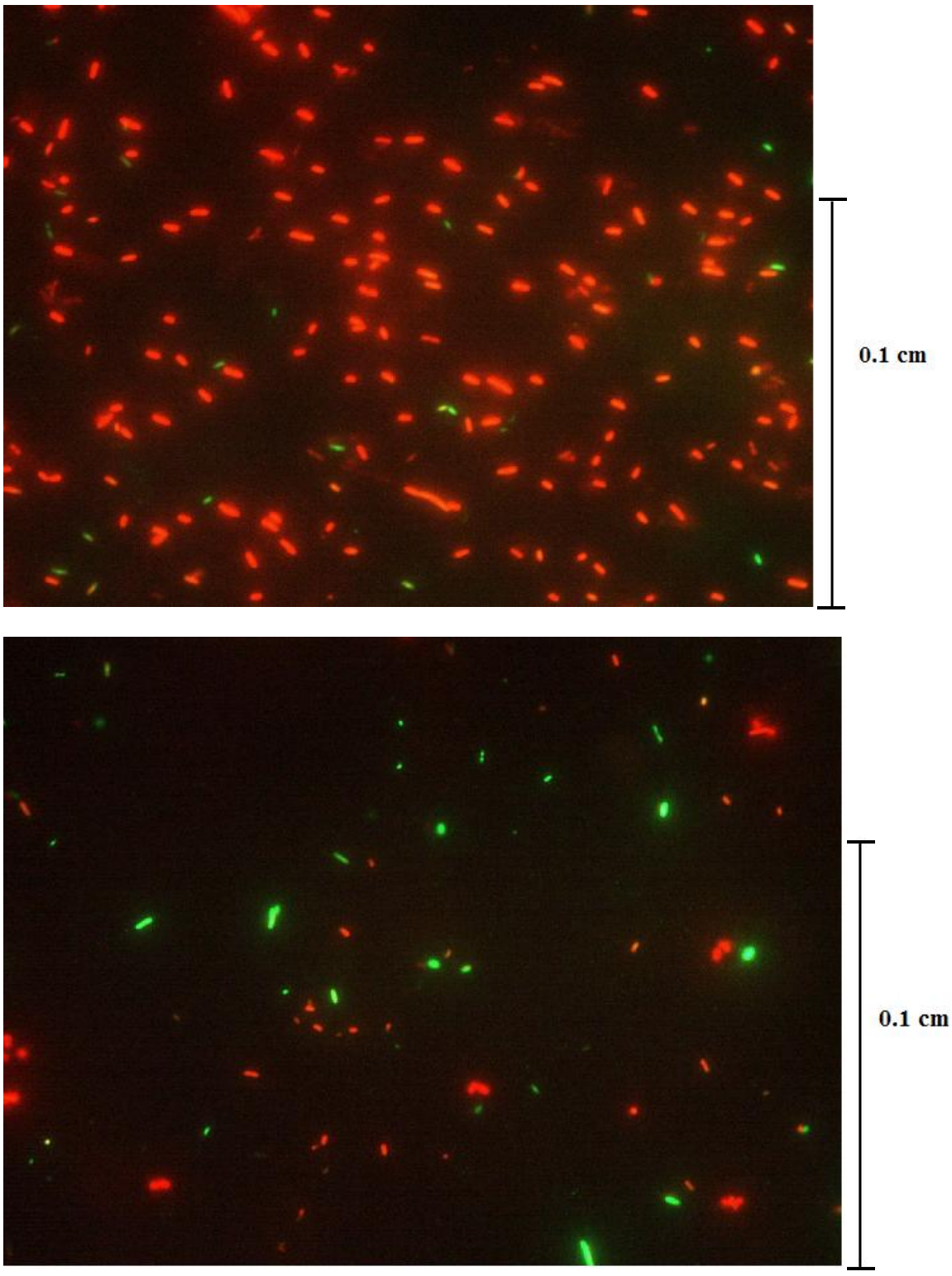

Figure 15: Live/Dead picture of *E. coli* O117:K98:H4 with (top) and without (bottom) cecropin P1 cys on a gold QCM-D crystal.

For *E. coli* O117:K98:H11, more bacteria adhered to the surface with cecropin P1 and in a more uniform layer, than on surfaces without cecropin P1. The amount of live bacteria (green) and dead bacteria (red) were counted for each image. The average number of bacteria present per picture and the average percentage of dead bacteria per picture were calculated (Figures 16 and 17).

.

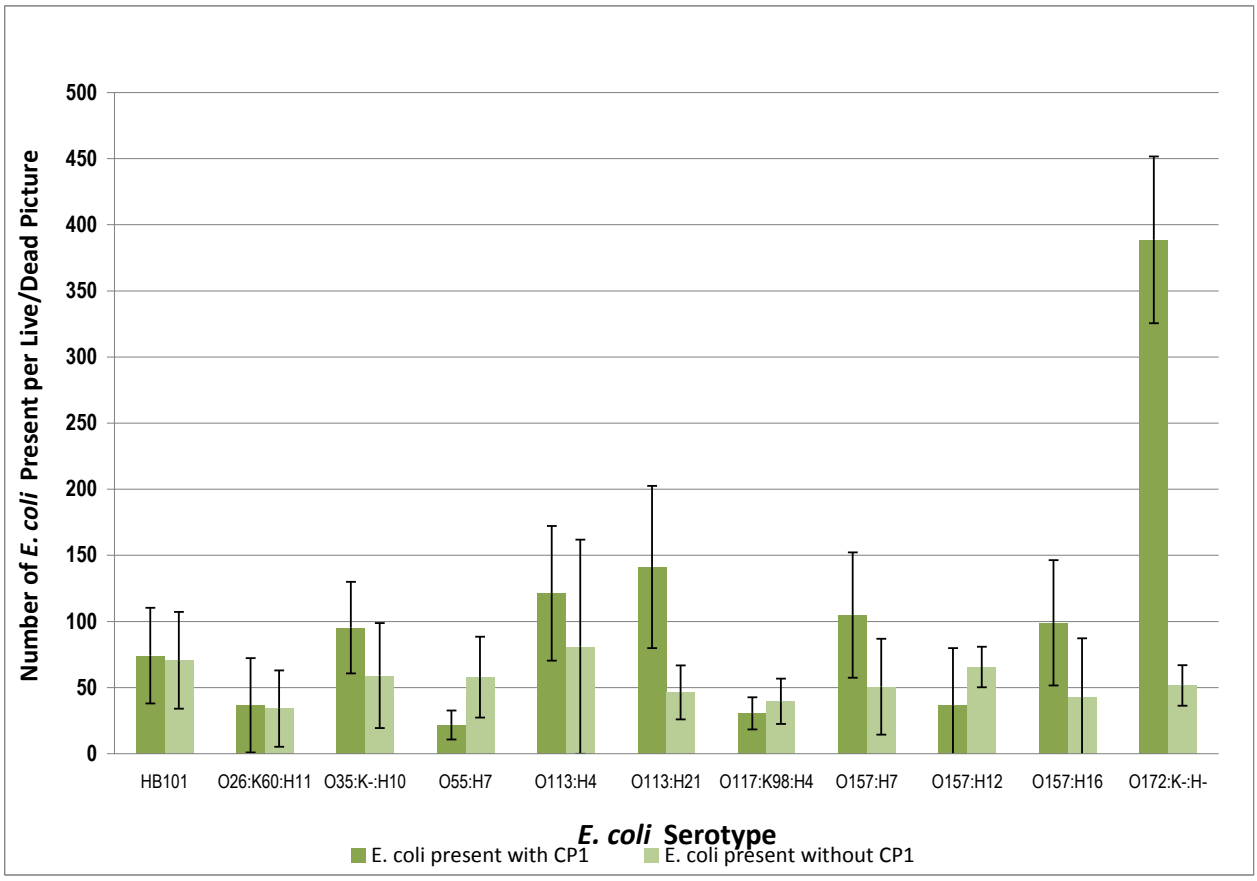

Figure 16: Graph of the number of *E. coli* cells present per live/dead picture with cecropin P1 and without cecropin P1.

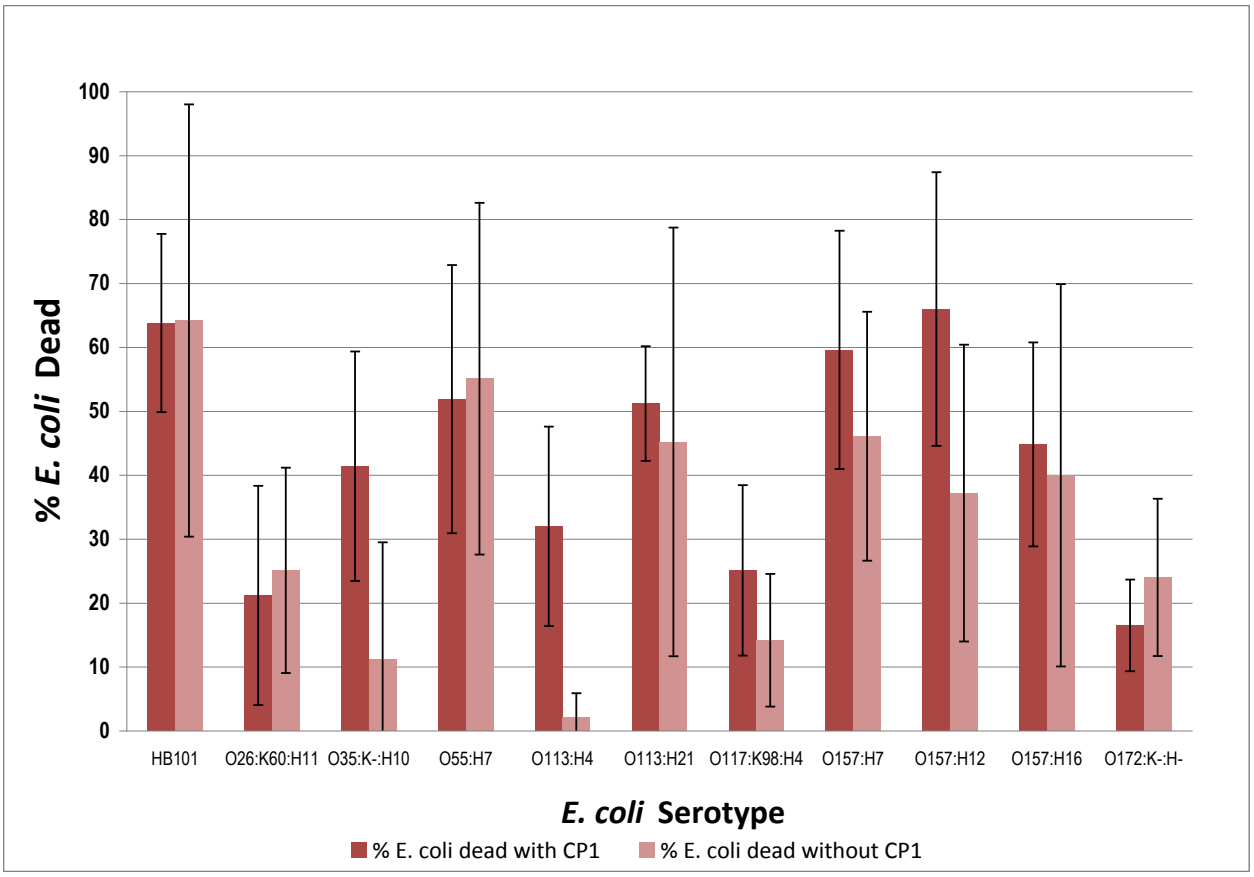

Figure 17: Graph of percentage of *E. coli* cells dead per live/dead picture with cecropin P1 and without cecropin P1.

One of the goals of this project was to examine the binding potential of different strains of *E. coli* to the AMP cecropin P1. Nine out of the eleven strains of bacteria (O35:K-:H10, O113:H21, O157:H7, O157:H16, O113:H4, HB101, O26:K60:H11, O117:K98:H4 and O172:K-:H-) yielded a higher amount of bacteria per picture present on the gold crystal when cecropin P1 was used as opposed to control experiments in the absence of cecropin P1. However, the amount of bacteria that bound to the cecropin P1 was not the same for all of the strains. *E. coli* O172:K-:H- had the highest amount of bacteria present with cecropin P1. Surprising results were those of *E. coli* O55:H7 and O157:H12, where the experiments done without cecropin P1 yielded more bacteria per picture than the experiments run with cecropin P1.

Another goal of this project was to study the affect of cecropin P1 in killing different strains of *E. coli*. The experiments resulted in six out of the eleven strains of *E. coli* yielding a higher percentage of bacteria dead with cecropin P1 applied to the gold crystal prior to the bacteria than those without cecropin P1. The six strains of *E. coli* were O35:K-:H10, O113:H21, O157:H7, O157:H12, O157:H16, O113:H4. It is possible that these types of bacteria are more vulnerable to the cecropin P1 than others. The remaining five strains (HB101, O26:K60:H11, O55:H7, O117:K98:H4, O172:K-:H-) yielded opposite results, where the higher percentage of *E. coli* dead was found in the experiments run without cecropin P1. It may be possible that some strains of the bacteria are not affected by cecropin P1.

SigmaStat 2.03 software was used to calculate the p value for the reliability (Tables 9 and 10) results. If the p value was <0.05 for a completed experiment, then difference in the results was statistically significant, meaning that the difference could not have been caused by random chance.

Table 6: Statistic significance for results of average number of *E. coli* cells present per live/dead picture.

***E. coli* Strain**	**P-value**	**Statistically Significant**
HB101	0.703	NO
O26:K60:H11	0.771	NO
O35:K-:H10	<0.001	YES
O55:H7	<0.001	YES
O113:H4	0.024	YES
O113:H21	<0.001	YES
O117:K98:H4	0.021	YES
O157:H7	<0.001	YES
O157:H12	<0.001	YES
O157:H16	<0.001	YES
O172:K-:H-	<0.001	YES

Table7: Statistic significance for results of average % of *E. coli* dead per live/dead picture.

***E. coli* Strain**	**P-value**	**Statistically Significant**
HB101	0.952	NO
O26:K60:H11	0.376	NO
O35:K-:H10	<0.001	YES
O55:H7	0.614	NO
O113:H4	<0.001	YES
O113:H21	0.348	NO
O117:K98:H4	<0.001	YES
O157:H7	0.008	YES
O157:H12	<0.001	YES
O157:H16	0.441	NO
O172:K-:H-	0.005	YES

Nine of the eleven strains of bacteria tested yielded statistically significant increases in bacterial binding when the AMP was present. The strains were O35:K-:H10, O55:H7, O113:H4, O113:H21, O117:K98:H4, O157:H7, O157:H16, O172:K-:H- and O35:K-:H10. Two strains, O55:H7, O157:H12 yielded a statistically significant decrease in bacterial binding to Cecropin P1 where as O35:K-:H10 showed a statistically significant increase in bacterial binding with Cecropin P1. The remaining bacteria; HB101, O26:K60:H11 and O35:K-:H10 showed no preference with respect to binding to gold or a CP1-coated surface. This result was expected for HB101, since that is our control bacterium and it lacks the O-antigen.

The research also determined which strains of *E. coli* were deactivated by the AMP cecropin P1. Three strains, O35:K-:H10, O157:H12 and O117:K98:H4 did not show any preferential binding to cecropin, but did yield results that show the bacteria, when in presence of cecropin, yield a higher percentage of bacteria dead than in the absence of cecropin P1. Also, while *E. coli* O172:K-:H- showed a preferential binding to cecropin P1, more bacteria were seen dead in the absence of cecropin P1, than in the presence of

the AMP. Therefore, while cecropin P1 has the ability to bind a certain strain of bacteria, the ability to bind necessarily influence the effectiveness of killing the bacterium.

This means that binding alone cannot be used as a way to characterize the effectiveness of an AMP against a potential pathogen. Three out of the six strains of bacteria that bound to the cecropin P1 also yielded higher percentages of dead bacteria when the cecropin P1 was present. These strains were O113:H4, O157:H7 and O35:K-:H10. Therefore, using cecropin P1 with these three types of *E. coli* has the potential to be the most successful method for binding and deactivating the bacteria. This result is particularly exciting since *E. coli* O157:H7 is one of the most serious food borne pathogens we face.

5 Conclusions and Recommendations

Using the data obtained from both QCM-D plots and live/dead kit cell counts, the following conclusions concerning how cecropin P1 affected cell adherence to the gold crystal surface were made. Additionally, results from the live/dead kit were used to determine the AMP's effectiveness in killing each strain of *E. coli*. Finally, recommendations on improving the procedure and future research are discussed in this section.

5.1 Number of E. coli Cells Present on Gold Crystals

The two methods used to determine the presence of *E. coli* cells on the gold crystals, QCM-D and live/dead kit, yielded results that did not always agree. In figure 18, the blue points represent bacteria deposited on crystals with cecropin P1 while the pink points represent bacteria deposited on crystals without cecropin P1.

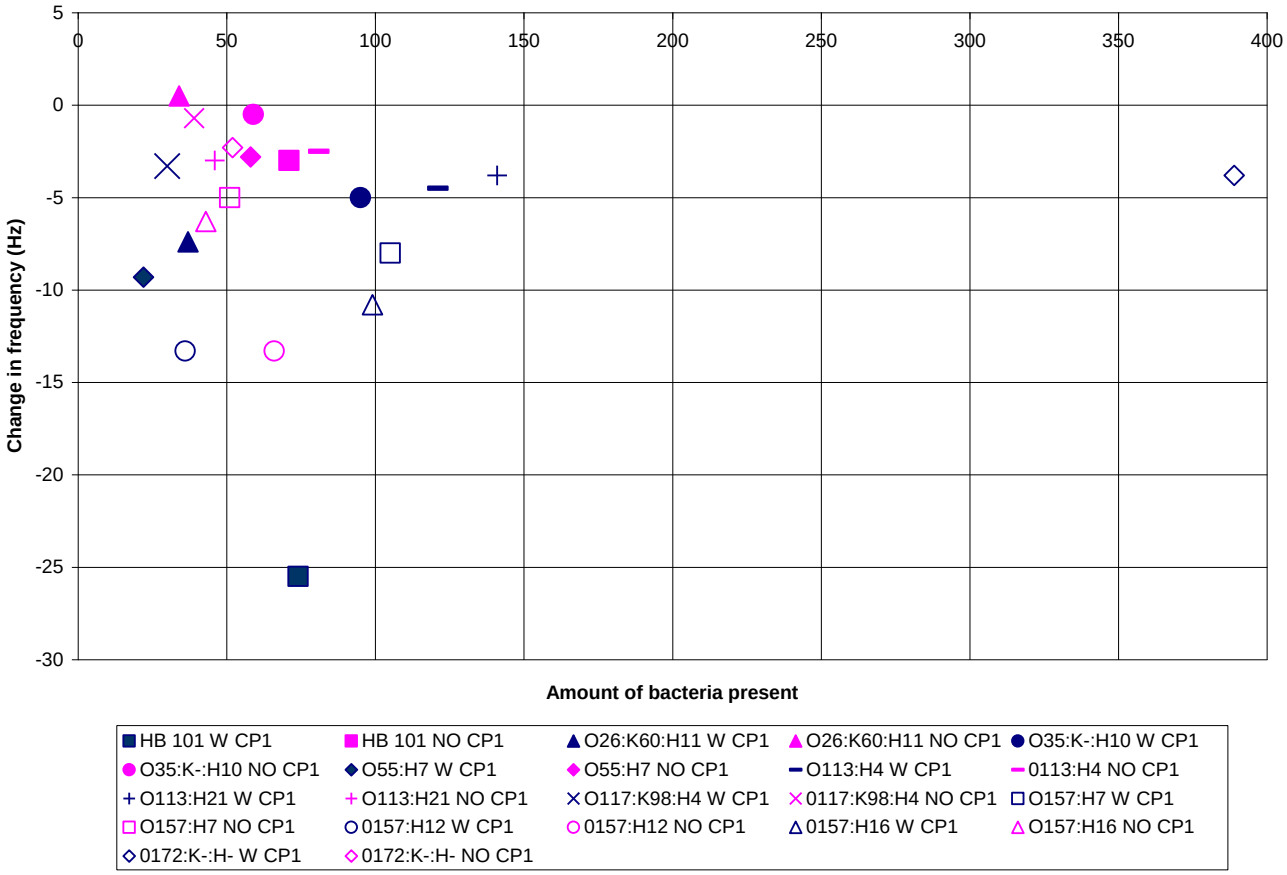

Figure 18: Amount of bacteria present per picture in live/dead kit versus frequency change measured by QCM-D.

Ideally, the change in frequency should become more negative with an increasing amount of bacteria present. However, this trend was not observed in these experiments, which could have been caused by washing procedures conducted prior to live/dead kit experiments.

Table 8 also illustrates the discrepancies between the QCM-D and the live/dead kit concerning how much bacteria was deposited on the gold crystals.

Table 8: *E. coli* strains with and without a statistically significant increase in the number of bacteria present on the crystal with cecropin P1 (versus without cecropin P1) as determined by the QCM-D and/or live/dead kit.

	Statistically Significant Increase of *E. coli* with CP1-cys	
***E. coli* Strain**	**QCM-D**	**Live/dead Kit**
HB101	NO	NO
O26:K60:H11	YES	NO
O35:K-:H10	YES	YES
O55:H7	YES	NO
O113:H4	YES	YES
O113:H21	NO	YES
O117:K98:H4	NO	NO
O157:H7	NO	YES
O157:H12	NO	NO
O157:H16	NO	YES
O172:K-:H-	NO	YES

For two strains (O26:K60:H11 and O55:H7) the QCM-D showed a statistically significant increase in *E. coli* adhered to crystals with cecropin P1, while the live/dead staining did not show an increase. Additionally, the live/dead kit showed a statistically significant increase in the amount of bacteria present for four strains strains of *E. coli* (O113:H21, O157:H7, O157:H16 and O172:K-:H-) while the QCM-D did not.

We offer some possible suggestions to explain these results. For the quantification of bacterial viability using the live/dead staining procedure, pictures were captured at arbitrary locations, and they may not have been accurate depictions of the entire *E. coli* population on the gold crystal. If the cecropin P1 was not evenly distributed over the surface of the crystal, then bacterial binding may have also been non-uniform. Thus, we recommend more pictures be taken to provide a larger, more representative depiction of the surface. Additionally, it may be beneficial to use atomic force microscopy (AFM) to

characterize the surface roughness, which can be related to the coverage of both *E. coli* and cecropin P1 deposited on each surface.

Despite the exhibited discrepancies, both methods showed that both *E. coli* O113:H4 and *E. coli* O35:K-:H10 exhibited a statistically significant increase in bacterial cells deposited on the crystal surface with cecropin P1 compared to crystals without the AMP. Thus, these experiments confirm that O113:H4 and O35:K-:H10 adhered to cecropin P1.

One goal of these experiments was to determine which portion of the *E. coli* lipopolysaccharide interacted with cecropin P1. One theory was that the number of sugars in the LPS might affect the binding capabilities of the bacteria, but this was not shown by the data. Of the two strains that most clearly adhered to the cecropin were *E. coli* O113:H4 and O35:K-:H10, the former has an indeterminable sugar backbone, while the latter has a five sugar backbone. Of the strains that exhibited preferential binding either in QCM-D experiments or through the live/dead kit, all had LPS backbones made up of various numbers of sugars, and thus no relationship between the number of sugars and binding efficiency was found. However, there was a difference between HB101, the laboratory strain without an O-antigen, and the majority of the pathogenic strains with an O-antigen. HB101 did not exhibit preferential binding with cecropin P1 in the QCM-D or live/dead kit experiments, indicating that it did not adhere to crystals with cecropin P1 any better than those without the AMP. This suggests that cecropin P1 may bind with some portion of the O-antigen, but the location has yet to be determined.

5.2 Percentage of E. coli Dead

The primary purpose of the live/dead kit was to determine the percentage of dead *E. coli* found on the gold crystals with and without exposure to cecropin P1. Four strains (O35:K-:H10, O157:H7, O157:H12 and O113:H4) showed a statistically significant increase in the percentage of dead bacteria on the crystals with cecropin P1, compared to those without the AMP. Of those four strains, O157:H12 did not show preferential binding to cecropin P1 crystals in either the QCM-D or live/dead experiments. O157:H7 showed preferential binding to crystals with cecropin P1 in live/dead experiments, but not in those using the QCM-D. Thus, for these three strains, it can be concluded that even though the adherence mechanism is not fully known or understood, the AMPs are effective in killing these particular types of *E.coli*.

However, *E. coli* O113:H4 and O35:K-:H10 indicated preferential binding in both QCM-D and live/dead experiments and also showed an increase in the percentage of bacteria dead on gold crystals where cecropin P1 was bound to the surface. Therefore, it can be concluded that, out of the eleven strains, *E. coli* O113:H4 and O35:K-:H10 were bound by cecropin P1 and also killed by the AMP. As stated previously, O113:H4 is categorized as verotoxin producing *E. coli*, which can lead to hemorrhaging of the intestinal tract and blood clotting disorders, and although O35:K-:H10 is less common, it still can cause food contamination and cause illness in humans. The results of this project show potential for cecropin P1's activity against *E. coli*, and therefore further experimentation should be conducted to definitively determine if cecropin P1 adheres and kills the remaining strains.

6 References

An, Y.H. and Friedman, R.J. 1998. **Concise Review of Mechanisms of Bacterial Adhesion.** *Journal of Biomedical Research; 43: 338-348*

Beveridge, T.J. 1999. **Structures of Gram-Negative Cell Walls and Their Derived Membrane Vesicles.** *Journal of Bacteriology; 181: 4725-4733*

Beveridge, T.J. and Graham, L.L. 1991. **Surface Layers of Bacteria.** *Microbiological Reviews; 55: 684-705*

Boman, H.G., Agerberth, B., and Boman, A. 1993. **Mechanisms of Action on *Escherichia coli* of Cecropin P1 and PR-39, Two Antimicrobial Peptides from Pig Intestine.** *Infection and Immunity; 61: 2978-2984*

Brogden, K.A., Ackermann, M., McCray Jr., P.B., and Tack, B.F. 2003. **Antimicrobial peptides in animals and their role in host defenses.** *International Journal of Antimicrobial Agents; 22: 465-478*

Bulet, P., Hetru, C., Dimarcq, J., and Hoffman, D. 1999. **Antimicrobial peptides in insects; structure and function.** *Developmental and Comparative Immunology; 23: 329-344*

Caroff, M., and Karibian, D. 2003. **Structure of bacterial lipopolysaccharides.** *Carbohydrate Research; 338: 2431-2447*

Carter, R.M., Mekalanos, J.J., Jacobs, M.B., Lubrano, G.J., and Guilbault, G.G. 1995. **Quartz crystal microbalance detection of *Vibrio cholera* O139 serotype.** *Journal of Immunological Methods; 187: 121-125*

Center for Disease Control and Prevention. 1994. **Addressing Emerging Infectious Disease Threats: A Prevention Strategy for the United States.** *U.S. Dept. Health and Human Services, Public Health Service, Atlanta, GA, USA*

Center for Disease Control and Prevention. **Multistate Outbreak of *E. Coli* O157 Infections Linked to Topp's Brand Ground Beef Patties**. 26 Oct. 2007. http://www.cdc.gov/ecoli/2007/october/100207.html

Center for Disease Control and Prevention (CDC). **Multistate Outbreak of *E. coli* O157 Infections, November-December 2006.** 14 Dec 2006. http://www2a.cdc.gov/HAN/ArchiveSys/ViewMsgV.asp?AlertNum=00255

Center for Disease Control and Prevention (CDC). **Update of Multi-State Outbreak of *E.coli* O157:H7 Infections from Fresh Spinach.** 6 Oct 2006. http://www.cdc.gov/ecoli/2006/september/updates/100606.htm

Epand, R. and Vogel, H. 1999. **Diversity of Antimicrobial Peptides and their Mechanisms of Action.** *Biochimica et Biophysics Acta; 1462: 11-28*

Fredriksson, C., Kihlman, S., Rodahl, M., and Kasemo, B. 1998. **The Piezoelectric Quartz Crystal Mass and Dissipation Sensor: A Means of Studying Cell Adhesion.** *Langmuir; 14: 249-251*

Hancock, R.E. and Diamond, G. 2000. **The Role of Cationic Antimicrobial Peptides in Innate Host Defenses.** *Trends Microbiol; 8: 402-410*

Höök, F., Rodahl, M., Brzezinski, P., and Kasemo, B. 1998. **Energy Dissipation Kinetics for Protein and Antibody-Antigen Adsorption under Shear Oscillation on a Quartz Crystal Microbalance.** *Langmuir; 14: 729-734*

Izadpanah, A. and Galla, R.L. 2005. **Antimicrobial Peptides**. *Continuing Medical Education: Journal of the American Academy of Dermatology; 25: 381-390*

Jenkins, M., Horsfall, M., Mathew, D., Scanlon M., Jayasekara, R. and Lonergan, G. 2004. **Application of a Quartz Crystal Microbalance to Evaluate Biodegradability of Starch by Bacillus Subtilis**. *Biotechnology Letters; 26: 1095-1099*

Jensen, H., and Unnevehr, L. 1995. **The economics of regulation and information related to foodborne microbial pathogens.** *Tracking Foodborne Pathogens from Farm to Table: Data Needs to Evaluate Control Options, USDA, Economic Research Service, Food and Consumer Economics Division; 125-133*

Kwon, K.D., Green H., Bjöörn, P., and Kubicki, J.D. 2006. **Model Bacterial Extracellular Polysachharide Adsorption Onto Silica and Alumina: Quartz Crystal Microbalance with Dissipation Monitoring of Dextran Adsorption.** *Environmental Science & Technology; 40: 7739-7744*

Miller, A.J., Smith, J.L., and Buchanan, R.L. 1998. **Factors affecting the emergence of new pathogens and research strategies leading to their control.** *Journal of Food Safety; 18: 243-263*

Mouenuddin, M., Wachsmuth, I.K., Moseley, S.L., Bopp, C.A., and Blake, P.A. 1989. **Serotype, Antimicrobial Resistance, and Adherence Properties of *Escherichia coli* Strains Associated with Outbreaks of Diarrheal Illness in Children in the United States.** *Journal of Clinical Microbiology; 27: 2234-2239*

Otto, K., Elwing, O., and Hermansson, M. 1999. **Effect of Ionic Strength on Initial Interactions of *Escherichia coli* with Surfaces, Studied On-Line by a Novel Quartz Crystal Microbalance Technique.** *Journal of Bacteriology; 181: 5210-5218*

Q-Sense, Inc. 2007. **QCM-D Basic Training Course**. *The New Jersey Center for Biomaterials, Rutgers University*

Reddy, K.V.R., Yedery, R.D., and Aranha, C. 2004. **Antimicrobial Peptides: Premises and Promises.** *International Journal of Antimicrobial Agents; 24: 536-547*

Rodahl, M., Höök, F., Fredriksson, C., Keller, C.A., Krozer, A., Brzezinski, P., Voinova, M., and Kasemo, B. 1997. **Simultaneous frequency and dissipation factor QCM measurements of biomolecular adsorption and cell adhesion.** *Faraday Discussions; 107: 229-246*

Rosenfeld, Y., Shai, Y. 2006. **Lipopolysaccaride (Endotoxin)- Host Defense Antibacterial Peptides Interaction: Role in Bacterial Resistance and Prevention of Sepsis.** *Biochimica er Biophysics Acta; 1756: 1513-1522*

Sauerbrey, G. 1959. **Verwendung von Schwingquarzen zur Wägung Dünner Schichten und zur Mikrowägung.** *Zeitschrift für Physik; 155: 206–222*

Schofield, A.L., Rudd, T.R., Martin, D.S., Fernig, D.G., and Edwards, C. 2007. **Real-time monitoring of the development and stability of biofilms of *Streptococcus mutans* using the quartz crystal microbalance with dissipation monitoring.** *Biosensors and Bioelectronics; 23: 407-413*

Scott, M.G., Vreugdenhil, A.C., Buurman, W.A., Hancock, R.E., and Gold, M.R. 2000. **Cutting Edge: Cationic Antimicrobial Peptides Block the Binding of Lipopolysaccharide (LPS) to LPS Binding Protein.** J. Immunology; *164: 549-553*

Shai, Y. 1999. **Mechanism of the binding, insertion, and destabilization of phospholipids bilayer membranes by α-helical antimicrobial and cell non-selective membrane-lytic peptides.** *Biochimica et Biophysica Acta; 1462: 55-70*

Stephan, R., Ragettli, S. and Untermann, F. 2000. **Prevalence and characteristics of verotoxin-producing *Echerichia coli* (VTEC) in stool samples from asymptomatic human carriers working in the meat processing industry in Switzerland.** *Journal of Applied Microbiology; 82: 335-341.*

Vunnam, S., Juvvadi, P., and Merrifield, R.B. 1997. **Synthesis and antibacterial action of cecropin and proline-arginine-rich peptides from pig intestine**. *The Journal of Peptide Research; 49: 59-66*

Appendix A: QCM-D Frequency and Dissipation Plots

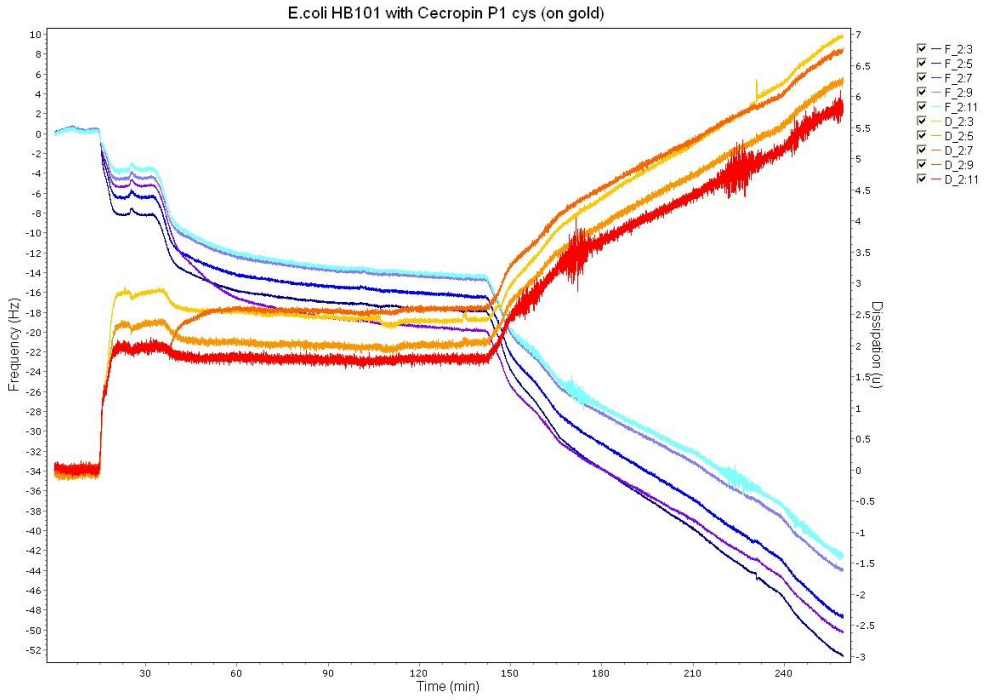

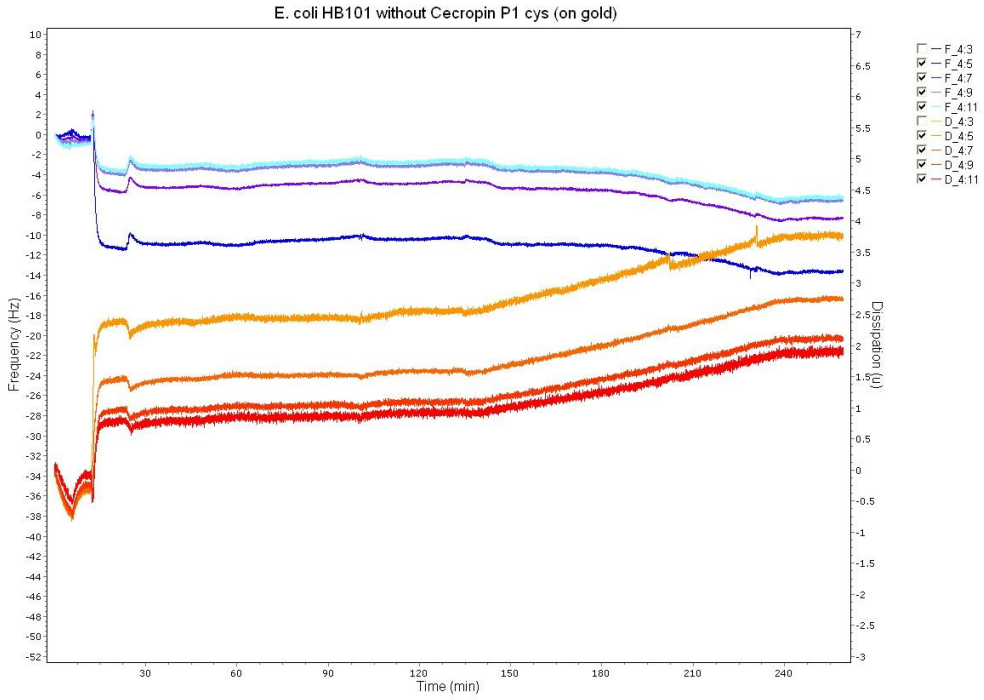

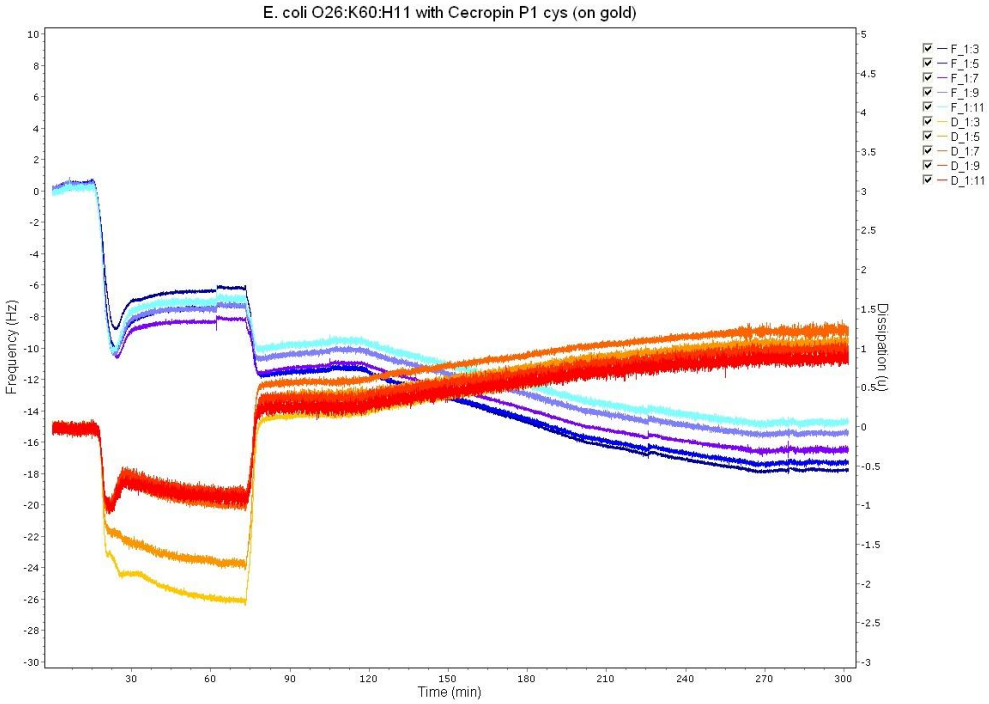
E. coli O26:K60:H11 with Cecropin P1 cys (on gold)
Frequency (Hz)
Dissipation (y)
Time (min)
F_1:3
F_1:5
F_1:7
F_1:9
F_1:11
D_1:3
D_1:5
D_1:7
D_1:9
D_1:11

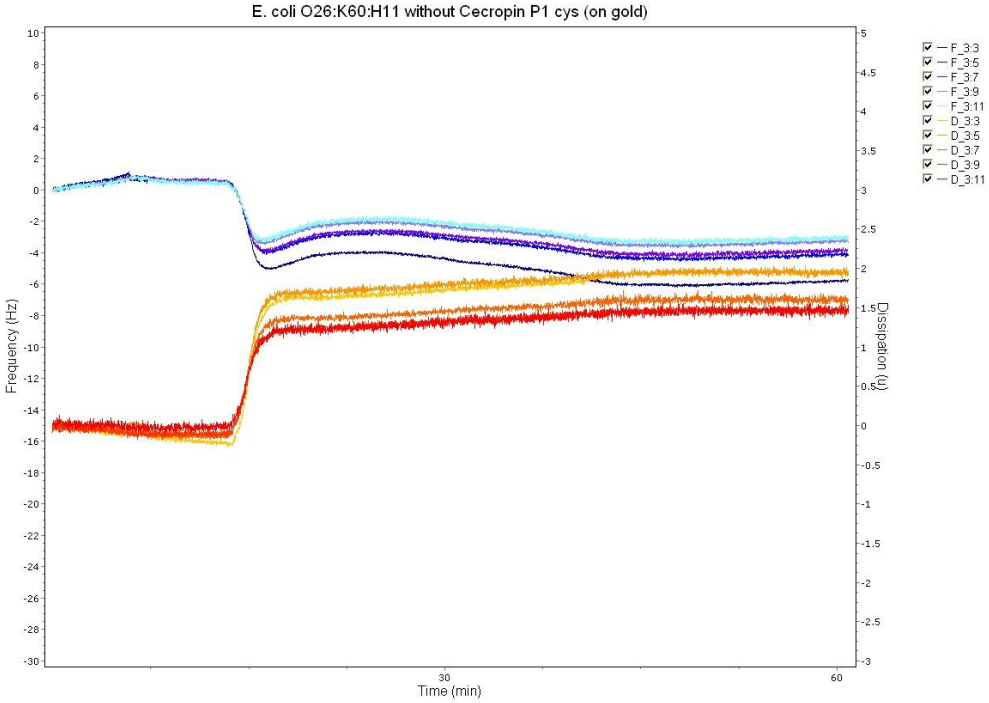
E. coli O26:K60:H11 without Cecropin P1 cys (on gold)
Frequency (Hz)
Dissipation (y)
Time (min)
F_3:3
F_3:5
F_3:7
F_3:9
F_3:11
D_3:3
D_3:5
D_3:7
D_3:9
D_3:11

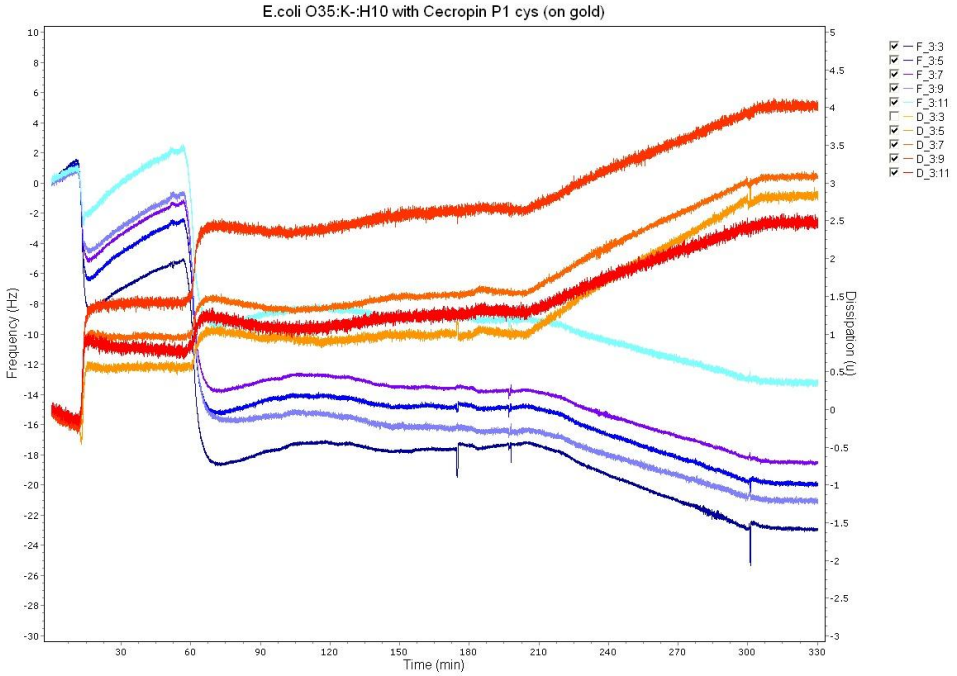
E.coli O35:K-:H10 with Cecropin P1 cys (on gold)
Frequency (Hz)
Dissipation (u)
Time (min)
F_3:3
F_3:5
F_3:7
F_3:9
F_3:11
D_3:3
D_3:5
D_3:7
D_3:9
D_3:11

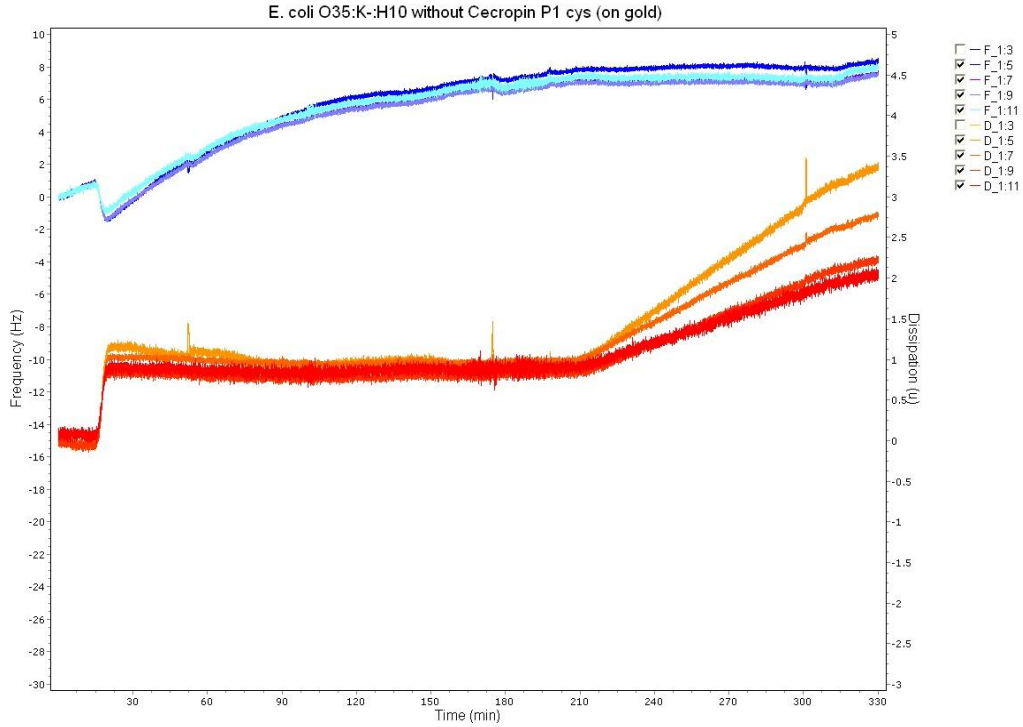
E. coli O35:K-:H10 without Cecropin P1 cys (on gold)
Frequency (Hz)
Dissipation (u)
Time (min)
F_1:3
F_1:5
F_1:7
F_1:9
F_1:11
D_1:3
D_1:5
D_1:7
D_1:9
D_1:11

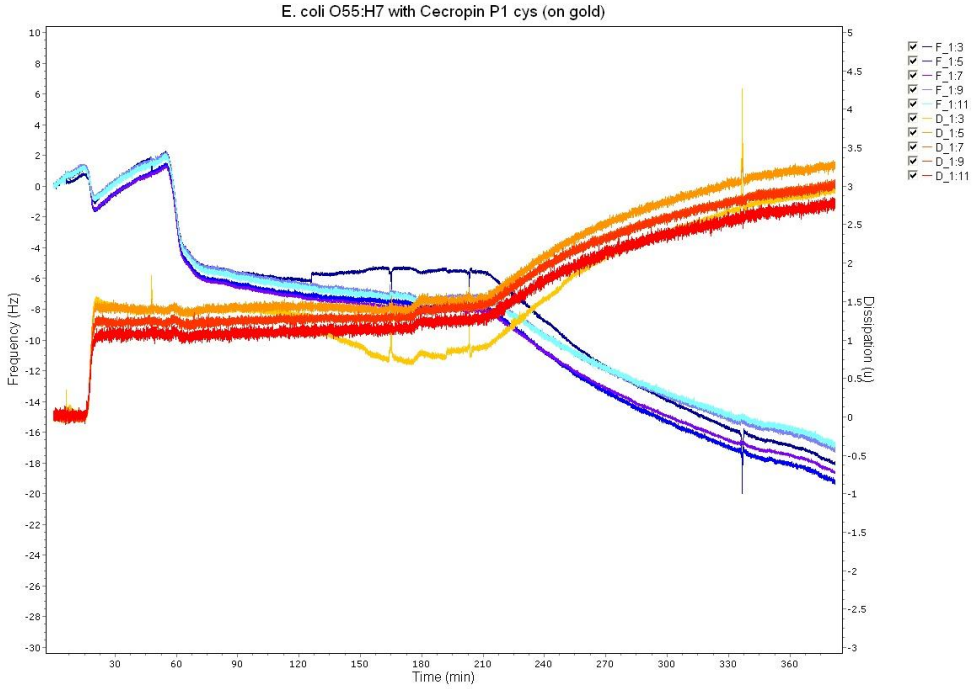
E. coli O55:H7 with Cecropin P1 cys (on gold)
Frequency (Hz)
Dissipation (Δ)
Time (min)
F_1:3
F_1:5
F_1:7
F_1:9
F_1:11
D_1:3
D_1:5
D_1:7
D_1:9
D_1:11

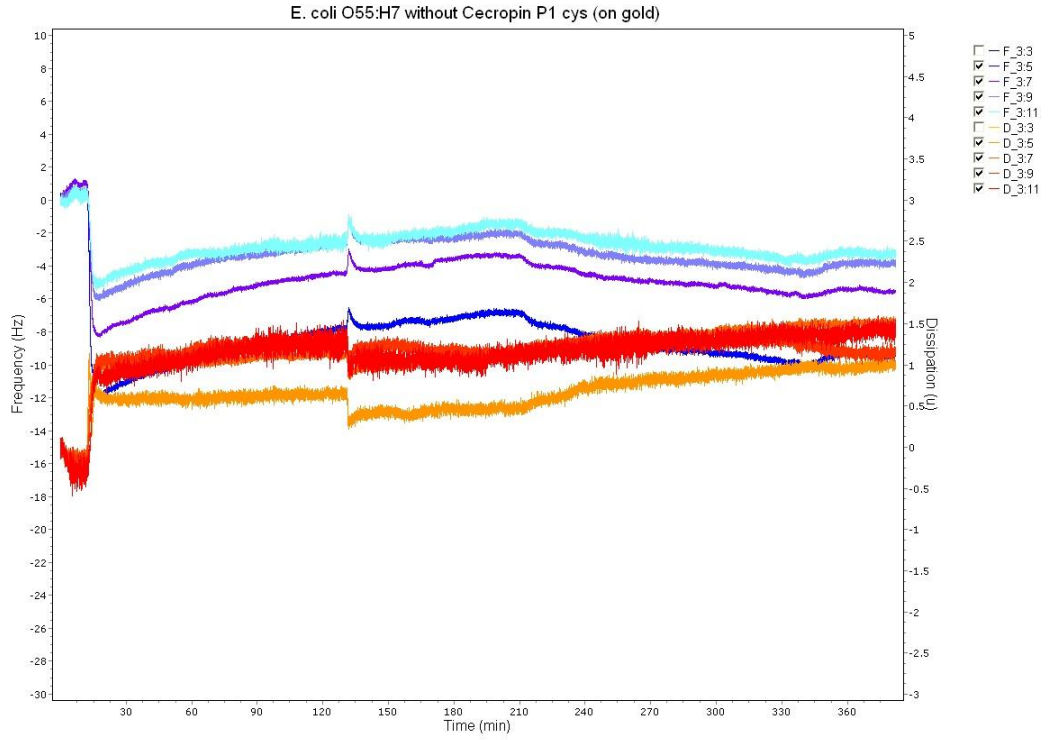
E. coli O55:H7 without Cecropin P1 cys (on gold)
Frequency (Hz)
Dissipation (Δ)
Time (min)
F_3:3
F_3:5
F_3:7
F_3:9
F_3:11
D_3:3
D_3:5
D_3:7
D_3:9
D_3:11

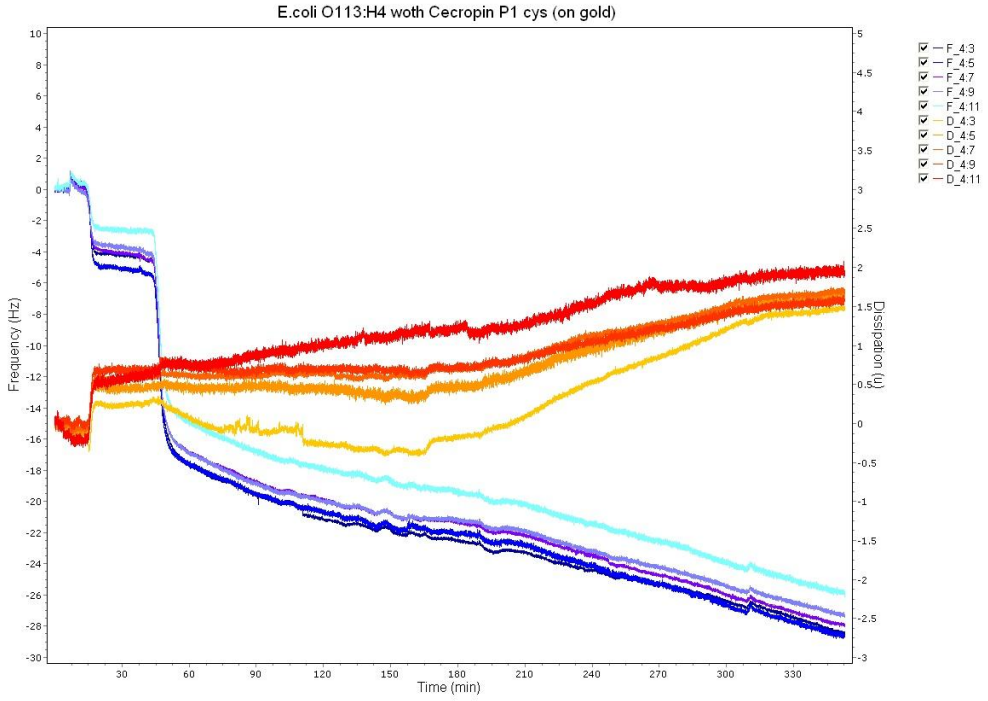
E.coli O113:H4 woth Cecropin P1 cys (on gold)
Frequency (Hz)
Dissipation (µ)
Time (min)
F_4:3
F_4:5
F_4:7
F_4:9
F_4:11
D_4:3
D_4:5
D_4:7
D_4:9
D_4:11

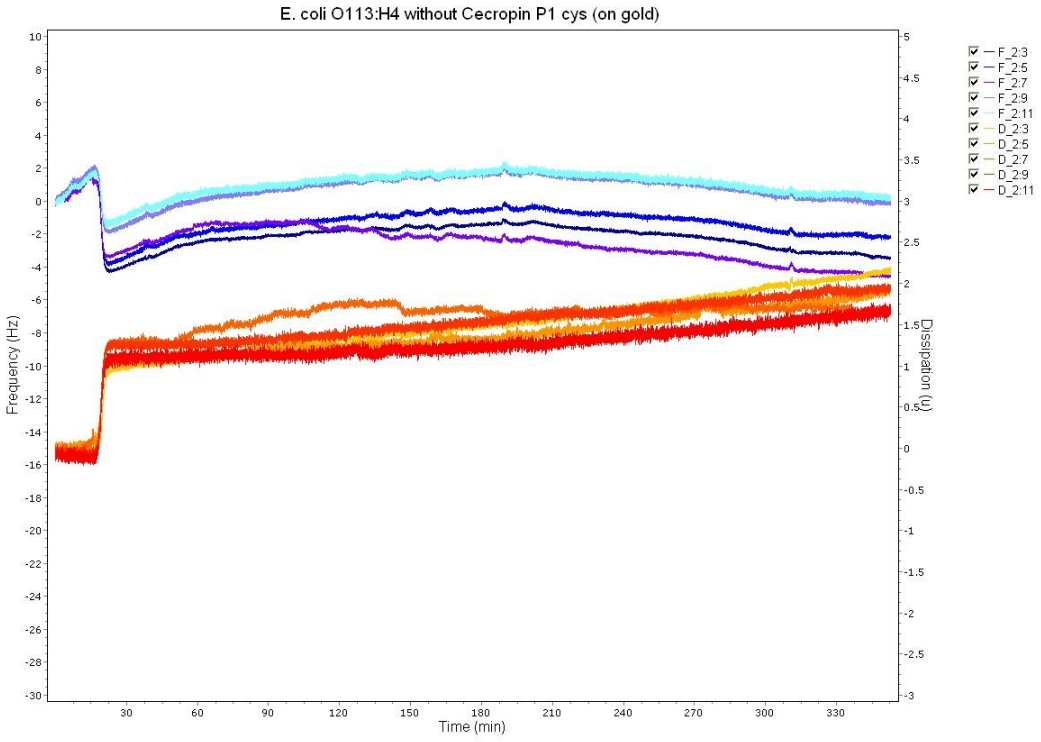
E. coli O113:H4 without Cecropin P1 cys (on gold)
Frequency (Hz)
Dissipation (µ)
Time (min)
F_2:3
F_2:5
F_2:7
F_2:9
F_2:11
D_2:3
D_2:5
D_2:7
D_2:9
D_2:11

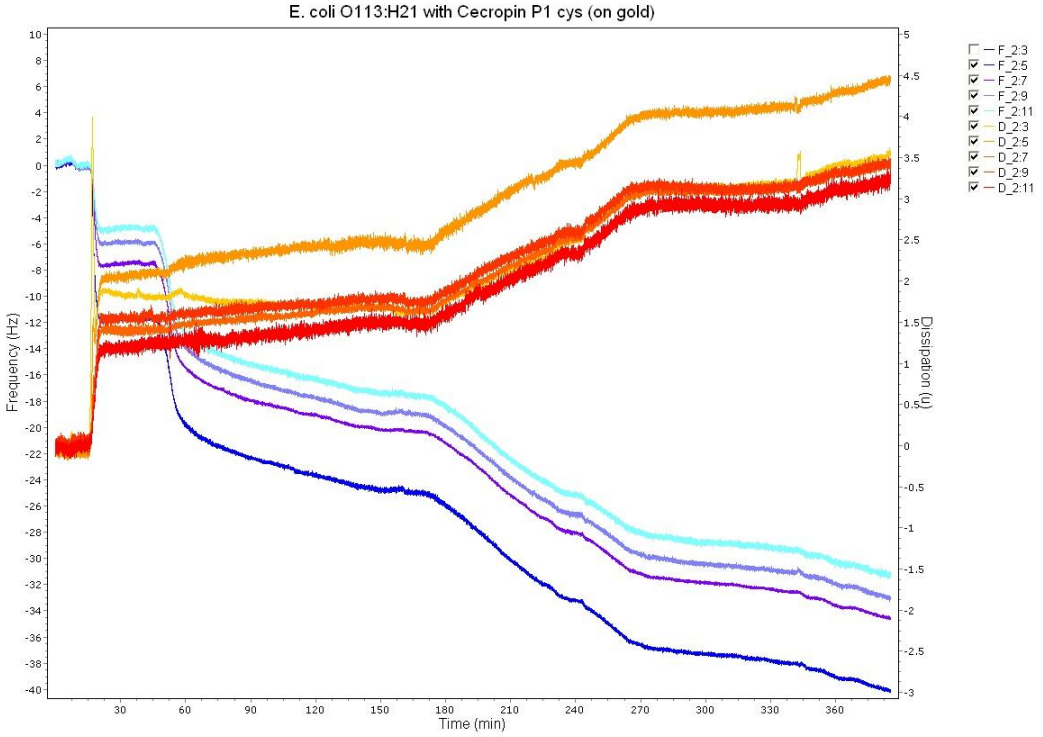
E. coli O113:H21 with Cecropin P1 cys (on gold)
Frequency (Hz)
Dissipation (µ)
Time (min)
F_2:3
F_2:5
F_2:7
F_2:9
F_2:11
D_2:3
D_2:5
D_2:7
D_2:9
D_2:11

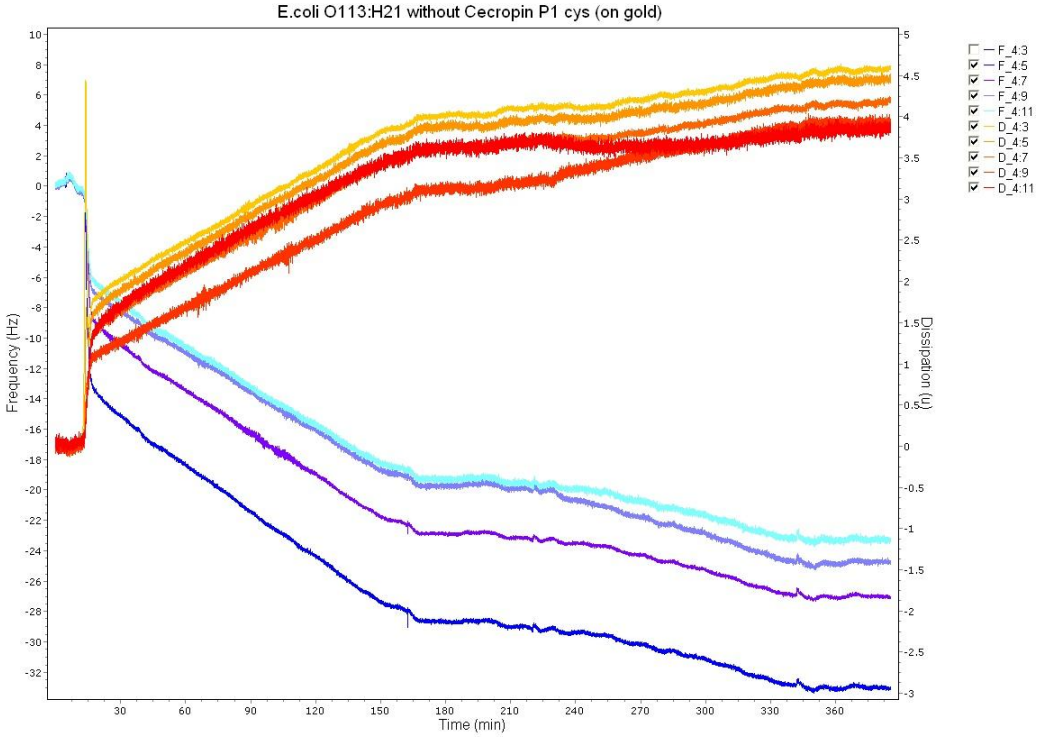
E.coli O113:H21 without Cecropin P1 cys (on gold)
Frequency (Hz)
Dissipation (µ)
Time (min)
F_4:3
F_4:5
F_4:7
F_4:9
F_4:11
D_4:3
D_4:5
D_4:7
D_4:9
D_4:11

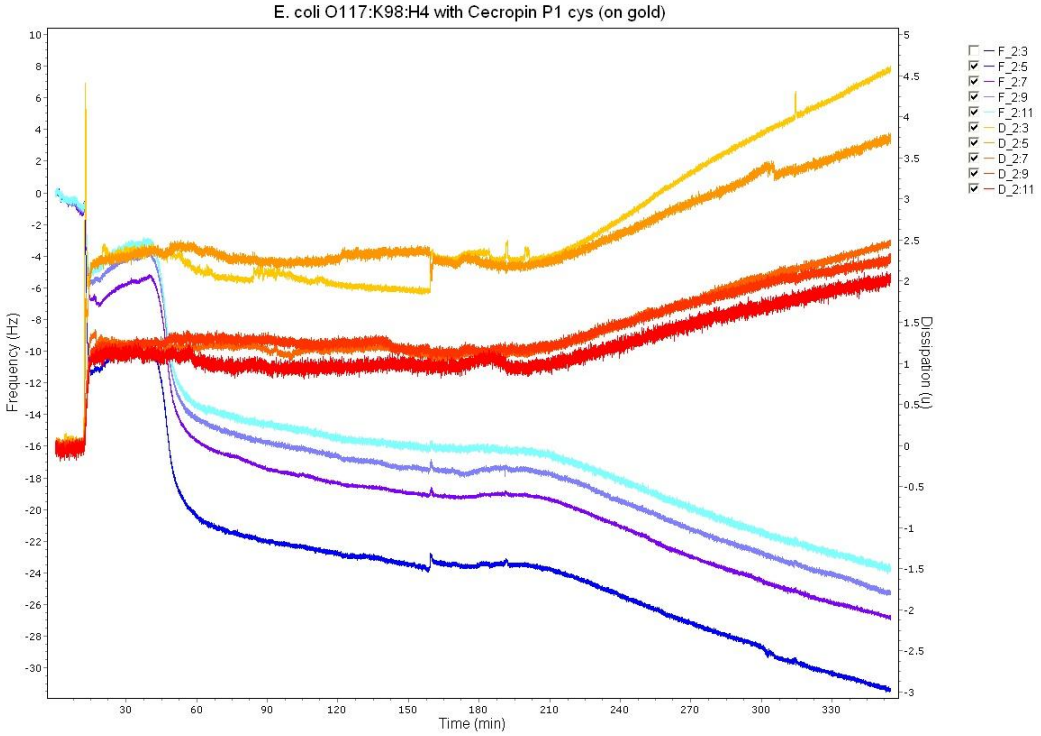
E. coli O117:K98:H4 with Cecropin P1 cys (on gold)
Frequency (Hz)
Dissipation (µ)
Time (min)
F_2:3
F_2:5
F_2:7
F_2:9
F_2:11
D_2:3
D_2:5
D_2:7
D_2:9
D_2:11

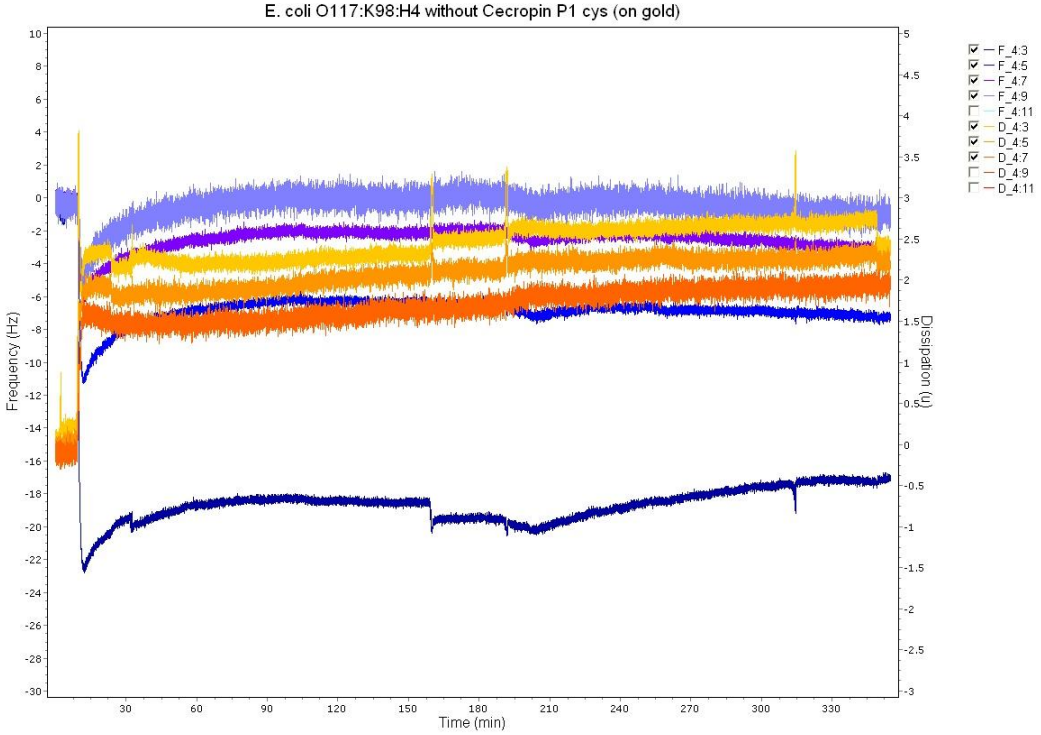
E. coli O117:K98:H4 without Cecropin P1 cys (on gold)
Frequency (Hz)
Dissipation (µ)
Time (min)
F_4:3
F_4:5
F_4:7
F_4:9
F_4:11
D_4:3
D_4:5
D_4:7
D_4:9
D_4:11

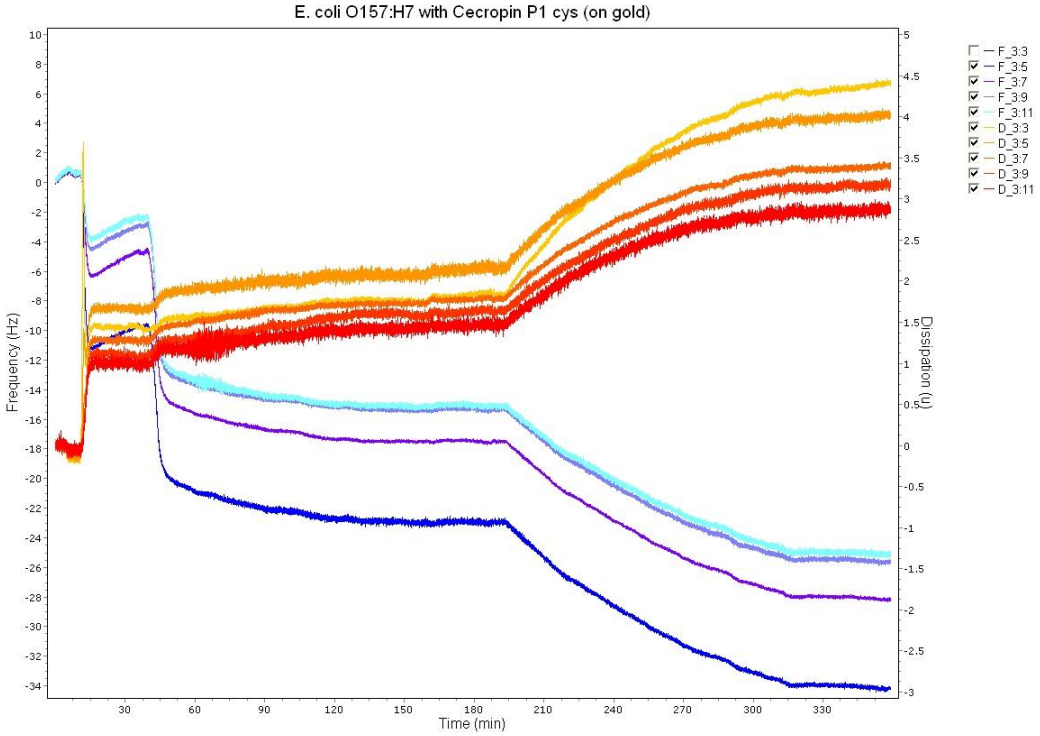
E. coli O157:H7 with Cecropin P1 cys (on gold)
Frequency (Hz)
Dissipation (1)
Time (min)
F_3:3
F_3:5
F_3:7
F_3:9
F_3:11
D_3:3
D_3:5
D_3:7
D_3:9
D_3:11

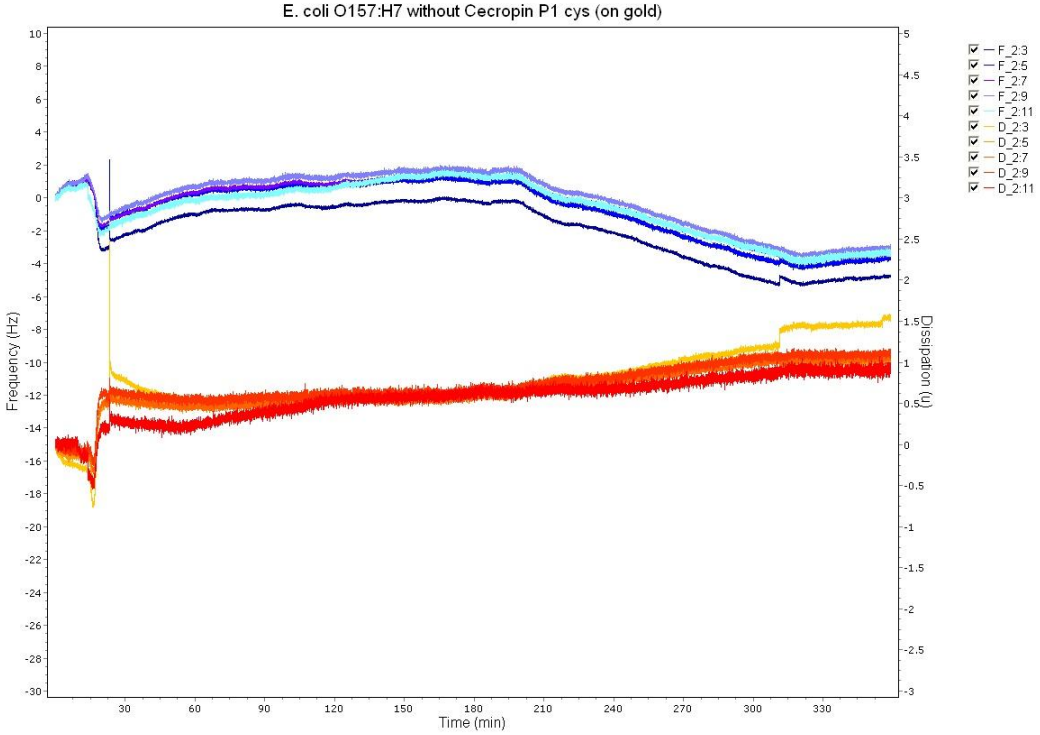
E. coli O157:H7 without Cecropin P1 cys (on gold)
Frequency (Hz)
Dissipation (1)
Time (min)
F_2:3
F_2:5
F_2:7
F_2:9
F_2:11
D_2:3
D_2:5
D_2:7
D_2:9
D_2:11

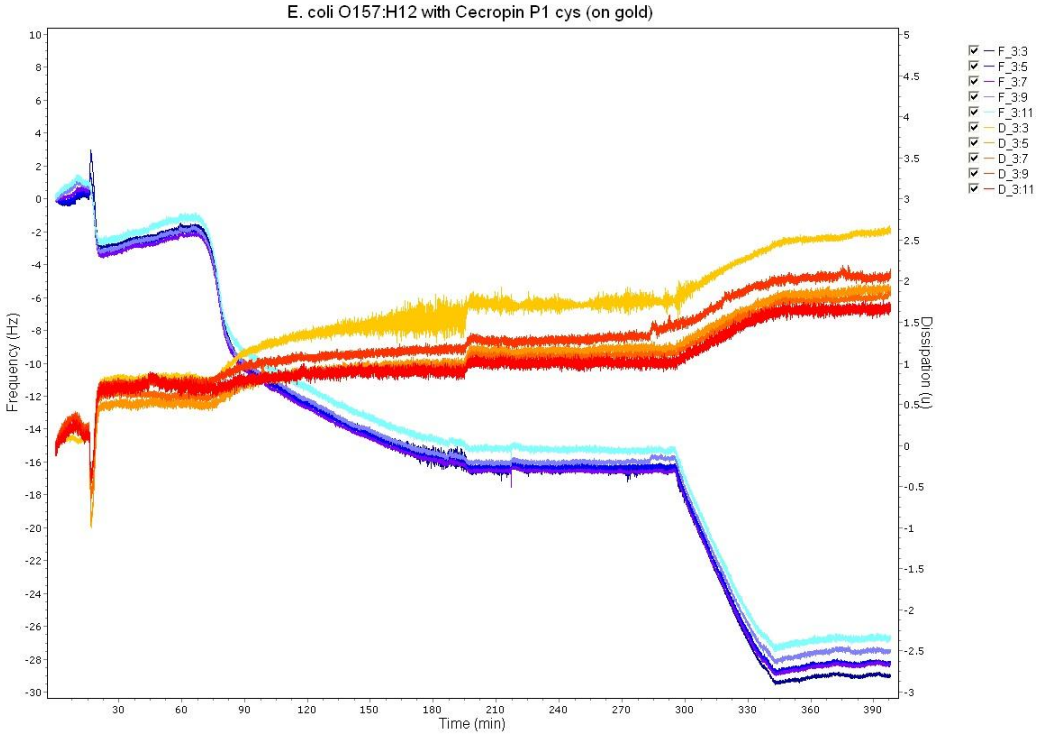
E. coli O157:H12 with Cecropin P1 cys (on gold)
Frequency (Hz)
Dissipation (μ)
Time (min)
F_3:3
F_3:5
F_3:7
F_3:9
F_3:11
D_3:3
D_3:5
D_3:7
D_3:9
D_3:11

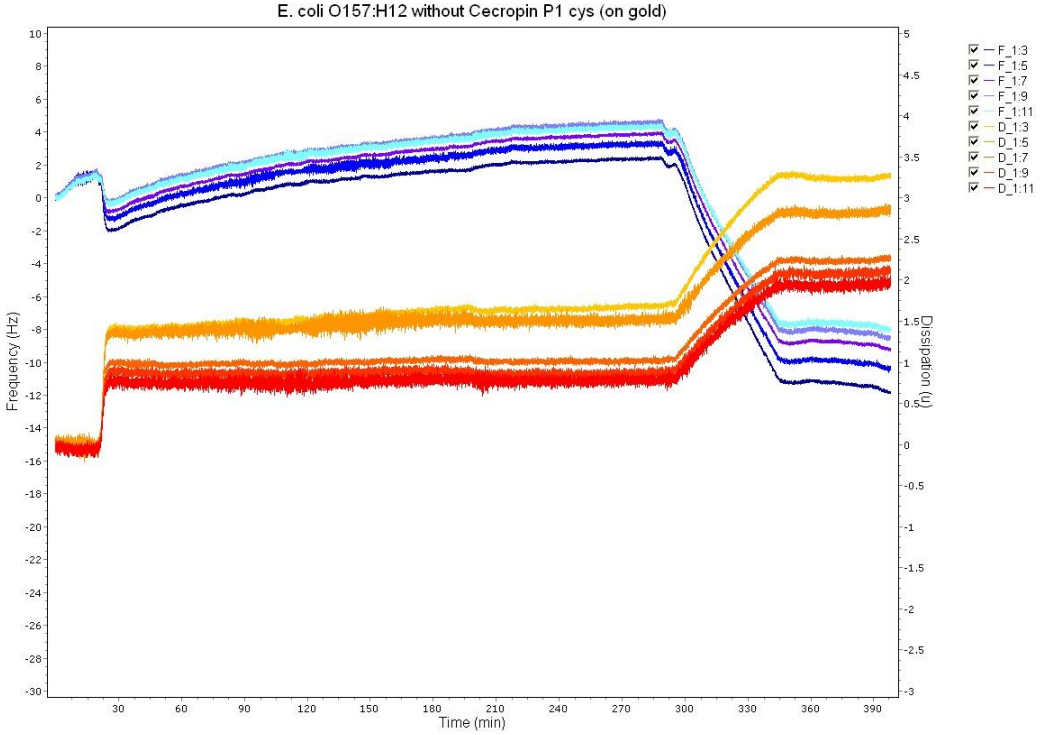
E. coli O157:H12 without Cecropin P1 cys (on gold)
Frequency (Hz)
Dissipation (μ)
Time (min)
F_1:3
F_1:5
F_1:7
F_1:9
F_1:11
D_1:3
D_1:5
D_1:7
D_1:9
D_1:11

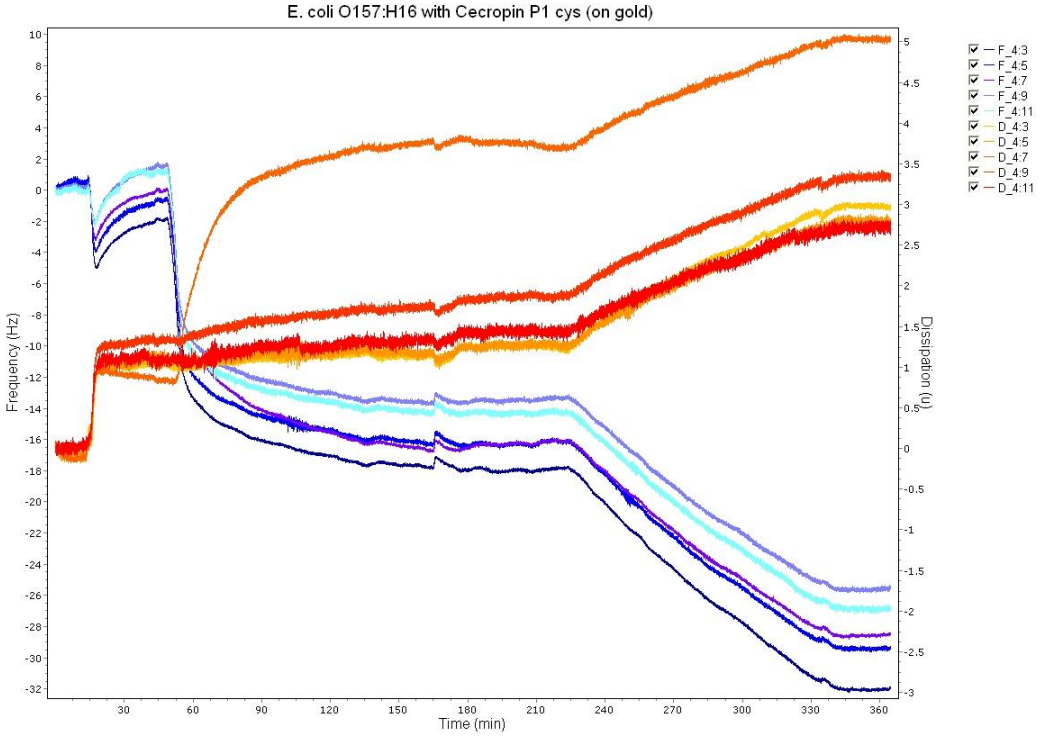
E. coli O157:H16 with Cecropin P1 cys (on gold)
Frequency (Hz)
Dissipation (µ)
Time (min)
F_4:3
F_4:5
F_4:7
F_4:9
F_4:11
D_4:3
D_4:5
D_4:7
D_4:9
D_4:11

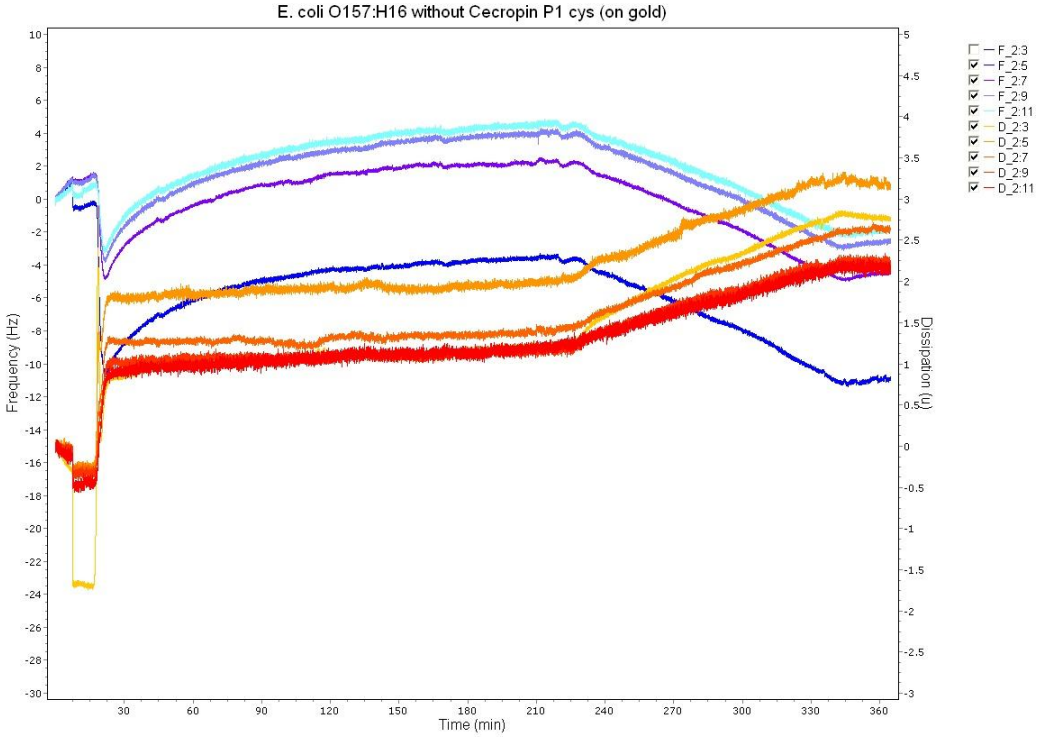
E. coli O157:H16 without Cecropin P1 cys (on gold)
Frequency (Hz)
Dissipation (µ)
Time (min)
F_2:3
F_2:5
F_2:7
F_2:9
F_2:11
D_2:3
D_2:5
D_2:7
D_2:9
D_2:11

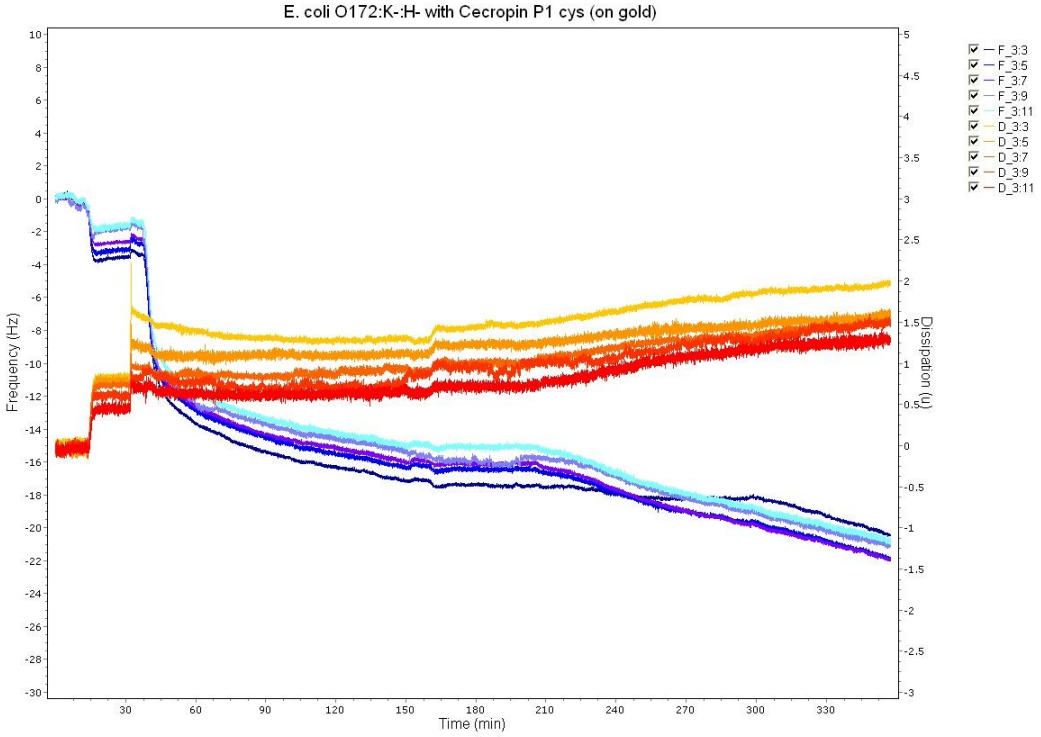
E. coli O172:K-:H- with Cecropin P1 cys (on gold)
Frequency (Hz)
Dissipation (µ)
Time (min)
F_3:3
F_3:5
F_3:7
F_3:9
F_3:11
D_3:3
D_3:5
D_3:7
D_3:9
D_3:11

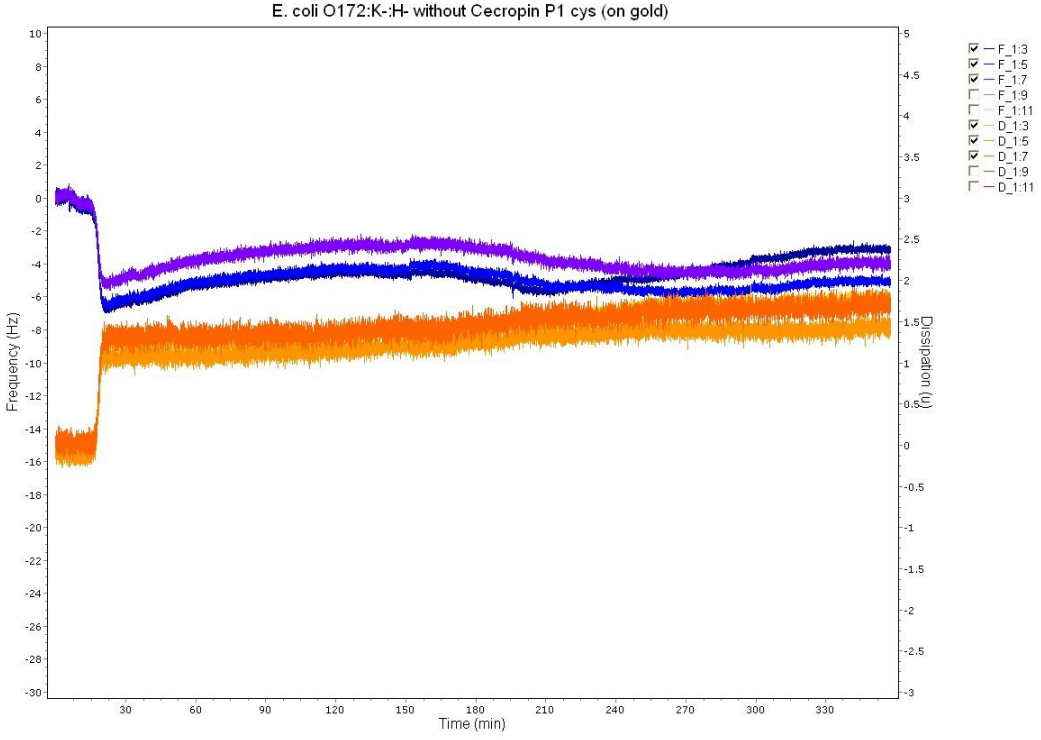
E. coli O172:K-:H- without Cecropin P1 cys (on gold)
Frequency (Hz)
Dissipation (µ)
Time (min)
F_1:3
F_1:5
F_1:7
F_1:9
F_1:11
D_1:3
D_1:5
D_1:7
D_1:9
D_1:11

Appendix B: QCM-D Frequency and Dissipation Shifts

			Δf (Hz)				
E. coli Strain	Crystal #	With CP1?	PBS (1st)	Cecropin P1 cys	PBS (2nd)	*E. coli*	PBS (3rd)
HB101 *didn't do second was for this strain	2	yes	-6.0	-10.0		-32.0	-8.0
	3	yes	-5.0	-15.0		-19.0	-1.0
	4	no	-5.0			-3.0	-1.0
O26:K60:H11 *didn't do PBS before CP1 and also CP1 was in water	1	yes		-8.0	-3.0	-5.0	-0.5
	2	yes		-9.0	-3.0	-6.5	-0.5
	3	yes		-8.0	-6.0	-10.0	-0.5
	4	yes		-9.0	-3.5	-8.0	-0.5
	3	no	-4.0			0.5	
O35:K-:H10	1	no	7.0			0.5	1.5
	2	yes	-4.0	-11.0	1.0	-6.0	-0.5
	3	yes	-2.0	-5.5	0.0	-5.0	-0.5
	4	no	7.0			-0.5	0.5
	1	no	-3.0			-1.0	-0.5
	2	no	-3.5			-0.5	-0.5
	4	yes	-5.5	-15.0	0.5	-3.5	-2.0
O55:H7	1	yes	1.5	-9.0	0.5	-8.5	-2.0
	2	yes	1.0	-10.0	0.5	-10.0	-2.5
	3	no	-2.5			-2.5	1.5
	4	no	-1.5			-3.0	0.0
O113:H4	1	no	6.5			-2.5	0.5
	2	no	-2.0			-2.5	-0.5
	3	yes	-6.0	-12.0	0.0	-4.5	-1.5
	4	yes	-4.0	-15.0	0.5	-4.5	-1.5
O113:H21	1	yes	-5.0	-13.0	-7.0	-3.0	-1.0
	2	yes	-7.0	-12.0	-6.0	-4.5	-1.5
	3	no	-20.5			-2.0	-1.0
	4	no	-18.5			-4.0	0.5
O117:K98:H4	2	yes	-4.5	-13.5	-0.5	-6.0	-2.0
	4	no	-2.0			-1.0	0.0
	1	no	-1.0			0.5	0.0
	2	no	-0.5			-0.5	0.0
	3	yes	-3.0	-13.0	0.0	-2.5	-1.5
	4	yes	-2.0	-12.5	1.0	-2.0	0.0
O157:H7	2	no	1.5			-5.0	1.0
	3	yes	-4.0	-12.0	0.0	-10.0	-0.5
	4	yes	-4.5	-13.5	-2.0	-6.0	-0.5
O157:H12	1	no	3.5			-11.5	-0.5
	2	no	6.5			-12.0	0.0
	3	yes	-2.5	-14.4	0.0	-13.0	0.0
	4	yes	-1.0	-19.0	0.5	-13.5	0.5
O157:H16	1	yes	-4.0	-13.5	0.0	-10.0	0.5
	2	no	-4.0			-7.0	0.5
	3	no	-3.5			-5.5	1.0
	4	yes	-2.0	-16.5	0.0	-11.5	0.0
O172:K-:H-	1	no	-4.5			-2.0	1.0
	2	no	-3.0			-2.5	0.0
	3	yes	-3.0	-13.5	0.0	-3.5	-2.0
	4	yes	-3.0	-14.5	0.5	-4.0	-1.5

			ΔD (μ)				
E. coli Strain	Crystal #	With CP1?	PBS (1st)	Cecropin P1 cys	PBS (2nd)	*E. coli*	PBS (3rd)
HB101 *didn't do second wash for this strain	2	yes	2.250	0.000		3.750	0.750
	3	yes	1.750	0.625		2.625	0.250
	4	no	1.000			0.750	0.000
O26:K60:H11 *didn't do PBS before CP1 and also CP1 was in	1	yes		-1.000	1.250	0.750	0.125
	2	yes		-1.000	1.500	0.500	0.125
	3	yes		-0.500	0.750	1.000	0.125
	4	yes		0.125	1.125	0.625	0.125
	3	no					
O35:K-:H10	1	no	1.000			1.000	0.250
	2	yes	1.125	0.500	0.125	1.000	0.375
	3	yes	0.875	0.500	0.000	2.750	0.125
	4	no	-0.125			3.000	0.000
	1	no	1.250			1.000	0.250
	2	no	2.625			0.875	0.250
	4	yes	1.875	0.125	0.125	0.750	0.250
O55:H7	1	yes	1.250	0.000	0.125	1.250	0.250
	2	yes	1.000	0.000	0.125	1.500	0.375
	3	no	1.000			0.375	0.000
	4	no	1.250			0.250	0.125
O113:H4	1	no	0.125			0.250	0.000
	2	no	1.250			0.500	0.125
	3	yes	1.125	0.500	0.250	1.375	0.125
	4	yes	0.500	0.250	0.000	0.750	0.125
O113:H21	1	yes	1.125	0.250	1.250	0.625	0.125
	2	yes	1.625	0.250	1.375	0.375	0.250
	3	no	2.875			0.250	0.125
	4	no	3.500			0.750	0.125
O117:K98:H4	2	yes	1.750	0.250	0.000	0.750	0.250
	4	no	1.750			0.125	0.000
	1	no	2.250			0.250	0.125
	2	no	1.250			0.250	0.125
	3	yes	1.125	0.250	0.000	0.375	0.250
	4	yes	1.125	0.250	0.000	0.375	0.250
O157:H7	2	no	0.500			0.500	0.125
	3	yes	1.375	0.500	0.125	1.625	0.125
	4	yes	0.625	0.125	0.125	0.625	0.000
O157:H12	1	no	1.250			1.500	0.125
	2	no	0.125			1.500	0.000
	3	yes	0.750	0.500	0.000	1.875	0.125
	4	yes	3.000	1.250	0.000	0.875	0.250
O157:H16	1	yes	1.000	0.125	0.125	1.000	0.250
	2	no	1.250			1.000	-0.125
	3	no	0.750			0.750	0.000
	4	yes	1.125	0.250	0.125	1.500	0.125
O172:K-:H-	1	no	1.375			0.375	0.125
	2	no	2.000			0.375	0.000
	3	yes	0.750	0.250	0.000	0.500	0.125
	4	yes	0.750	0.000	0.000	0.375	0.125

Appendix C: Live/Dead Cell Count Raw Data

Strain:	**O26:K60:H11**	**O26:K60:H11**	**O26:K60:H11**	**O26:K60:H11**	**O157:H12**	**O157:H12**	**O157:H12**	**O157:H12**
Picture:	**Crystal 1 CP1**	**Crystal 2 CP1**	**no CP1-cys**	**no CP1-cys**	**no CP1-cys 1**	**no CP1- cys 2**	**CP1-cys 3**	**CP1-cys 4**
1 Live	8	32	44	5	4	34	8	17
1 Dead	3	9	14	1	16	20	19	25
% Dead 1	27.27272727	21.95121951	24.13793103	16.66666667	80	37.03703704	70.37037037	59.52380952
Bacteria per pic	11	41	58	6	20	54	27	42
2 Live	8	10	41	26	10	36	7	16
2 Dead	7	1	15	17	14	14	19	9
% Dead 2	46.66666667	9.090909091	26.78571429	39.53488372	58.33333333	28	73.07692308	36
Bacteria per pic	15	11	56	43	24	50	26	25
3 Live	16	61	63	34	3	37	8	17
3 Dead	6	4	5	1	10	17	27	31
% Dead 3	27.27272727	6.153846154	7.352941176	2.857142857	76.92307692	31.48148148	77.14285714	64.58333333
Bacteria per pic	22	65	68	35	13	54	35	48
4 Live	13	9	14	12	4	27	8	46
4 Dead	1	2	21	9	18	6	23	21
% Dead 4	7.142857143	18.18181818	60	42.85714286	81.81818182	18.18181818	74.19354839	31.34328358
Bacteria per pic	14	11	35	21	22	33	31	67
5 Live	15	25	31	12	15	52	10	30
5 Dead	3	7	32	3	8	12	59	31
% Dead 5	16.66666667	21.875	50.79365079	20	34.7826087	18.75	85.50724638	50.81967213
Bacteria per pic	18	32	63	15	23	64	69	61
6 Live	7	35	87	16	13	26	6	16
6 Dead	2	6	37	6	14	12	72	14
% Dead 6	22.22222222	14.63414634	29.83870968	27.27272727	51.85185185	31.57894737	92.30769231	46.66666667
Bacteria per pic	9	41	124	22	27	38	78	30
7 Live	16	30	35	59	43	32	7	14
7 Dead	1	88	4	3	1	21	33	35
% Dead 7	5.882352941	74.57627119	10.25641026	4.838709677	2.272727273	39.62264151	82.5	71.42857143
Bacteria per pic	17	118	39	62	44	53	40	49
8 Live	15	48	36	12	9	43	6	6
8 Dead	6	10	7	9	24	5	14	45
% Dead 8	28.57142857	17.24137931	16.27906977	42.85714286	72.72727273	10.41666667	70	88.23529412
Bacteria per pic	21	58	43	21	33	48	20	51
9 Live	9	42	56	9	9	50	10	27
9 Dead	6	0	19	5	10	6	13	20
% Dead 9	40	0	25.33333333	35.71428571	52.63157895	10.71428571	56.52173913	42.55319149
Bacteria per pic	15	42	75	14	19	56	23	47
10 Live	28	30	57	15	39	35	12	72
10 Dead	3	3	27	3	6	5	20	20
% Dead 10	9.677419355	9.090909091	32.14285714	16.66666667	13.33333333	12.5	62.5	21.73913043
Bacteria per pic	31	33	84	18	45	40	32	92
11 Live	33	16	16	11	12	23	8	35
11 Dead	2	0	0	7	11	6	65	75
% Dead 11	5.714285714	0	0	38.88888889	47.82608696	20.68965517	89.04109589	68.18181818
Bacteria per pic	35	16	16	18	23	29	73	110
12 Live	8	29	11	8	13	39	8	20
12 Dead	7	18	5	2	18	4	59	79
% Dead 12	46.66666667	38.29787234	31.25	20	58.06451613	9.302325581	88.05970149	79.7979798
Bacteria per pic	15	47	16	10	31	43	67	99
13 Live	13	88	7	26	8	58	11	100
13 Dead	1	45	2	2	9	8	54	40
% Dead 13	7.142857143	33.83458647	22.22222222	7.142857143	52.94117647	12.12121212	83.07692308	28.57142857
Bacteria per pic	14	133	9	28	17	66	65	140
14 Live	43	5		10	9	35	13	29
14 Dead	4	3		10	10	10	77	198
% Dead 14	8.510638298	37.5		50	52.63157895	22.22222222	85.55555556	87.2246696
Bacteria per pic	47	8	0	20	19	45	90	227
15 Live	140	10		2	6	32	12	87
15 Dead	3	5		2	7	10	76	30
% Dead 15	2.097902098	33.33333333		50	53.84615385	23.80952381	86.36363636	25.64102564
Bacteria per pic	143	15	0	4	13	42	88	117
Avg % Dead per pic	20.10049454	22.38408607	22.42618931	27.68647429	52.66556515	21.76185446	78.41448594	53.48732497
Avg of crystals % dead		21.2422903		25.0563318		37.2137098		65.95090546
St. Dev of % dead		17.15029328		16.06286447		23.22164434		21.40488291
Average bacteria/ pic	28.46666667	44.73333333	45.73333333	22.46666667	24.86666667	47.66666667	50.93333333	80.33333333
Avg bacteria per pic		36.6		34.1		36.26666667		65.63333333
St Dev of bacteria per pic		35.67148963		28.8531956		15.30592253		43.48640956

Strain:	O172:H-	O172:H-	O172:H-	O172:H-	O113:H4	O113:H4	O113:H4	O113:H4
Picture:	no cys crystal 1	no cys crystal	cys crystal 3	cys crystal 4	no cys crystal	no cys crystal 2	cys crystal 3	cys crystal 4
1 Live	54	41	360	280	90	109	71	77
1 Dead	6	17	45	37	11	0	20	64
% Dead 1	10	29.31034483	11.11111111	11.67192429	10.89108911	0	21.97802198	45.39007092
Bacteria per pic	60	58	405	317	101	109	91	141
2 Live	27	18	388	344	47	59	67	71
2 Dead	29	11	64	57	1	0	8	32
% Dead 2	51.78571429	37.93103448	14.15929204	14.21446384	2.083333333	0	10.66666667	31.06796117
Bacteria per pic	56	29	452	401	48	59	75	103
3 Live	30	25	320	340	98	46	66	90
3 Dead	33	24	56	49	2	0	4	36
% Dead 3	52.38095238	48.97959184	14.89361702	12.59640103	2	0	5.714285714	28.57142857
Bacteria per pic	63	49	376	389	100	46	70	126
4 Live	20	28	400	332	71	77	76	62
4 Dead	11	15	56	47	3	0	15	50
% Dead 4	35.48387097	34.88372093	12.28070175	12.40105541	4.054054054	0	16.48351648	44.64285714
Bacteria per pic	31	43	456	379	74	77	91	112
5 Live	37	39	504	220	55	78	66	70
5 Dead	10	20	40	44	4	0	15	66
% Dead 5	21.27659574	33.89830508	7.352941176	16.66666667	6.779661017	0	18.51851852	48.52941176
Bacteria per pic	47	59	544	264	59	78	81	136
6 Live	31	30	328	288	40	58	56	104
6 Dead	14	15	40	44	8	0	9	54
% Dead 6	31.11111111	33.33333333	10.86956522	13.25301205	16.66666667	0	13.84615385	34.17721519
Bacteria per pic	45	45	368	332	48	58	65	158
7 Live	26	9	260	264	94	56	62	52
7 Dead	10	18	40	51	3	0	12	73
% Dead 7	27.77777778	66.66666667	13.33333333	16.19047619	3.092783505	0	16.21621622	58.4
Bacteria per pic	36	27	300	315	97	56	74	125
8 Live	47	15	304	312	60	32	70	52
8 Dead	11	12	52	59	2	0	14	71
% Dead 8	18.96551724	44.44444444	14.60674157	15.90296496	3.225806452	0	16.66666667	57.72357724
Bacteria per pic	58	27	356	371	62	32	84	123
9 Live	42	25	408	312	55	98	81	72
9 Dead	12	20	67	64	0	0	14	89
% Dead 9	22.22222222	44.44444444	14.10526316	17.0212766	0	0	14.73684211	55.27950311
Bacteria per pic	54	45	475	376	55	98	95	161
10 Live	49	37	384	268	496	61	45	92
10 Dead	19	26	40	60	1	0	15	71
% Dead 10	27.94117647	41.26984127	9.433962264	18.29268293	0.201207243	0	25	43.55828221
Bacteria per pic	68	63	424	328	497	61	60	163
11 Live	31	55	400	336	63	51	84	142
11 Dead	16	24	88	80	0	0	23	68
% Dead 11	34.04255319	30.37974684	18.03278689	19.23076923	0	0	21.4953271	32.38095238
Bacteria per pic	47	79	488	416	63	51	107	210
12 Live	57	41	280	364	75	64	57	156
12 Dead	12	21	104	70	0	0	23	97
% Dead 12	17.39130435	33.87096774	27.08333333	16.12903226	0	0	28.75	38.33992095
Bacteria per pic	69	62	384	434	75	64	80	253
13 Live	25	33	340	240	56	66	50	118
13 Dead	17	41	46	164	2	3	19	67
% Dead 13	40.47619048	55.40540541	11.91709845	40.59405941	3.448275862	4.347826087	27.53623188	36.21621622
Bacteria per pic	42	74	386	404	58	69	69	185
14 Live	31	49	424	272	34	53	29	133
14 Dead	13	38	50	69	0	0	23	49
% Dead 14	29.54545455	43.67816092	10.54852321	20.23460411	0	0	44.23076923	26.92307692
Bacteria per pic	44	87	474	341	34	53	52	182
15 Live	27	21	300	196	86	52	66	113
15 Dead	13	18	100	104	1	3	132	50
% Dead 15	32.5	46.15384615	25	34.66666667	1.149425287	5.454545455	66.66666667	30.67484663
Bacteria per pic	40	39	400	300	87	55	198	163
Avg % Dead per pic	30.19336272	41.64332363	14.31521803	18.60440371	3.572820169	0.653491436	23.23372554	40.79168803
Avg of crystals % dead		23.94556211		16.45981087		2.113155802		32.01270678
St. Dev of % dead		12.29828346		7.167225691		3.783126221		15.61562002
Average bacteria/ pic	50.66666667	52.4	419.2	357.8	97.2	64.4	86.13333333	156.0666667
Avg bacteria per pic		51.53333333		388.5		80.8		121.1
St Dev of bacteria per pic		15.27164001		63.067971		81.05102692		50.93359436

	Strain:						
	HB 101	**HB 101**	**HB 101**	**HB 101**	**O35:K-:H10**	**O35:K-:H10**	**O35:K-:H10**
Picture:	**no cys crystal 1**	**cys crystal 2**	**cys crystal 2**	**no cys crystal**	**cys crystal 2**	**cys crystal 3**	**no cys crystal**
1 Live	12	43	4	20	23	63	672
1 Dead	72	1	83	44	46	17	0
% Dead 1	85.71428571	2.272727273	95.40229885	68.75	66.66666667	21.25	0
Bacteria per pic	84	44	87	64	69	80	672
2 Live	21	25	5	24	25	87	79
2 Dead	32	7	54	42	29	51	10
% Dead 2	60.37735849	21.875	91.52542373	63.63636364	53.7037037	36.95652174	11.23595506
Bacteria per pic	53	32	59	66	54	138	89
3 Live	25	34	4	55	26	56	64
3 Dead	14	9	80	41	12	49	0
% Dead 3	35.8974359	20.93023256	95.23809524	42.70833333	31.57894737	46.66666667	0
Bacteria per pic	39	43	84	96	38	105	64
4 Live	99	31	10	47	58	60	12
4 Dead	52	44	85	92	13	15	8
% Dead 4	34.43708609	58.66666667	89.47368421	66.18705036	18.30985915	20	40
Bacteria per pic	151	75	95	139	71	75	20
5 Live	5	99	3	29	196	10	11
5 Dead	16	0	96	76	0	66	9
% Dead 5	76.19047619	0	96.96969697	72.38095238	0	86.84210526	45
Bacteria per pic	21	99	99	105	196	76	20
6 Live	13	34	5	27	50	44	2
6 Dead	24	17	53	80	30	13	0
% Dead 6	64.86486486	33.33333333	91.37931034	74.76635514	37.5	22.80701754	0
Bacteria per pic	37	51	58	107	80	57	2
7 Live	40	5	2	33	37	76	4
7 Dead	43	3	91	79	39	43	0
% Dead 7	51.80722892	37.5	97.84946237	70.53571429	51.31578947	36.13445378	0
Bacteria per pic	83	8	93	112	76	119	4
8 Live	19	26	2	29	67	32	45
8 Dead	44	28	83	75	54	23	16
% Dead 8	69.84126984	51.85185185	97.64705882	72.11538462	44.62809917	41.81818182	26.2295082
Bacteria per pic	63	54	85	104	121	55	61
9 Live	11	141	4	49	67	44	100
9 Dead	13	46	66	82	46	39	11
% Dead 9	54.16666667	24.59893048	94.28571429	62.59541985	40.7079646	46.98795181	9.90990991
Bacteria per pic	24	187	70	131	113	83	111
10 Live	10	7	3	39	30	41	8
10 Dead	19	14	56	55	79	39	0
% Dead 10	65.51724138	66.66666667	94.91525424	58.5106383	72.47706422	48.75	0
Bacteria per pic	29	21	59	94	109	80	8
11 Live	25	7	27	19	32	58	7
11 Dead	17	50	50	49	66	53	0
% Dead 11	40.47619048	87.71929825	64.93506494	72.05882353	67.34693878	47.74774775	0
Bacteria per pic	42	57	77	68	98	111	7
12 Live	20	31	7	11	74	49	46
12 Dead	15	18	40	66	34	16	0
% Dead 12	42.85714286	36.73469388	85.10638298	85.71428571	31.48148148	24.61538462	0
Bacteria per pic	35	49	47	77	108	65	46
13 Live	18	7	20	11	37	71	40
13 Dead	30	48	104	31	45	30	0
% Dead 13	62.5	87.27272727	83.87096774	73.80952381	54.87804878	29.7029703	0
Bacteria per pic	48	55	124	42	82	101	40
14 Live	8	96	11	12	40	105	27
14 Dead	15	44	78	40	47	54	0
% Dead 14	65.2173913	31.42857143	87.64044944	76.92307692	54.02298851	33.96226415	0
Bacteria per pic	23	140	89	52	87	159	27
15 Live	8	109	10	17	60	100	49
15 Dead	23	0	63	79	35	57	3
% Dead 15	74.19354839	0	86.30136986	82.29166667	36.84210526	36.30573248	5.769230769
Bacteria per pic	31	109	73	96	95	157	52
Avg % Dead per pic	58.93721247	37.39004664	90.16934893	69.53223924	44.09731048	38.70313319	9.209640262
Avg of crystals % dead	64.23472585		63.77969779			41.40022184	
St. Dev of % dead	13.93060251		33.82028545			17.93894696	15.34941138
Average bacteria/ pic	50.86666667	68.26666667	79.93333333	90.2	93.13333333	97.4	81.53333333
Avg bacteria per pic	70.53333333		74.1			95.26666667	
St Dev of bacteria per pic	36.60764319		36.18568015			34.55623436	166.4781696

	Strain:							
	O55:H7	**O55:H7**	**O55:H7**	**O55:H7**	**O157:H7**	**O157:H7**	**O157:H7**	**O157:H7**
Picture:	**crystal 1 CP1**	**crystal 2 CP1**	**crystal 3 no CP1**	**crystal 4 no CP1**	**crystal 1 no CP1**	**crystal 2 no CP1**	**crystal 3 CP1**	**crystal 4 CP1**
1 Live	18	2	30	37	89	14	36	10
1 Dead	7	35	27	57	44	12	87	37
% Dead 1	28	94.59459459	47.36842105	60.63829787	33.08270677	46.15384615	70.73170732	78.72340426
Bacteria per pic	25	37	57	94	133	26	123	47
2 Live	14	4	39	43	61	14	77	9
2 Dead	6	20	20	32	10	17	61	44
% Dead 2	30	83.33333333	33.89830508	42.66666667	14.08450704	54.83870968	44.20289855	83.01886792
Bacteria per pic	20	24	59	75	71	31	138	53
3 Live	7	1	1	49	39	17	69	10
3 Dead	4	10	25	28	47	5	66	25
% Dead 3	36.36363636	90.90909091	96.15384615	36.36363636	54.65116279	22.72727273	48.88888889	71.42857143
Bacteria per pic	11	11	26	77	86	22	135	35
4 Live	9	6	11	12	74	14	62	3
4 Dead	6	23	17	6	34	12	48	40
% Dead 4	40	79.31034483	60.71428571	33.33333333	31.48148148	46.15384615	43.63636364	93.02325581
Bacteria per pic	15	29	28	18	108	26	110	43
5 Live	11	20	4	17	28	10	50	8
5 Dead	11	20	49	18	16	2	63	40
% Dead 5	50	50	92.45283019	51.42857143	36.36363636	16.66666667	55.75221239	83.33333333
Bacteria per pic	22	40	53	35	44	12	113	48
6 Live	19	16	1	17	5	2	71	7
6 Dead	17	10	64	14	16	8	67	56
% Dead 6	47.22222222	38.46153846	98.46153846	45.16129032	76.19047619	80	48.55072464	88.88888889
Bacteria per pic	36	26	65	31	21	10	138	63
7 Live	4	5	0	26	49	6	67	3
7 Dead	7	10	9	29	15	12	79	36
% Dead 7	63.63636364	66.66666667	100	52.72727273	23.4375	66.66666667	54.10958904	92.30769231
Bacteria per pic	11	15	9	55	64	18	146	39
8 Live	13	16	2	28	45	10	85	7
8 Dead	7	7	37	19	20	10	77	45
% Dead 8	35	30.43478261	94.87179487	40.42553191	30.76923077	50	47.5308642	86.53846154
Bacteria per pic	20	23	39	47	65	20	162	52
9 Live	8	4	3	33	59	12	55	11
9 Dead	6	14	37	17	31	11	60	37
% Dead 9	42.85714286	77.77777778	92.5	34	34.44444444	47.82608696	52.17391304	77.08333333
Bacteria per pic	14	18	40	50	90	23	115	48
10 Live	10	9	1	27	52	7	93	29
10 Dead	6	12	66	9	33	16	90	59
% Dead 10	37.5	57.14285714	98.50746269	25	38.82352941	69.56521739	49.18032787	67.04545455
Bacteria per pic	16	21	67	36	85	23	183	88
11 Live	7	7	2	36	67	7	70	52
11 Dead	0	6	35	29	28	17	74	53
% Dead 11	0	46.15384615	94.59459459	44.61538462	29.47368421	70.83333333	51.38888889	50.47619048
Bacteria per pic	7	13	37	65	95	24	144	105
12 Live	6	9	95	26	21	7	71	36
12 Dead	7	13	18	11	43	13	68	39
% Dead 12	53.84615385	59.09090909	15.92920354	29.72972973	67.1875	65	48.92086331	52
Bacteria per pic	13	22	113	37	64	20	139	75
13 Live	14	6	83	33	48	15	94	66
13 Dead	8	19	15	29	37	10	82	54
% Dead 13	36.36363636	76	15.30612245	46.77419355	43.52941176	40	46.59090909	45
Bacteria per pic	22	25	98	62	85	25	176	120
14 Live	7	32	99	25	69	12	77	48
14 Dead	13	30	47	32	24	8	106	23
% Dead 14	65	48.38709677	32.19178082	56.14035088	25.80645161	40	57.92349727	32.3943662
Bacteria per pic	20	62	146	57	93	20	183	71
15 Live	9	9	76	11	65	1	87	70
15 Dead	10	6	27	13	42	7	78	18
% Dead 15	52.63157895	40	26.21359223	54.16666667	39.25233645	87.5	47.27272727	20.45454545
Bacteria per pic	19	15	103	24	107	8	165	88
Avg % Dead per pic	41.22804895	62.55085589	66.61091852	43.5447284	38.57187062	53.59544305	51.12362503	68.11442437
Avg of crystals % dead		51.88945242		55.07782346		46.08365683		59.6190247
St. Dev of % dead		20.96488841		27.50471963		19.4693945		18.65103511
Average bacteria/ pic	18.06666667	25.4	62.66666667	50.86666667	80.73333333	20.53333333	144.6666667	65
Avg bacteria per pic		21.73333333		56.76666667		50.63333333		104.8333333
St Dev of bacteria per pic		10.93218385		30.57008154		36.30947756		47.38112772

	Strain:					
	O113:H21	**O113:H21**	**O113:H21**	**O113:H21**	**O117:K98:H4**	**O117:K98:H4**
Picture:	**crystal 1 CP1**	**crystal 2 CP1**	**crystal 4 no CP1**	**crystal 4 no CP1**	**crystal 1**	**crystal 2**
1 Live	34	124	5	41	29	10
1 Dead	37	95	18	4	160	72
% Dead 1	52.11267606	43.37899543	78.26086957	8.888888889	84.65608466	87.80487805
Bacteria per pic	71	219	23	45	189	82
2 Live	61	92	2	20	200	120
2 Dead	59	96	2	2	192	184
% Dead 2	49.16666667	51.06382979	50	9.090909091	48.97959184	60.52631579
Bacteria per pic	120	188	4	22	392	304
3 Live	64	85	18	19	38	152
3 Dead	62	99	26	1	180	184
% Dead 3	49.20634921	53.80434783	59.09090909	5	82.56880734	54.76190476
Bacteria per pic	126	184	44	20	218	336
4 Live	40	87	4	47	63	72
4 Dead	40	77	28	0	185	176
% Dead 4	50	46.95121951	87.5	0	74.59677419	70.96774194
Bacteria per pic	80	164	32	47	248	248
5 Live	38	88	4	2	143	104
5 Dead	35	105	57	20	194	208
% Dead 5	47.94520548	54.40414508	93.44262295	90.90909091	57.56676558	66.66666667
Bacteria per pic	73	193	61	22	337	312
6 Live	41	123	20	27	28	100
6 Dead	44	125	20	33	234	216
% Dead 6	51.76470588	50.40322581	50	55	89.3129771	68.35443038
Bacteria per pic	85	248	40	60	262	316
7 Live	45	118	51	24	233	68
7 Dead	33	95	0	45	219	72
% Dead 7	42.30769231	44.60093897	0	65.2173913	48.45132743	51.42857143
Bacteria per pic	78	213	51	69	452	140
8 Live	25	126	16	21	44	164
8 Dead	27	96	16	50	204	96
% Dead 8	51.92307692	43.24324324	50	70.42253521	82.25806452	36.92307692
Bacteria per pic	52	222	32	71	248	260
9 Live	38	109	41	31	56	100
9 Dead	54	135	11	29	244	110
% Dead 9	58.69565217	55.32786885	21.15384615	48.33333333	81.33333333	52.38095238
Bacteria per pic	92	244	52	60	300	210
10 Live	32	123	50	5	60	148
10 Dead	45	57	0	34	216	65
% Dead 10	58.44155844	31.66666667	0	87.17948718	78.26086957	30.51643192
Bacteria per pic	77	180	50	39	276	213
11 Live	47	79	66	5	32	156
11 Dead	33	90	0	59	188	64
% Dead 11	41.25	53.25443787	0	92.1875	85.45454545	29.09090909
Bacteria per pic	80	169	66	64	220	220
12 Live	12	89	57	29	47	39
12 Dead	36	84	14	61	192	9
% Dead 12	75	48.55491329	19.71830986	67.77777778	80.33472803	18.75
Bacteria per pic	48	173	71	90	239	48
13 Live	30	114	17	21	46	32
13 Dead	66	79	1	36	190	88
% Dead 13	68.75	40.93264249	5.555555556	63.15789474	80.50847458	73.33333333
Bacteria per pic	96	193	18	57	236	120
14 Live	30	106	33	31	78	17
14 Dead	71	85	1	12	124	200
% Dead 14	70.2970297	44.5026178	2.941176471	27.90697674	61.38613861	92.16589862
Bacteria per pic	101	191	34	43	202	217
15 Live	47	83	9	13	74	50
15 Dead	58	85	17	62	148	20
% Dead 15	55.23809524	50.5952381	65.38461538	82.66666667	66.66666667	28.57142857
Bacteria per pic	105	168	26	75	222	70
Avg % Dead per pic	54.80658054	47.51228871	38.86986034	51.58256346	73.48900993	54.81616932
Avg of crystals % dead		51.15943463		45.2262119		36.74450496
St. Dev of % dead		8.959951674		33.53429533		20.48651123
Average bacteria/ pic	85.6	196.6	40.26666667	52.26666667	269.4	206.4
Avg bacteria per pic		141.1		46.26666667		237.9
St Dev of bacteria per pic		61.35389148		20.37058957		89.15788011

	Strain:				
	O117:K98:H4	**O157:H16**	**O157:H16**	**O157:H16**	**O157:H16**
Picture:	**crystal 4 NO CP1**	**crystal 1 with CP1**	**crystal 4 with CP1**	**crystal 2 no CP1**	**crystal 3 no CP1**
1 Live	29	42	7	27	1
1 Dead	20	52	37	37	0
% Dead 1	40.81632653	55.31914894	84.09090909	57.8125	0
Bacteria per pic	49	94	44	64	1
2 Live	50	81	16	80	132
2 Dead	45	59	14	38	42
% Dead 2	47.36842105	42.14285714	46.66666667	32.20338983	24.13793103
Bacteria per pic	95	140	30	118	174
3 Live	41	49	30	14	2
3 Dead	52	42	23	49	4
% Dead 3	55.91397849	46.15384615	43.39622642	77.77777778	66.66666667
Bacteria per pic	93	91	53	63	6
4 Live	50	56	12	33	3
4 Dead	26	104	19	47	1
% Dead 4	34.21052632	65	61.29032258	58.75	25
Bacteria per pic	76	160	31	80	4
5 Live	54	64	10	56	1
5 Dead	30	80	16	43	2
% Dead 5	35.71428571	55.55555556	61.53846154	43.43434343	66.66666667
Bacteria per pic	84	144	26	99	3
6 Live	70	64	32	32	5
6 Dead	17	84	17	5	2
% Dead 6	19.54022989	56.75675676	34.69387755	13.51351351	28.57142857
Bacteria per pic	87	148	49	37	7
7 Live	27	100	35	4	5
7 Dead	18	74	23	34	0
% Dead 7	40	42.52873563	39.65517241	89.47368421	0
Bacteria per pic	45	174	58	38	5
8 Live	38	84	50	27	4
8 Dead	19	56	30	71	3
% Dead 8	33.33333333	40	37.5	72.44897959	42.85714286
Bacteria per pic	57	140	80	98	7
9 Live	70	56	40	16	0
9 Dead	20	42	30	29	0
% Dead 9	22.22222222	42.85714286	42.85714286	64.44444444	
Bacteria per pic	90	98	70	45	0
10 Live	42	48	70	19	3
10 Dead	35	53	44	18	6
% Dead 10	45.45454545	52.47524752	38.59649123	48.64864865	66.66666667
Bacteria per pic	77	101	114	37	9
11 Live	43	76	68	63	0
11 Dead	30	96	36	0	2
% Dead 11	41.09589041	55.81395349	34.61538462	0	100
Bacteria per pic	73	172	104	63	2
12 Live	70	102	48	70	2
12 Dead	40	120	22	0	3
% Dead 12	36.36363636	54.05405405	31.42857143	0	60
Bacteria per pic	110	222	70	70	5
13 Live	55	80	60	36	8
13 Dead	37	14	34	2	16
% Dead 13	40.2173913	14.89361702	36.17021277	5.263157895	66.66666667
Bacteria per pic	92	94	94	38	24
14 Live	50	85	32	120	8
14 Dead	24	10	54	0	8
% Dead 14	32.43243243	10.52631579	62.79069767	0	50
Bacteria per pic	74	95	86	120	16
15 Live	82	101	40	39	2
15 Dead	45	11	34	2	1
% Dead 15	35.43307087	9.821428571	45.94594595	4.87804878	33.33333333
Bacteria per pic	127	112	74	41	3
Avg % Dead per pic	37.34108603	42.9265773	46.74907218	37.90989921	42.03776683
Avg of crystals % dead			44.83782474		39.97383302
St. Dev of % dead	9.0849055		15.95689847		29.90131198
Average bacteria/ pic	81.93333333	132.3333333	65.53333333	67.4	17.73333333
Avg bacteria per pic			98.93333333		42.56666667
St Dev of bacteria per pic	21.68102089		47.35918025		44.50856821

Appendix D: Live/Dead Tables

Table 7: Number of *E. coli* present on crystal per picture with cecropin P1 and without cecropin P1.

E. coli Strain	*E. coli* present with CP1	*E. coli* present without CP1
HB101	74	71
O26:K60:H11	37	34
O35:K-:H10	95	59
O55:H7	22	58
O113:H4	121	81
O113:H21	141	46
O117:K98:H4	30	39
O157:H7	105	51
O157:H12	36	66
O157:H16	99	43
O172:K-:H-	389	52

Table 8: Percentage of *E. coli* dead per picture with cecropin P1 and without cecropin P1.

E. coli Strain	% *E. coli* dead with CP1	% *E. coli* dead without CP1
HB101	64	64
O26:K60:H11	21	25
O35:K-:H10	41	11
O55:H7	52	55
O113:H4	32	2
O113:H21	51	45
O117:K98:H4	25	14
O157:H7	60	46
O157:H12	66	37
O157:H16	45	40
O172:K-:H-	17	24

Appendix E: Growth Curves

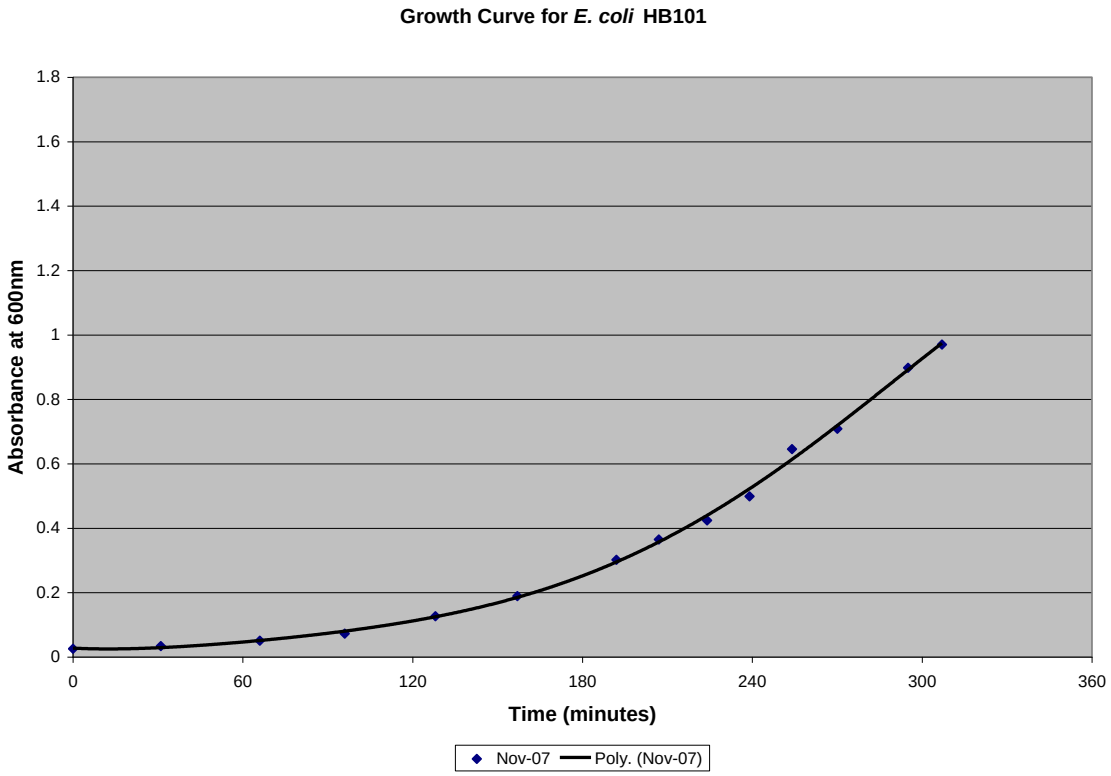

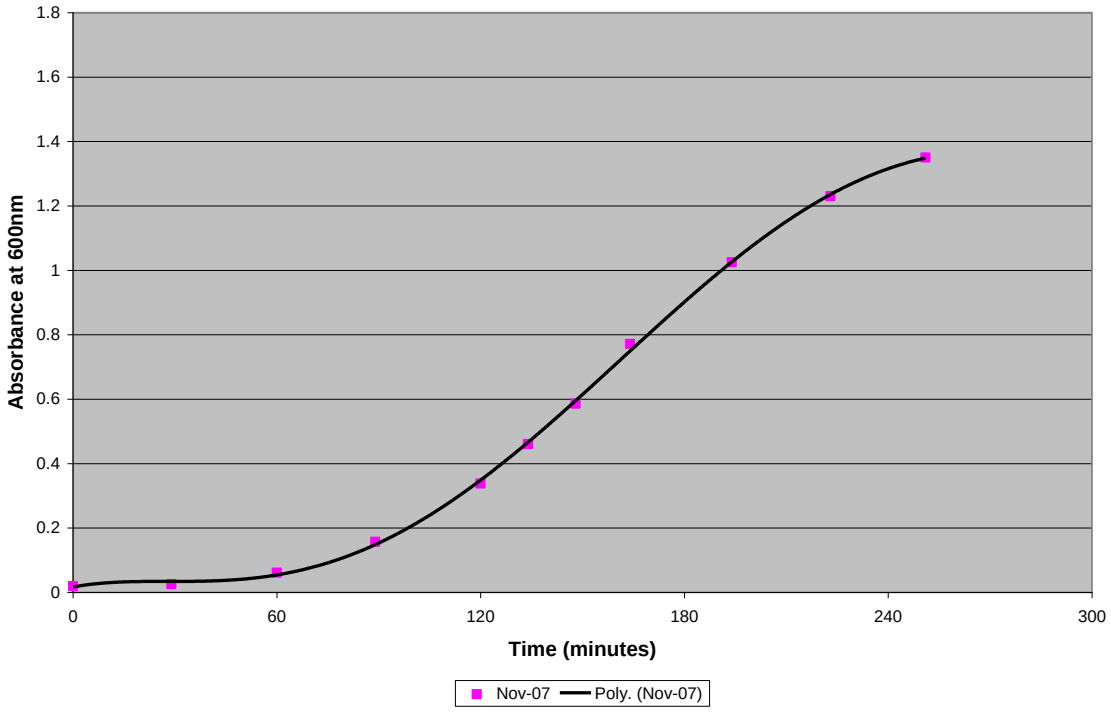

Growth Curve for *E. coli* O55:H7

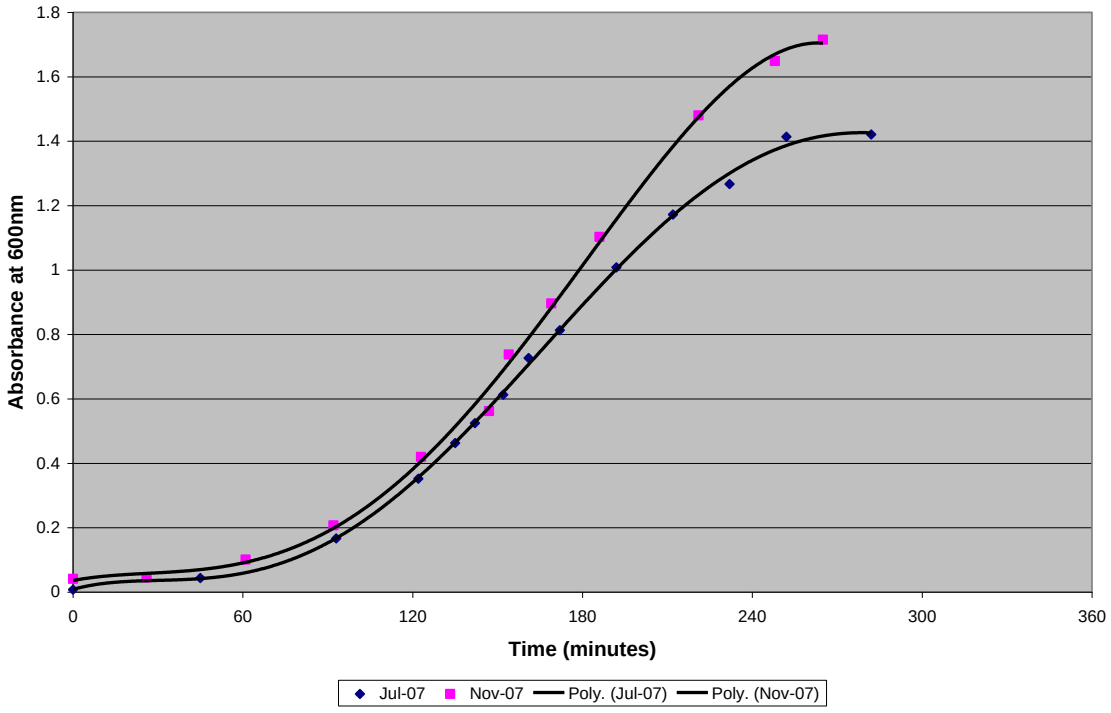

Growth Curve for *E. coli* O113:H4

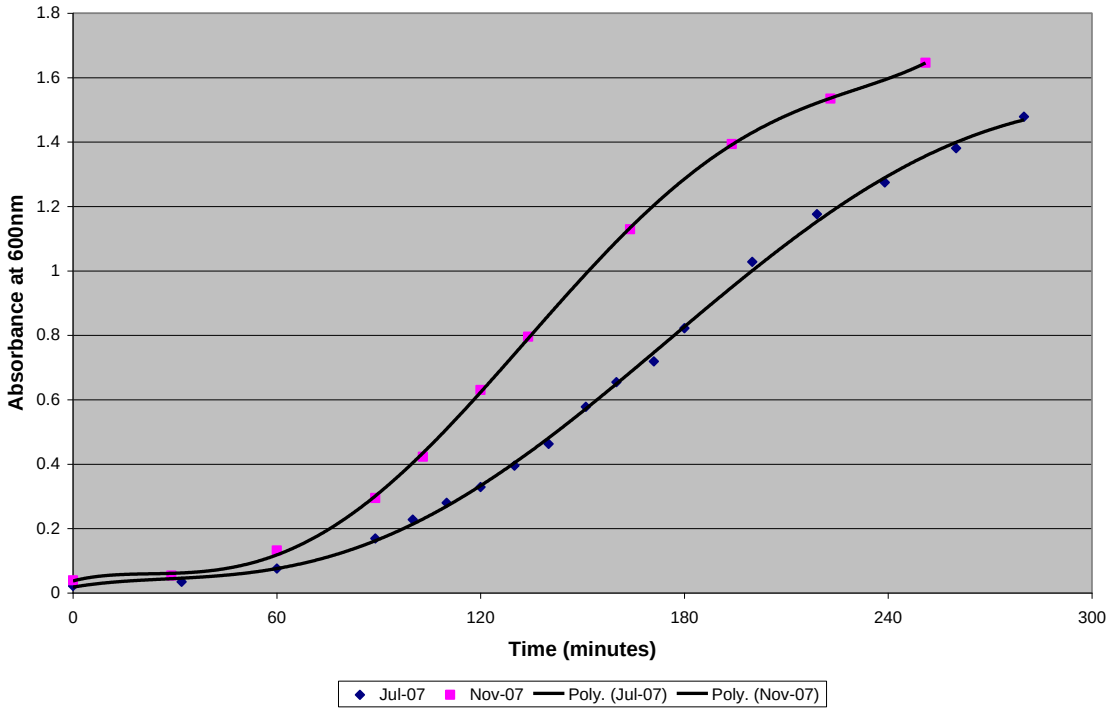

Growth Curve for *E. coli* O113:H21

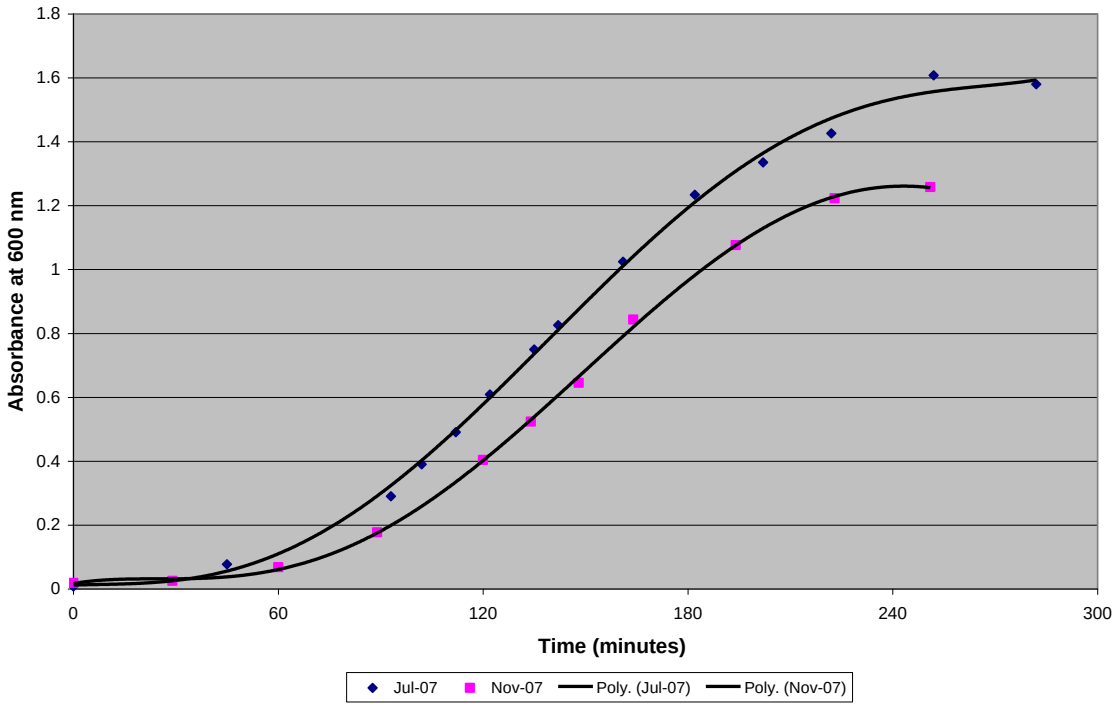

Growth Curve for *E. coli* O157:H7

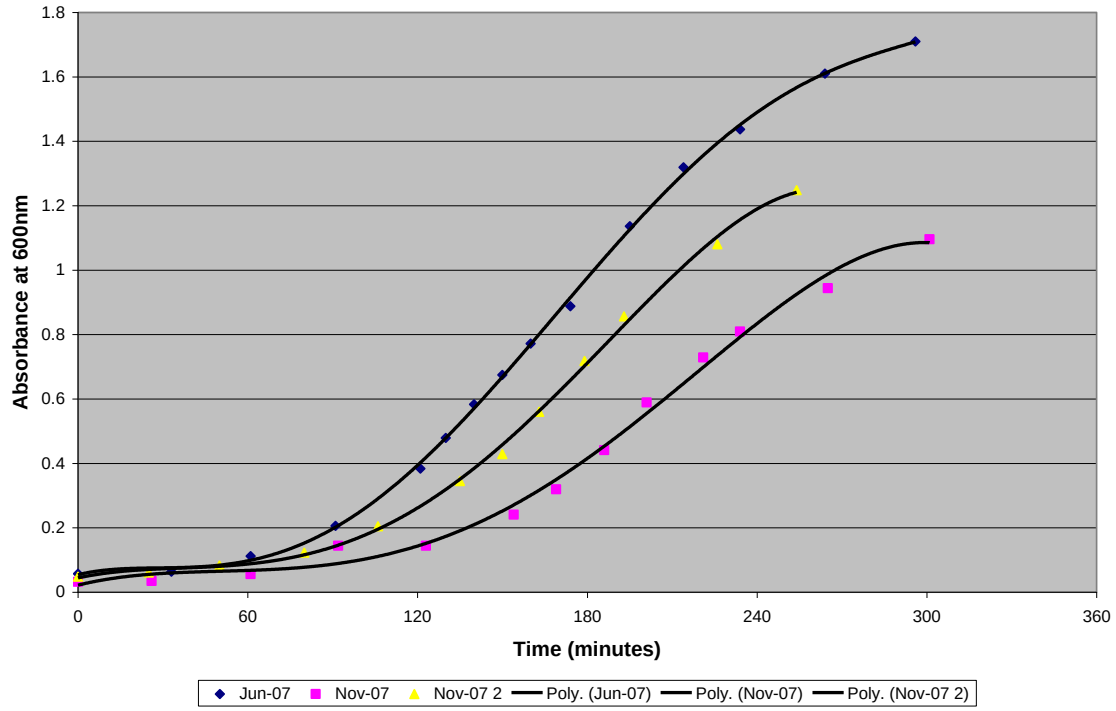

Growth Curve for *E. coli* O157:H12

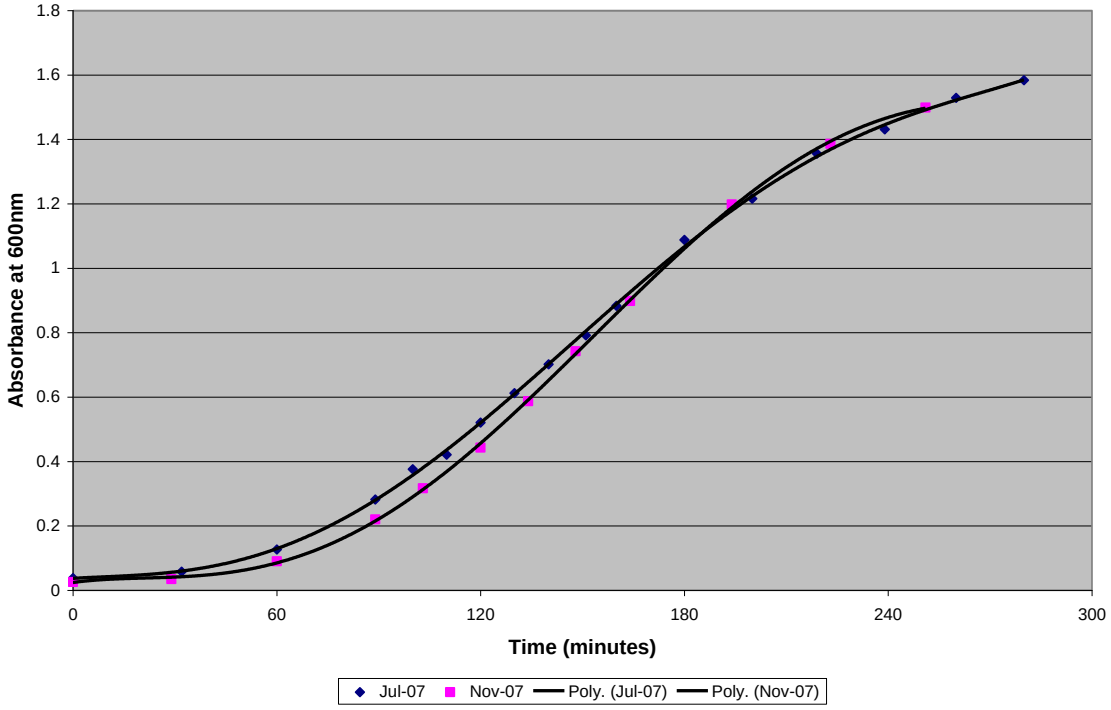

Growth Curve for *E. coli* O157:H16

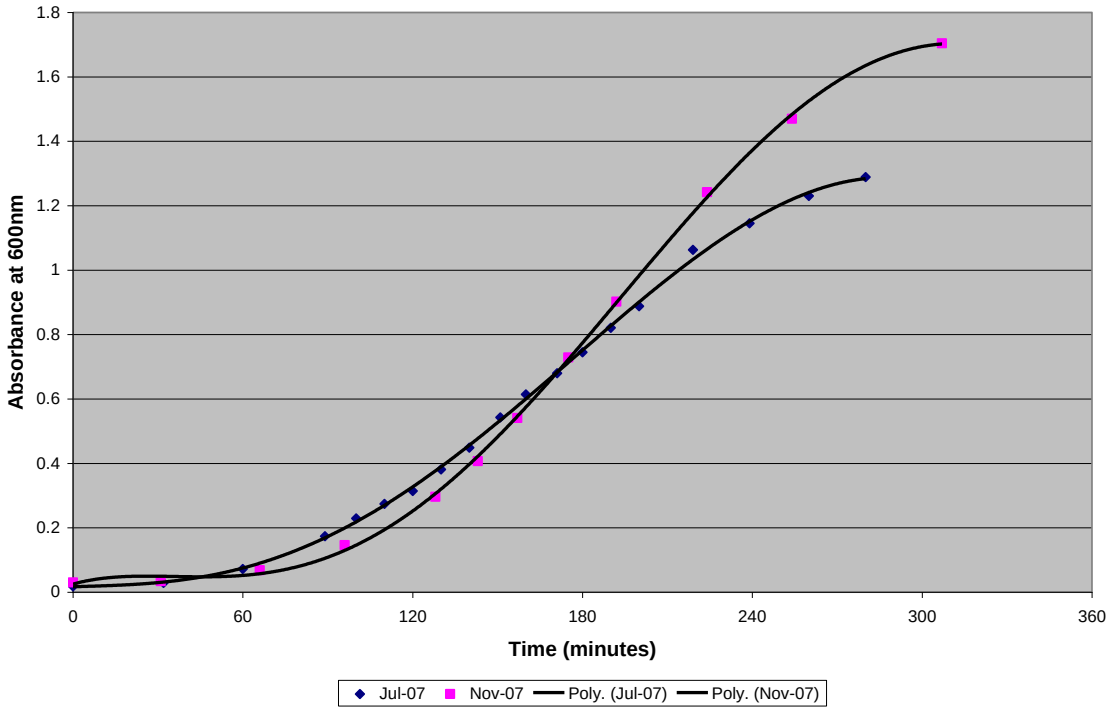

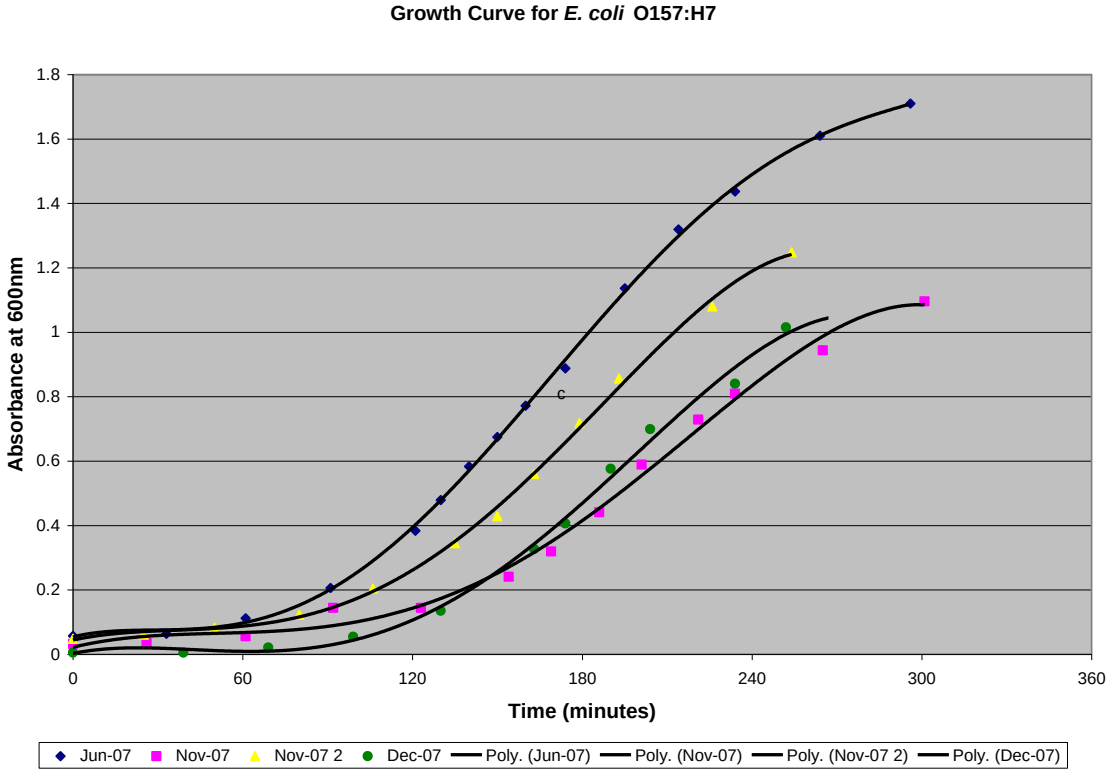
Growth Curve for E. coli O157:H7
Absorbance at 600nm
Time (minutes)
Jun-07
Nov-07
Nov-07 2
Dec-07
Poly. (Jun-07)
Poly. (Nov-07)
Poly. (Nov-07 2)
Poly. (Dec-07)

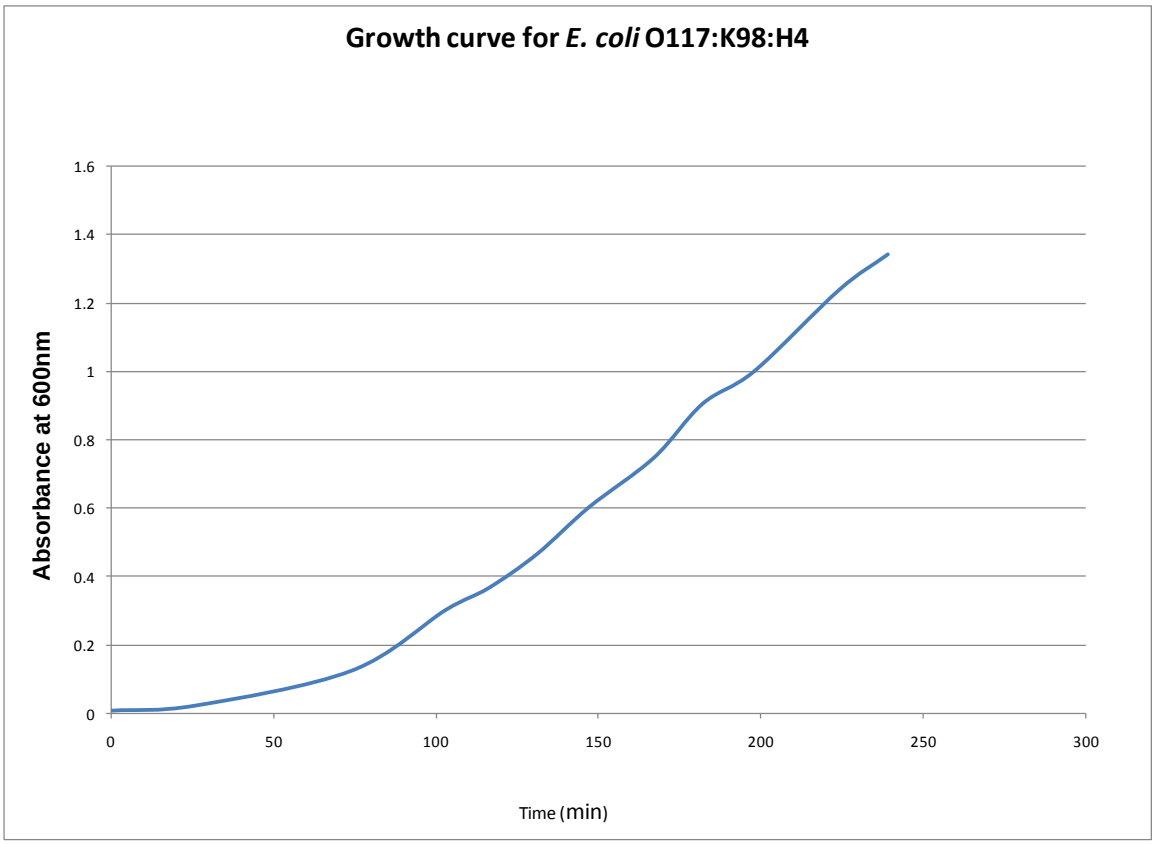
Growth curve for E. coli O117:K98:H4
Absorbance at 600nm
Time (min)

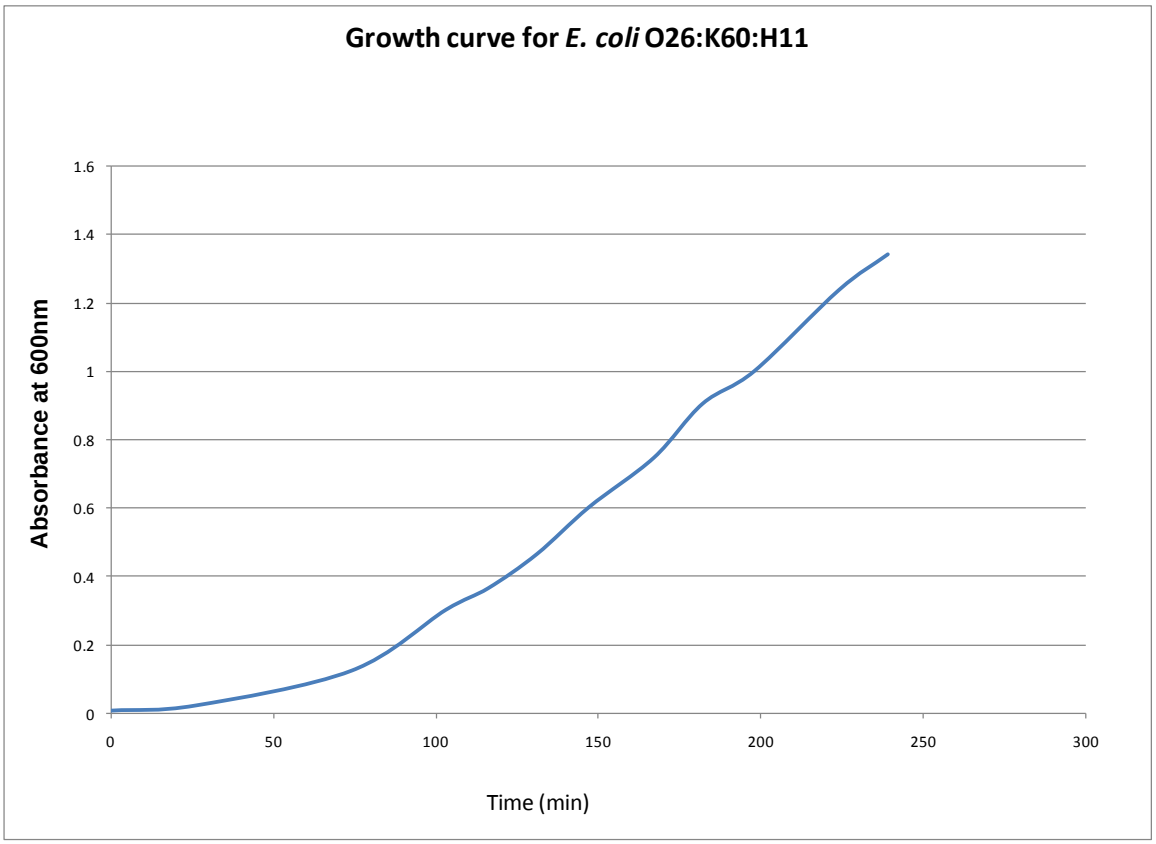
Growth curve for E. coli O26:K60:H11
Absorbance at 600nm
1.6
1.4
1.2
1
0.8
0.6
0.4
0.2
0
0
50
100
150
200
250
300
Time (min)

Appendix F: Frequency and Dissipation Results Table

Average frequency and dissipation shifts measured in QCM-D when *E.coli* was added, with and without cecropin P1 cys bound to the gold crystal surface.

	Average Shift Measured When *E. coli* Added			
	Δf (Hz)		ΔD (μ)	
***E. coli* Strain**	**With CP1-cys**	**No CP1-cys**	**With CP1-cys**	**No CP1-cys**
HB101	-25.5	-3.0	3.200	0.800
O26:K60:H11	-7.4	0.5	0.700	0.125
O35:K-:H10	-5.0	-0.5	1.525	1.406
O55:H7	-9.3	-2.8	1.400	0.300
O113:H4	-4.5	-2.5	1.100	0.400
O113:H21	-3.8	-3.0	0.500	0.500
O117:K98:H4	-3.3	-0.7	0.542	0.167
O157:H7	-8.0	-5.0	1.100	0.500
O157:H12	-13.3	-11.8	1.400	1.500
O157:H16	-10.8	-6.3	1.250	0.875
O172:K-:H-	-3.8	-2.3	0.400	0.400
Averages	**-8.9**	**-3.4**	**1.245**	**0.684**